Online ISSN : 2249-4596
Print ISSN : 0975-5861
DOI : 10.17406/GJRE

Global Journal

of Researches in Engineering: I

Numerical Methods

Application of Numerical Methods

Finite and Numerical Simulations

Highlights

Estimate of Rheology Constants

Modeling Filters of Six Symmetrical

Discovering Thoughts, Inventing Future

VOLUME 20 ISSUE 1 VERSION 1.0

Global Journal of Researches in Engineering: I
Numerical Methods

Global Journal of Researches in Engineering: I
Numerical Methods
Volume 20 Issue 1 (Ver. 1.0)

Open Association of Research Society

Incorporation No.: 0423089
License No.: 42125/022010/1186
Registration No.: 430374
Import-Export Code: 1109007027
Employer Identification Number (EIN):
USA Tax ID: 98-0673427

Global Journals Inc.

*(A Delaware USA Incorporation with "Good Standing"; **Reg. Number: 0423089**)*

Sponsors: Open Association of Research Society
Open Scientific Standards

Publisher's Headquarters office

Global Journals® Headquarters
945th Concord Streets,
Framingham Massachusetts Pin: 01701,
United States of America
USA Toll Free: +001-888-839-7392
USA Toll Free Fax: +001-888-839-7392

Offset Typesetting

Global Journals Incorporated
2nd, Lansdowne, Lansdowne Rd., Croydon-Surrey,
Pin: CR9 2ER, United Kingdom

Packaging & Continental Dispatching

Global Journals Pvt Ltd
E-3130 Sudama Nagar, Near Gopur Square,
Indore, M.P., Pin:452009, India

Find a correspondence nodal officer near you

To find nodal officer of your country, please email us at *local@globaljournals.org*

eContacts

Press Inquiries: *press@globaljournals.org*
Investor Inquiries: *investors@globaljournals.org*
Technical Support: *technology@globaljournals.org*
Media & Releases: *media@globaljournals.org*

Pricing (Excluding Air Parcel Charges):

Yearly Subscription (Personal & Institutional)
250 USD (B/W) & 350 USD (Color)

Editorial Board

Global Journal of Research in Engineering

Prof. (LU), (UoS) Dr. Miklas Scholz

Cand Ing, BEng (equiv), PgC, MSc, Ph.D., CWEM, CEnv, CSci, CEng, FHEA, FIEMA, FCIWEM, FICE, Fellow of IWA, VINNOVA Fellow, Marie Curie Senior, Fellow, Chair in Civil Engineering (UoS) Wetland Systems, Sustainable Drainage, and Water Quality

Dr. Kitipong Jaojaruek

B. Eng, M. Eng, D. Eng (Energy Technology, Asian Institute of Technology). Kasetsart University Kamphaeng Saen (KPS) Campus Energy Research Laboratory of Mechanical Engineering

Dr. Yudong Zhang

B.S., M.S., Ph.D. Signal and Information Processing, Southeast University Professor School of Information Science and Technology at Nanjing Normal University, China

Dr. Burcin Becerik-Gerber

University of Southern Californi Ph.D. in Civil Engineering Ddes, from Harvard University M.S. from University of California, Berkeley M.S. from Istanbul, Technical University

Dr. Minghua He

Department of Civil Engineering Tsinghua University Beijing, 100084, China

Hiroshi Sekimoto

Professor Emeritus Tokyo Institute of Technology Japan Ph.D., University of California Berkeley

Dr. Philip G. Moscoso

Technology and Operations Management IESE Business School, University of Navarra Ph.D. in Industrial Engineering and Management, ETH Zurich M.Sc. in Chemical Engineering, ETH Zurich, Spain

Dr. Shaoping Xiao

BS, MS Ph.D. Mechanical Engineering, Northwestern University The University of Iowa, Department of Mechanical and Industrial Engineering Center for Computer-Aided Design

Dr. Stefano Mariani

Associate Professor, Structural Mechanics, Department of Civil and Environmental Engineering, Ph.D., in Structural Engineering Polytechnic University of Milan Italy

Dr. A. Stegou-Sagia

Ph.D., Mechanical Engineering, Environmental Engineering School of Mechanical Engineering, National Technical University of Athens, Greece

Dr. Ciprian Lapusan

Ph. D in Mechanical Engineering Technical University of Cluj-Napoca Cluj-Napoca (Romania)

Diego Gonzalez-Aguilera

Ph.D. Dep. Cartographic and Land Engineering, University of Salamanca, Avilla, Spain

Dr. Francesco Tornabene

Ph.D. in Structural Mechanics, University of Bologna Professor Department of Civil, Chemical, Environmental and Materials Engineering University of Bologna, Italy

Dr. Maria Daniela

Ph.D in Aerospace Science and Technologies Second University of Naples, Research Fellow University of Naples Federico II, Italy

Dr. Omid Gohardani

Ph.D. Senior Aerospace/Mechanical/ Aeronautical, Engineering professional M.Sc. Mechanical Engineering, M.Sc. Aeronautical Engineering B.Sc. Vehicle Engineering Orange County, California, US

Dr. Paolo Veronesi

Ph.D., Materials Engineering, Institute of Electronics, Italy President of the master Degree in Materials Engineering Dept. of Engineering, Italy

Contents of the Issue

Global Journal of Researches in Engineering: I
Numerical Methods
Volume 20 Issue 1 Version 1.0 Year 2020
Type: Double Blind Peer Reviewed International Research Journal
Publisher: Global Journals
Online ISSN: 2249-4596 & Print ISSN: 0975-5861

Solar Synchronous Orbits. Predicting the Mean Local Time of the Ascending Node

By Andrey Nazarenko

Abstract- Based on the orbital data of the Meteor M1 spacecraft, the possible causes of the deviations of the mean local time of the ascending node (MLTAN) from the initial value are considered. It has been established that the main cause of deviations is the change in inclination. This occurs as a result of solar gravitational disturbances and leads to a change in the MLTAN under the law, which at intervals of up to 7 years is close to parabola. In general, these variations are long-period with the period of 28 years. The simplified system of differential equations describing the evolution of inclination and MLTAN has been proposed. The results of the integration of this system of equations are well consistent with the real data on the evolution of the parameters of the orbit of the Meteor M1 spacecraft.

Keywords: *local time, ascending node, inclination, evolution equations.*

GJRE-I Classification: *FOR Code: 230116*

Strictly as per the compliance and regulations of:

Solar Synchronous Orbits. Predicting the Mean Local Time of the Ascending Node

Солнечно синхронные орбиты. Прогнозирование местного солнечного времени восходящего узла

Andrey Nazarenko

Abstract- Based on the orbital data of the Meteor M1 spacecraft, the possible causes of the deviations of the mean local time of the ascending node (MLTAN) from the initial value are considered. It has been established that the main cause of deviations is the change in inclination. This occurs as a result of solar gravitational disturbances and leads to a change in the MLTAN under the law, which at intervals of up to 7 years is close to parabola. In general, these variations are long-period with the period of 28 years. The simplified system of differential equations describing the evolution of inclination and MLTAN has been proposed. The results of the integration of this system of equations are well consistent with the real data on the evolution of the parameters of the orbit of the Meteor M1 spacecraft.

Keywords: local time, ascending node, inclination, evolution equations.

Аннотация- **На основе орбитальных данных КА МЕТЕОР М1 рассмотрены возможные причины отклонений местного солнечного времени восходящего узла (МСВ ВУ) от начального значения. Установлено, что основной причиной отклонений является изменение наклонения. Это происходит в результате действия солнечных гравитационных возмущений и приводит к изменению МСВ ВУ по закону, который на интервале до 7 лет близок к параболе. В общем случае эти вариации являются долгопериодическими с периодом ≈28 лет. Предложена упрощенная система дифференциальных уравнений, описывающих эволюцию наклонения и МСВ ВУ. Результаты интегрирования этой системы уравнений хорошо согласуются с реальными данными об эволюции параметров орбиты КА МЕТЕОР М1.**

Ключевые слова: Местное время, долгота восходящего узла, наклонение, эволюция, интегрирование уравнений.

I. Введение

Спутники дистанционного зондирования Земли (ДЗЗ) широко применяются для оптических наблюдений объектов на поверхности Земли [1]. Параметры спутников на солнечно синхронных орбитах (ССО) выбираются так, чтобы условия наблюдения были наиболее благоприятными и стабильными. Это достигается таким выбором долготы восходящего узла и наклонения орбиты, чтобы поверхность Земли всегда была освещена Солнцем. Основой выбора параметров орбиты является известное соотношение для изменения долготы восходящего узла (ДВУ) под действием гравитационных возмущений за виток [2, 3, 4]

$$\delta\Omega = 2\pi \cdot \frac{3}{2} \cdot c_{20} \left(\frac{R_э}{p} \right)^2 \cdot \cos i + O\left(c_{20}^2\right) . \qquad (1)$$

Здесь:

c_{20} - параметр гравитационного поля Земли (≈-0.001), характезующий ее сжатие,

$R_э$ - средний экваториальный радиус Земли,

p – параметр орбиты,

i – наклонение орбиты.

Author: Retired Professor, Russian Academy of Sciences Russia, Russia. e-mail: anazarenko32@mail.ru

Зависимость (1) имеет погрешность порядка c_{20}^2, которая обусловлена влиянием других (более слабых) возмущающих факторов.

Для обеспечения благоприятных условий наблюдения долгота восходящего узла (ДВУ, Ω) выбирается так, чтобы прямое восхождение Солнца в момент пролета спутника через восходящий узел ($\alpha(t_\Omega)$) было меньше ДВУ в этот момент на заданную величину

$$\eta(t_\Omega) = \Omega(t_\Omega) - \alpha(t_\Omega) + \pi = const \,. \tag{2}$$

Эта величина называется местным солнечным временем восходящего узла и обычно обозначается как МСВ ВУ.

Для обеспечения стабильности условий наблюдения параметры орбиты выбираются так, чтобы выполнялось условие постоянства МСВ ВУ:

$$\eta(t_\Omega + T_{dr}) = \eta(t_\Omega), \tag{3}$$

где T_{dr} - драконический период спутника. Детализация условия (3):

$$\alpha(t_\Omega + T_{dr}) - \alpha(t_\Omega) = \Omega(t_\Omega + T_{dr}) - \Omega(t_\Omega) \,. \tag{4}$$

Здесь при расчете левой разности можно принять производную прямого восхождения по времени постоянной и равной

$$\dot{\alpha} = 2\pi / 365.25 \text{ рад/сутки} = 0.9856°/\text{сутки}. \tag{5}$$

С учетом этого обстоятельства и формулы (1) условие (4) принимает вид

$$\dot{\alpha} \cdot T_{dr} = \delta\Omega \,. \tag{6}$$

Выполнение условия (6) на всем интервале полета спутника обеспечивает постоянство МСВ ВУ. Однако при полете реального спутника МСВ ВУ меняется во времени. Актуальной задачей является выявление всех факторов, которые являются причиной непостоянства МСВ ВУ, и разработка простой инженерной методики для прогнозирования этой характеристики.

Основой проведенного анализа являются параметры орбиты спутника МЕТЕОР М1, который 17.09.2009 был выведен на круговую орбиту с параметрами: высота 832 км, наклонение 98.77°. Рассмотрен интервал времени с момента запуска до июня 2017 г (данные американского каталога ([5]). В известных публикациях [6, 7, 8] анализ эволюции МСВ ВУ по реальным данным рассмотрен недостаточно полно.

Author: Retired Professor, Russian Academy of Sciences Russia, Russia. e-mail: anazarenko32@mail.ru

II. Эволюция параметров орбиты спутника METEOP M1

На рисунках 1, 2, 3 и 4 представлены графики значений элементов орбиты спутника в функции времени. Из данных этого рисунка видно, что закономерности изменения рассматриваемых элементов орбит имеют вековой характер и являются очень похожими, а именно:

- наблюдается их уменьшение во времени по закону, близкому к параболе;
- за весь период полуось уменьшилась на 1 км, а период – на 0. 021 мин;
- уменьшение параметров происходило наиболее интенсивно на интервале времени с мая 2014 г по сентябрь 2015 г. Этот период характерен достижением максимума солнечной активности, что привело к увеличению плотности атмосферы и усилению торможения спутника.

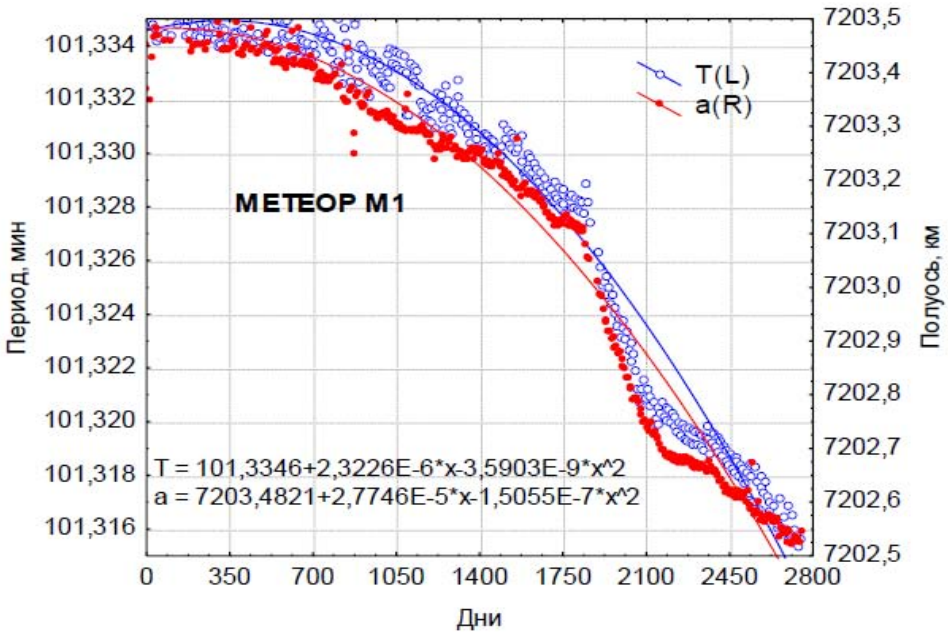

Рисунок 1: Эволюция периода и большой полуоси

Таким образом наиболее вероятной причиной вековых изменений периода и полуоси является влияние торможения КА в атмосфере Земли.

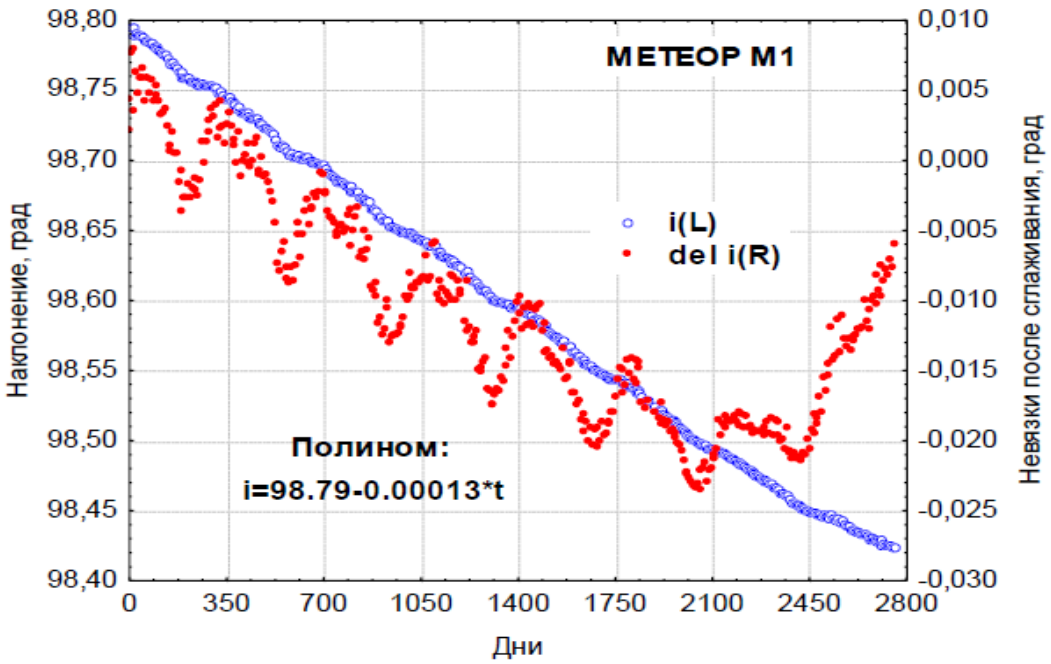

Рисунок 2: Эволюция наклонения орбиты

Представленные здесь данные об эволюции наклонения орбиты характерны наличием монотонной составляющей. На рассмотренном интервале времени наклонение уменьшилось на 0.37°. Известно, что при движении спутника в гравитационном поле Земли вековых возмущений наклонения не возникает. Атмосферные возмущения вносят в наклонение ничтожный вклад. Поэтому наблюдаемое изменение наклонения объясняется какими-то другими возмущающими факторами.

В отклонениях оценок наклонения от результатов сглаживания (полинома) видна периодическая составляющая с амплитудой ≈0.004° и периодом ≈1 год.

Они имеют второй порядок малости ($c_{20}^2 \approx 10^{-6}$). Такие возмущения четко видны на интервале времени до 2100-го дня. Равенство периода одному году позволяет предположить, что возникновение этих возмущений связано с влиянием солнечной гравитации.

На интервале времени после 2100-го дня наблюдаются существенные отклонения оценок наклонения от линейной зависимости, которые достигают значения 0.022°. Происхождение этих существенных отклонений на данном этапе неизвестно. Возможная причина аномальных отклонений в эволюции наклонения на интервале времени после 2100-го дня будет рассмотрена ниже.

Представленные на рисунке 3 данные об эволюции долготы восходящего узла характерны наличием существенной вековой составляющей. В

соответствии с формулой (1) она имеет порядок c_{20}. За сутки это возмущение приводит к перемещению восходящего узла на ≈1°. Именно это обстоятельство должно обеспечивать выполнение условия (6), необходимого для нормального функционирования КА на солнечно синхронных орбитах. За прошедшее время восходящий узел совершил 7 полных оборотов. В этих условиях затруднительно построить отклонения реальных оценок ДВУ от их сглаженных значений, как это было сделано выше для данных об эволюции периода, полуоси и наклонения.

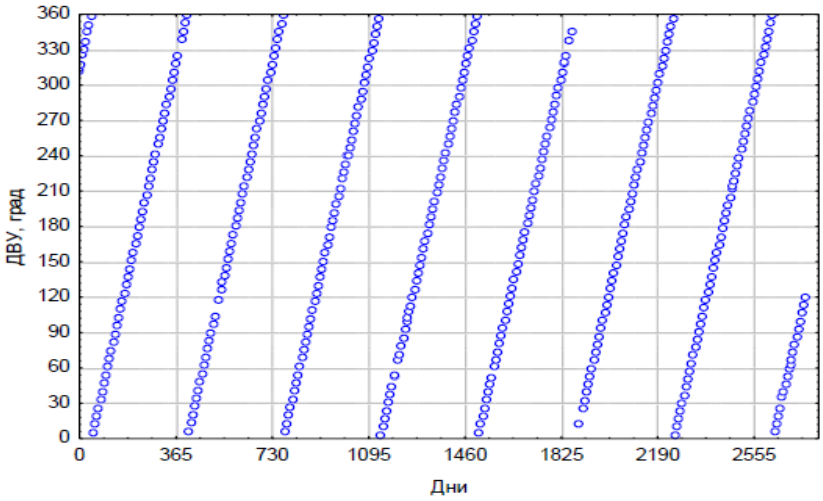

Рисунок 3: Эволюция долготы восходящего узла

Для более детального анализа эволюции ДВУ было выбрано два годичных интервала, на которых данный параметр орбиты изменялся от 0° до 360°. Соответствующие оценки представлены на рисунке 4.

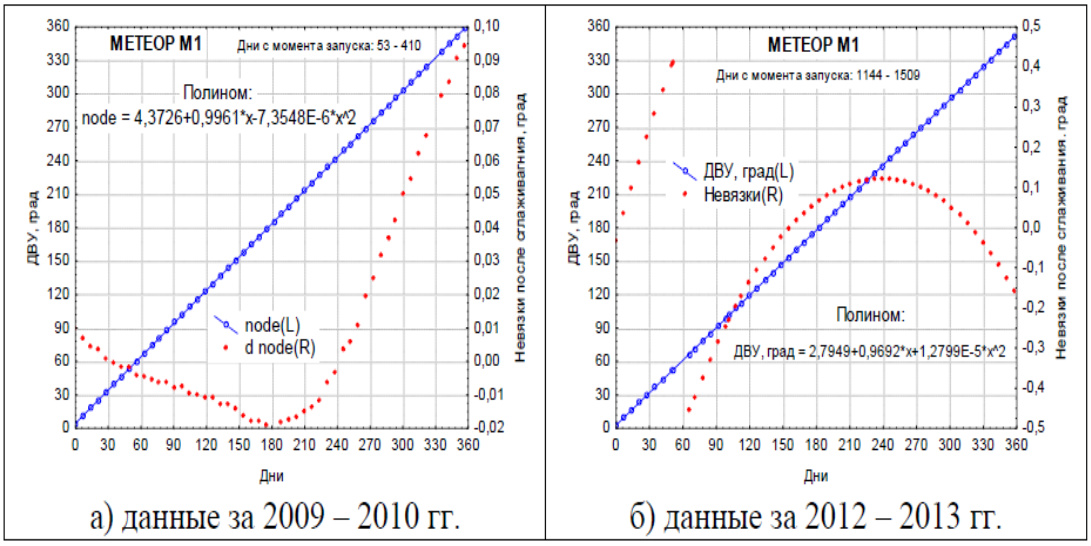

Рисунок 4: Детальные данные об эволюции долготы восходящего узла

На этих рисунках приведены исходные оценки, результаты аппроксимации вековой составляющей полиномом второй степени ($\hat{\Omega} = a_0 + a_1 \cdot t + a_2 \cdot t^2$), а также остаточные невязки между исходными данными и полиномом. Соответствующие результаты аппроксимации приведены в таблице 1.

Таблица 1: Результаты аппроксимации значений долготы восходящего узла

Интервал времени	a_1, град/сутки	a_2, град/сутки^2	невязки $\Omega - \hat{\Omega}$, град
2009 – 2010 гг.	0.9961	-0.00000735	от -0.02 до 0.10
2012 – 2013 гг.	0.9692	+0.00001279	от -0.5 до 0.4

Эти результаты являются весьма интересными.

- На первом интервале коэффициент a_1 несколько больше «идеального» значения 0.9856 град/сутки, а на втором интервале – несколько меньше.

- Коэффициенты a_2 имеют разные знаки. Их вклад в эволюцию ДВУ на годичном интервале является относительно небольшим. В первом случае он составляет -0.95°, а во втором +1.65°.

- На первом интервале остаточные невязки намного меньше, чем на втором интервале, где они сопоставимы с вкладом квадратичной составляющей полинома.

- На первом интервале остаточные невязки меняются плавно, а на втором – имеют разрыв в окрестности точки «60-й день». Смещение оценок в момент разрыва составляет ≈1°. Данный факт позволяет сделать вывод, что на втором интервале оценка коэффициента a_2 является недостаточно достоверной. Причины разрыва – неизвестны.

Таким образом, отклонения фактичекских значений ДВУ от «идеальных» можно оценить следующим образом.

- На первом интервале: $\delta\Omega \approx (0.9961 - 09856) \cdot t - 0.00000735 \cdot t^2$; (8)
- На втором интервале: $\delta\Omega \approx (0.9692 - 09856) \cdot t$. (9)

На рисунке 5 представлены результаты расчета МСВ ВУ по формуле (2). Построена аппроксимация оценок МСВ ВУ (полином)

$$\hat{\eta}(t) = 20.93 + 0.0007 \cdot t - 0.000000513 \cdot t^2, \text{ [часы]}. \quad (10)$$

В соответствии с данными рисунка и этой аппроксимации оценки МСВ ВУ сначала увеличиваются от значения 20.89^h до 21.24^h, а затем уменьшается до значения 19.07^h на 2775-й день. Диапазон изменения оценок МСВ ВУ на этом интервале составляет 2.17^h.

Имеется хорошее согласие оценок МСВ ВУ по данным рисунка 5 с результатами анализа эволюции ДВУ, представленных на рисунке 4. На рисунке 5 два проанализированных годичных интервала выделены светло зелеными линиями. Эволюция МСВ ВУ на этих участках полностью согласуется с формой приведенных выше полиномов (8) и (9).

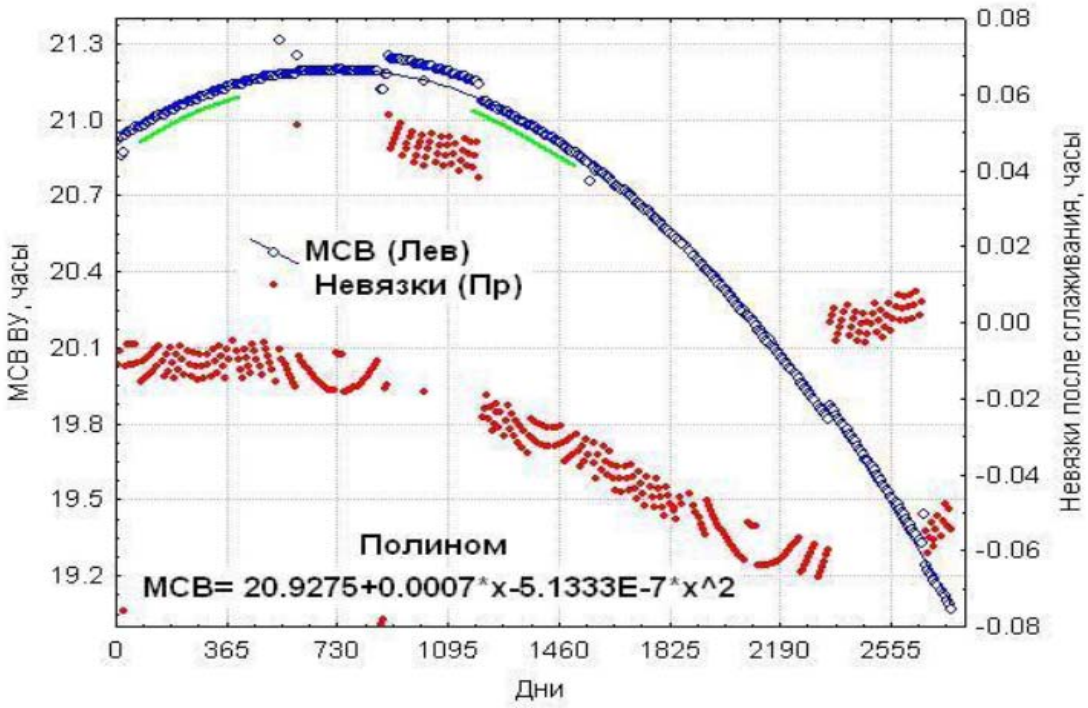

Рисунок 5: Эволюция местного солнечного времени восходящего узла

III. Влияние погрешностей начальных условий

Выше в разделе 1 отмечалось, что солнечно синхронные обиты проектируются так, чтобы МСВ ВУ было постоянным. Построенная в предыдущем разделе зависимость (10) описывает реальное изменение этой характеристики спутника МКТЕОР М1 на 7-ми летнем интервале его полета. Диапазон изменения МСВ ВУ на всем интервале составил 2.1^{h}. Возможными причинами изменения МСВ ВУ являются погрешности выведения КА, т.е. отличие реальных параметров орбиты от «идеальных». Оценим их влияние.

В соответствии с данными таблицы 1 скорость изменения ДВУ на начальном этапе его полета была рана

$$\dot{\Omega}(t=0)=\frac{d\hat{\Omega}}{dt}(t=0)=a_1=0.9961 \text{ град/сутки.}$$

Отличие этой оценки от «идеального» значения 0.9856 составляет

$$\delta\dot{\Omega}=0.9961-0.9856=0.0105 \text{ град/сутки.} \qquad (11)$$

Оценим влияние погрешностей полуоси (δa) и наклонения (δi) на эволюцию ДВУ. Воспользуемся формулами (1) и (6) для расчета величины $\dot{\Omega}$. Сохраняя уровень погрешностей порядка 10^{-6} и учитывая близость солнечно синхронных орбит к круговым, можем записать

$$\dot{\Omega} = \frac{\delta\Omega}{T_{dr}} = \frac{\delta\Omega}{T} = 2\pi \cdot \frac{3}{2} \cdot c_{20} \cdot \left(\frac{R}{a}\right)^2 \cdot \cos i \cdot \frac{\sqrt{\mu}}{2\pi} \cdot a^{-3/2} = \frac{3}{2} \cdot c_{20} \cdot R^2 \cdot \sqrt{\mu} \cdot \cos i \cdot a^{-7/2} + O\left(10^{-6}\right). \quad (12)$$

На основе этой формулы легко построить частные производные:

$$\partial\dot{\Omega}/\partial a = \dot{\Omega} \cdot \left(-\frac{7}{2} \cdot a^{-1}\right), \quad (13)$$

$$\partial\dot{\Omega}/\partial i = \dot{\Omega} \cdot (-tgi). \quad (14)$$

Эти производные имеют относительную погрешность порядка 10^{-6} и справедливы для любого момента времени. Для КА МЕТЕОР М1 эти производные равны: $\partial\dot{\Omega}/\partial a = \dot{\Omega} \cdot \left(-0.0005\,км^{-1}\right)$ и $\partial\dot{\Omega}/\partial i = \dot{\Omega} \cdot (6.45)$. Особенностью производных является то, что они имеют разные знаки. При известных отклонениях δa и δi от «идеальных» значений отклонение $\delta\dot{\Omega}$ будет равно

$$\delta\dot{\Omega} = \left(\partial\dot{\Omega}/\partial a\right) \cdot \delta a + \left(\partial\dot{\Omega}/\partial i\right) \cdot \delta i. \quad (15)$$

Для ориентировочных расчетов примем, что при выводе КА погрешности по радиусу и бинормали на превышают 1 км. В этом случае $\delta a = 1$ км и $\delta i = \delta a / a = 0.00014$ радиан. Из данных рисунков 1 и 2 видно, что эти оценки погрешностей можно считать гарантированными. Соответствующие отклонения примут значения:

$$\left(\partial\dot{\Omega}/\partial a\right) \cdot \delta a = -0.0005 \quad \text{и} \quad \left(\partial\dot{\Omega}/\partial i\right) \cdot \delta i = 0.0009 \quad \text{[град/сутки]}. \quad (16)$$

Эти отклонения намного меньше приведенного выше отличия (11) реальной скорости от «идеального» значения (0.0105 град/сутки).

Таким образом, наблюдаемые изменения МСВ ДУ не являются следствием погрешностей выведения спутника на орбиту.

IV. Влияние изменения полуоси под действием атмосферного торможения

Данные об эволюции большой полуоси *a* были представлены на рисунке 1. Отклонение текущего значения полуоси от начального аппроксимировано полиномом по времени *t* (в сутках):

$$\delta a(t) = a_1 \cdot t + a_2 \cdot t^2 \approx 2.77 \cdot 10^{-5} \cdot t - 1.5 \cdot 10^{-7} \cdot t^2, \text{ [км]}. \quad (17)$$

Влияние отклонения полуоси на ДВУ характеризуется формулой (13), которая применима для любого момента времени. Поэтому можем записать:

$$\delta\Omega(t) = \left(\partial\dot{\Omega}/\partial a\right)\cdot \delta a(t) \quad (18)$$

На этой основе суммарное отклонение ДВУ на всем интервале t_Σ полета КА может быть вычислено по формуле

$$\Delta\Omega(t_\Sigma) = \left(\partial\dot{\Omega}/\partial a\right)\cdot \int_0^{t_\Sigma} \delta a(t)\cdot dt = \left(\partial\dot{\Omega}/\partial t\right)\cdot\left(\frac{1}{2}a_1\cdot t_\Sigma^2 + \frac{1}{3}a_2\cdot t_\Sigma^3\right). \quad (19)$$

При вычислениях по этой формуле используются значения: $\dot{\Omega}=1$ град/сутки, a=7203 км, t_Σ=2775 дней.

В результате получена оценка: $\Delta\Omega(t_\Sigma) = -0.133^\circ$. Этому отклонению соответствует *уменьшение МСВ ВУ на 0.5 минут.*

Таким образом, наблюдаемое изменение большой полуоси КА МЕТЕОР М1 под действием торможения в атмосфере не оказывает существенного влияния на величину МСВ ВУ.

V. Влияние изменения наклонения орбиты на МСВ ВУ

Данные об эволюции наклонения i были представлены на рисунке 2. Отклонение текущего значения наклонения от начального аппроксимировано линейной зависимостью от времени t (в сутках):

$$\delta i(t) = a_1^{(i)}\cdot t \approx -0.00013\cdot t \text{, [град].} \quad (20)$$

Влияние отклонения наклонения на ДВУ характеризуется формулой (14), которая применима для любого момента времени. Поэтому можем записать:

$$\delta\Omega(t) = \left(\partial\dot{\Omega}/\partial i\right)\cdot \delta i(t)\cdot\frac{\pi}{180} \text{, [град].} \quad (21)$$

На этой основе суммарное отклонение ДВУ на всем интервале t_Σ полета КА может быть вычислено по формуле

$$\Delta\Omega(t_\Sigma) = \left(\partial\dot{\Omega}/\partial i\right)\cdot \int_0^{t_\Sigma} \delta i(t)\cdot dt\cdot\frac{\pi}{180} = a_2\cdot t_\Sigma^2 = \left(\partial\dot{\Omega}/\partial i\right)\cdot\frac{1}{2}a_1^{(i)}\cdot t_\Sigma^2\cdot\frac{\pi}{180}. \quad (22)$$

При вычислениях по этой формуле используются значения: $\dot{\Omega}=1$ град/сутки, *tgi*=-6.45, t_Σ=2775 дней. В результате получена оценка: $\Delta\Omega(t_\Sigma) = -56.3^\circ$. Этому отклонению соответствует *уменьшение МСВ ВУ на 225 мин.*

Таким образом, в результате линейного изменения наклонения орбиты отклонение МСВ ВУ от заданной величины изменятся по параболе и достигает значения **3часа 45 мин.**

Коэффициент $a_2 = a_2^{(\Omega)}$ при квадрате времени в формуле (22) равен

$$a_2^{(\Omega)} = \left(\partial\dot{\Omega}/\partial i\right).\frac{1}{2}a_1^{(i)} \cdot \frac{\pi}{180} = -7.31\times10^{-6} \text{ град/ сутки}^2. \quad (23)$$

Эта оценка согласуется со значением соответствующего коэффициента аппроксимирующего полинома для ДВУ, приведенным в таблице 1 (-7.35×10^{-6}), что свидетельствует о корректности изложенной выше методики.

Полученная оценка изменения МСВ ВУ в результате эволюции наклонения орбиты на интервале полета КА представляется весьма важной и нуждается в дополнительных комментариях.

а) Изменение МСВ ВУ на 3 часа 45 минут приводит к существенному ухудшению условий наблюдения поверхности Земли и, как следствие, к снижению эффективности работы КА.

б) Разработка рекомендаций по обеспечению стабилизации МСВ ВУ является актуальной задачей.

в) Из формул (13) и (14), а также изложенных выше материалов следует, что управление наклонением является наиболее эффективным способом обеспечения стабильности МСВ ВУ.

г) Простейшим способом уменьшения отклонений МСВ ВУ от базовой величины является внесение поправки в начальное значение наклонения [6, 7].

Это положение иллюстрирует рисунок 6. Здесь кривые “dMST METEOR M1” и “dMST Polynom” совпадают с теми, что были приведены выше на рисунке 5. Значение коэффициента $a_1 = a_1^{(\Omega)}$ в этом случае равно $0.0007 \cdot 360/24 = 0.0105$ град/сутки.

Кривая “Parabola” – это графическое представление функции (22), у которой коэффициент a_2 при квадрате времени имеет значение (23). Она построена для условий, когда в момент вывода спутника на орбиту условие (6) строго выполняется. Поэтому в этом случае коэффициент $a_1 = a^{(\Omega)}{}_1 = 0$.

Функция “Correction” построена на основе учета такого коэффициента a_1 в линейной составляющей полинома, который обеспечивает равенство по модулю максимальных отклонений МСВ ВУ разных знаков. Нетрудно показать, что это оптимальное значение равно

$$a_{1,opt}^{(\Omega)} = 2\cdot\left(\sqrt{2}-1\right)\cdot a_2 \cdot t_\Sigma = 0.01685, \text{ [град/сутки]}. \quad (24)$$

Отличие данного оптимального (24) значения коэффициента от того, который использовался при построении функции “dMST Polynom” ($a_1 = a_1^{(\Omega)}$ =0.0105) составляет

$$\delta a_1^{(\Omega)} = 0.01685 - 0.0105 = 0.00635, \text{ [град/ сутки].} \qquad (25)$$

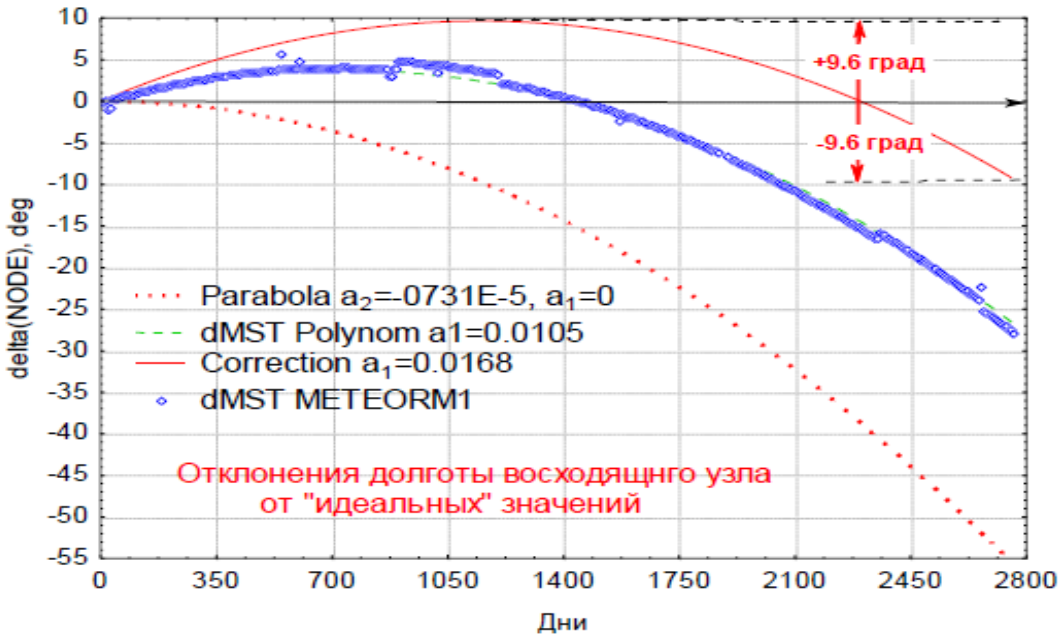

Рисунок 6: Отклонения ДВУ с учетом и без учета коррекции наклонения

Оценку (25) можно применить для определения поправки в наклонение, которая обеспечивает минимизацию отклонений МСВ ВУ от базовой величины. Для этого используется формула (21). С учетом формулы (14) и связи вариаций ДВУ и наклонения получим поправку к фактическому наклонению в момент выведения:

$$\delta i(0) = \frac{\delta a_1^{(\Omega)}}{\left(\partial\dot{\Omega}/\partial i\right)} \cdot \frac{180}{\pi} = \frac{0.00635}{1 \cdot 6.45} \cdot \frac{180}{\pi} = 0.056$$

градусов. (26)

Это как раз та поправка к наклонению спутника в момент его выведения, которую надо было бы учесть для оптимизации МВС ВУ на интервале полета в 2775 дней. Естественно, что возможность реализации такой поправки зависит от точности выведения КА на орбиту.

Приведенное выше значение коэффициента $a_1 = a_1^{(\Omega)}$=0.0105 град/сутки, соответствующее кривым “dMST METEOR M1” и “dMST Polynom”, позволяет определить отличие фактического наклонения в момент вывода от «идеального», при котором строго выполняется условие (6). Применяя для этих условий формулу (26), получим:

$$\delta i(0)_0 = \frac{a_1^{(\Omega)}}{\left(\partial\dot{\Omega}/\partial i\right)}\cdot\frac{180}{\pi} = \frac{0.0105}{1\cdot 6.45}\cdot\frac{180}{\pi} = 0.093$$

градусов. (27)

Именно на эту величину отличалось наклонение при выводе от того, при котором строго выполняется условие (6). Из данных рисунка 6 видно, что при фактическом наклонении в момент вывода обеспечивалась минимизация отклонений МСВ ВУ (не более 16 мин) на 5-ти летнем интервале его полета.

В заключение раздела заметим, что на данном этапе не рассмотрена природа существенного отклонения, наблюдаемого МСВ ВУ от базовой величины, которое изменятся по параболе и достигает значения 3часа 45 мин на 7-ми летнем интервале времени.

VI. Влияние погрешностей модели гравитационного поля Земли

В разделе 1 отмечалось, что формула (1), положенная в основу проектирования параметров КА на солнечно синхронных орбитах, имеет погрешность порядка 10^{-6} при прогнозе движения на 1 виток. Естественно, что с увеличением интервала прогноза погрешности растут. Поэтому для более точного и надежного выбора параметров КА используются современные модели движения спутников. Такого рода модели являются уникальными компьютерными программами, учитывающими многопараметрические модели гравитационного поля Земли и другие возмущающие факторы. При долговременных прогнозах они требуют существенных затрат машинного времени. Тем не менее, современные модели движения спутников не являются абсолютно точными. Погрешности возникают в связи с отсутствием полной информации о реальных возмущающих факторах.

В монографии [9] изложена методика оценки погрешностей прогнозирования движения спутников в гравитационном поле Земли. В результате применения опорной орбиты и линеаризации исходных дифференциальных уравнений движения спутника построены дифференциальные уравнения для отклонений от опорного вектора состояния (погрешностей)

$$\frac{d\delta x}{dt} = A(t)\cdot\delta x + B(t)\cdot q(t), \quad (28)$$

Рассматриваются возмущающие ускорения *q(t)*, которые не учитываются при интегрировании исходных уравнений (шум системы). Важным является то, что этот шум существенно отличается от белого шума, т.е. имеется корреляция значений шума в разные моменты времени. Построены статистические характеристики случайного процесса

$$M\, q(t)\cdot q^{T}(\tau) = K_q(t,\tau). \tag{29}$$

Расчет корреляционной матрицы погрешностей вектора состояния при прогнозировании движения производится по формуле

$$K_x(t) = \int_{t_0}^{t}\int_{t_0}^{t} U(t,\xi)\cdot B(\xi)\cdot K_q(\xi,\eta)\cdot B(\eta)^T\cdot U(t,\eta)^T\cdot d\xi\cdot d\eta \tag{30}$$

,

Матрица $U(t,t_0)$ называется фундаментальной матрицей решений уравнений (28), а также переходной матрицей.

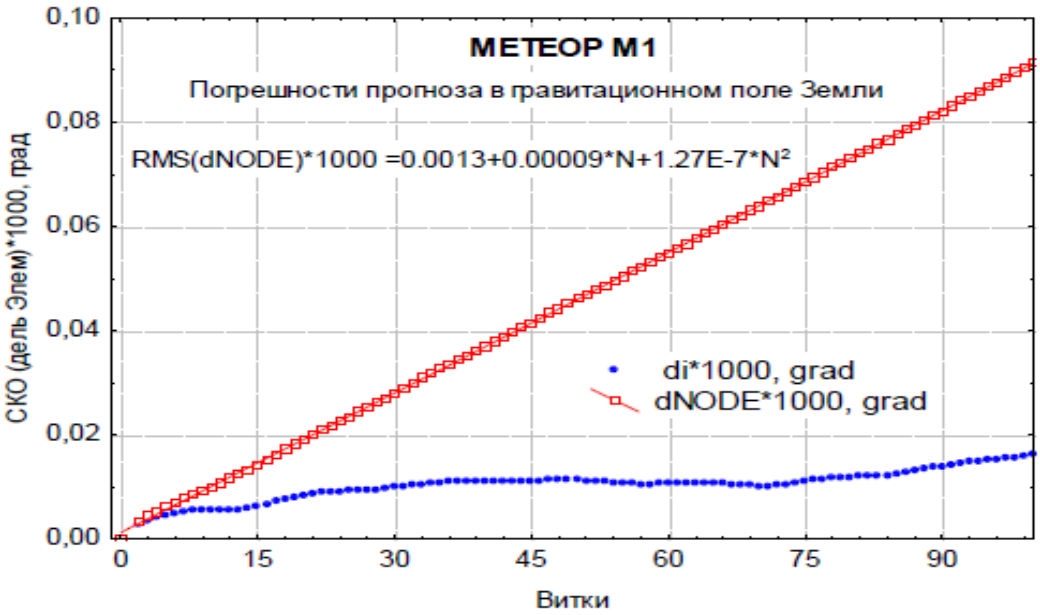

Рисунок 7: СКО погрешностей прогнозирования ДВУ и наклонения

Проведение вычислений по формуле (30) является весьма трудоемкой операцией. Она выполняется с использованием программы “Prilog_C.pas”, достаточно подробное описание которой изложено в монографии [9]. На рисунке 7 представлены результаты расчета СКО погрешностей прогнозирования ДВУ и наклонения КА МОНИТОР М1 на недельном интервале времени. Эти оценки построены для модели движения, в которой учитываются коэффициенты разложений гравитационного потенциала до 100-го порядка.

Рассмотрим результаты для ДВУ (NODE). На недельном интервале СКО погрешности имеет монотонно нарастающий характер и достигает значения 0.09×10^{-3} °. При оценке погрешностей прогноза на 7 лет (2775 дней) можно использовать допущение о сохранении полученной закономерности. В результате получим

$$\sigma\Omega(2775) \approx \sigma\Omega(7)\cdot 2775/7 = 0.09\cdot10^{-3}\cdot396 = 3.5\cdot10^{-7} = 0.033^{\circ}. \tag{31}$$

Этой оценке соответствует погрешность прогноза ДВУ не более 0.1°. Данное значение намного меньше оценок погрешностей, обусловленных другими источниками. Погрешности прогнозирования наклонения мы не рассматриваем потому, что они намного меньше и в гравитационном поле Земли не имеют вековой составляющей.

Таким образом, погрешности используемой модели гравитационного поля Земли не являются источником наблюдаемых отклонений МСВ ВУ от заданной величины.

VII. Влияние лунно-солнечных возмущений

Для анализа эволюции орбиты КА МЕТЕОР М1 использовалась современная компьютерная модель движения спутников. Ее достаточно подробное описание изложено в статьях [10-12]. Ниже на рисунках 8 – 10 представлены основные результаты расчетов.

На рисунках 8 и 9 представлены данные об эволюции периода: реальные значения и результаты прогноза (назад).

Естественно, что оценки реальных изменений периода совпадают с соответствующими данными рисунка 1. Расчетное значение периода при прогнозе с учетом возмущений от Луны и Солнца изменилось на 0.023 минуты, а при прогнозе без учета этих возмущений – на 0.026 мин. Разница составила 0.003 мин. В соответствии с материалами раздела 4 такие изменения периода (и соответствующие изменения полуоси) не оказывают существенного влияния на величину МСВ ВУ.

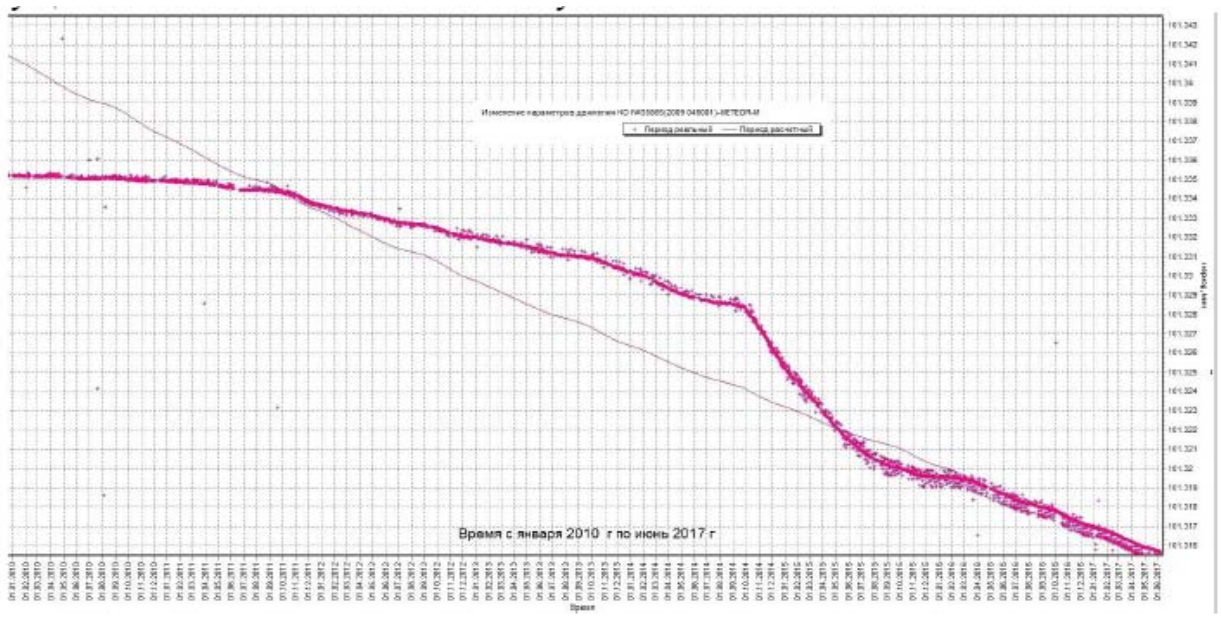

Рисунок 8: Период. Прогноз без учета Луны и Солнца

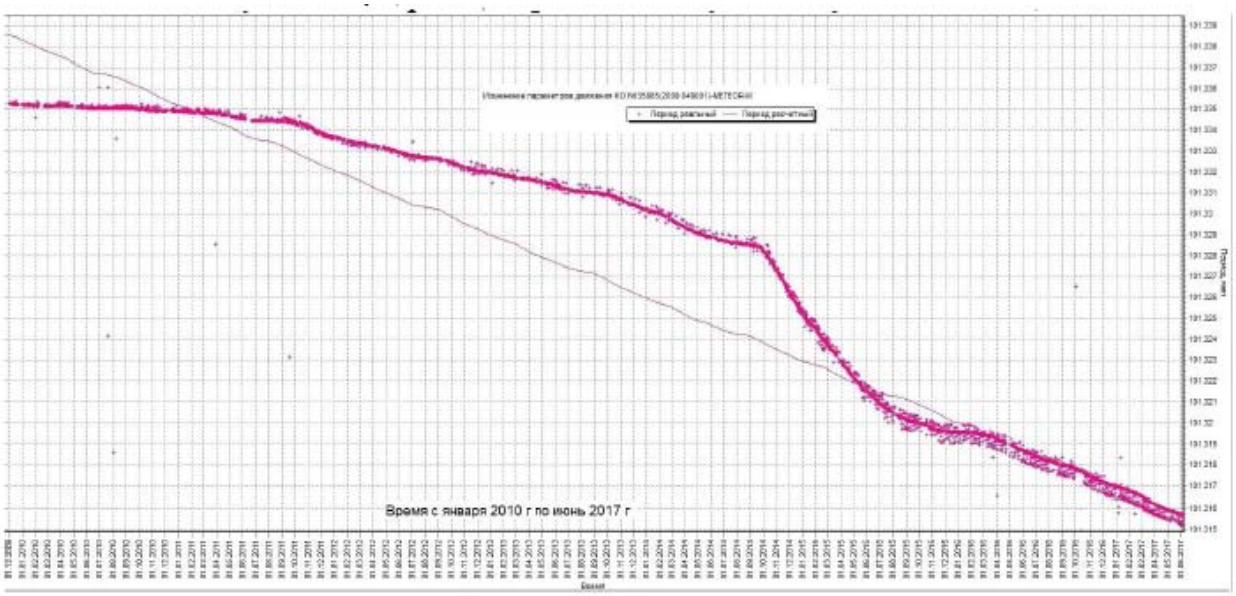

Рисунок 9: Период. Прогноз с учетом Луны и Солнца

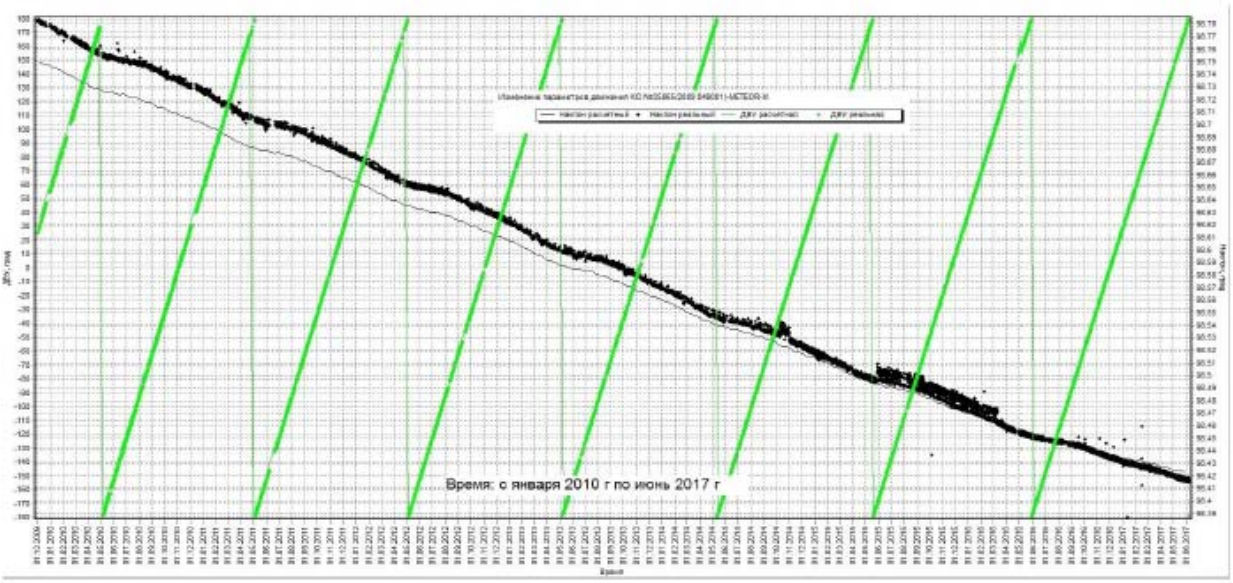

Рисунок 10: Реальные и прогнозные данные о наклонении

Здесь представлены данные об эволюции наклонения орбиты: реальные значения и результаты прогноза (назад) с учетом гравитационных возмущений от Луны и Солнца. Из этих результатов четко видно, что учет лунно-солнечных возмущений приводит к достаточно хорошему согласию расчетных и экспериментальных данных. В изменении наклонения преобладает вековая составляющая. Имеются также относительно небольшая составляющая с периодом 1 год. Суммарное изменения наклонения за время полета КА составило: 0.36° по данным измерений и 0.33° по результатам прогноза.

Таким образом, основной причиной наблюдаемых вариаций МСВ ВУ является изменение наклонения КА под действием лунно-солнечных гравитационных возмущений. Указанное изменение наклонения приводит в свою очередь к отклонению возмущений ДВУ первого порядка (1) от заданного значения. Эти отклонения имеют второй порядок малости (c_{20}^2), но они на интервале полета КА накапливаются, что и приводит к наблюдаемым отклонениям МСВ ВУ от заданного значения.

VIII. Прогнозирование наклонения и МСВ ВУ

Выше в разделе 7 выявление причин отклонений МСВ ВУ от заданного значения было выполнено двумя способами: на основе анализа известных орбитальных данных и на основе применения современной модели движения спутников. Важным результатом этого анализа является подтверждение факта, что основной причиной возникновения квадратичной составляющей в эволюции МСВ ВУ является изменение наклонения КА в результате действия лунно-солнечных гравитационных возмущений. Оценки вековой составляющей в эволюции наклонения, найденные двумя способами, практически совпали, а именно, в соответствии с выражением (20) значение коэффициента при вековой составляющей равно

$$a_1^{(i)} \approx -0.00013 \text{ градусов в сутки.} \qquad (32)$$

При проектировании солнечно-синхронных орбит надежным способом определения вековой компоненты в эволюции наклонения является применение современной компьютерной модели движения, учитывающей влияние лунно-солнечной гравитации и другие существенные возмущающие факторы. Такого рода компьютерные модели являются уникальными. Их применение требует существенных затрат машинного времени, особенно при рассмотрении ряда проектных вариантов.

В статье [7] изложен простой аналитический способ расчета вековой составляющей в эволюции наклонения. Ниже приведен фрагмент текста этой статьи.

В работе [3] приведены формулы для расчета величины δi для общего случая орбит, однако, учитывая особенности ССО, для анализа удобно соотношение для δi в зависимости от угла χ. Такое соотношение получено нами в работе [6]:

$$\delta i_S = \frac{4\mu_S r^3 \sin 2\chi \sin i_0}{\mu \rho_0^3}, \qquad (4)$$

где μ_S, μ — гравитационные постоянные Солнца и Земли, ρ_0 — среднее расстояние Земля — Солнце.

Как следует из выражения (4), знак δi_S определяется знаком функции $\sin 2\chi$. На рис. 4 приведены изменения наклонения Δi_S за пять лет в зависимости от номинального МСВ ВУ для разных высот.

Здесь: δi_S - возмущение за виток (в радианах), χ - разность ДВУ и прямого восхождения Солнца. При вычислениях по данной формуле использовались следующие значения аргументов:

$\mu_S = 1.327 \times 10^{11}$ км^3/с^2,
$r = 7210$ км,
$\chi = 315°$,
$i_0 = 98.77°$,
$\mu = 3.986 \times 10^5$ км^3/с^2,
$\rho_0 = 150 \times 10^6$ км.

В результате получена оценка

$\delta i_S = -1.464 \times 10^{-7}$ радиан.

При периоде КА 101.33 мин. этой оценке соответствует вековое возмущение

$$a_1^{[5]} \approx -0.000119 \text{ градусов в сутки.} \qquad (33)$$

Данная оценка на 9% меньше оценки (32), что свидетельствует о приемлемом согласии численного (более точного) и аналитического (приближенного) решений. Этот факт является важным. Он подтверждает возможность применения обоих способов для расчета вековой составляющей наклонения.

Применим результаты, изложенные в статье [7], для анализа эволюции МСВ ВУ КА МЕТЕОР М1. Из определения (2) МСВ ВУ следует, что

$$\sin(2\chi) = \sin(2\eta). \qquad (34)$$

С использованием обозначений формулы (20) дифференциальное уравнение для отклонений наклонения может быть записано так

$$\frac{di}{dt} = a_1^{(i)} \cdot \frac{\sin(2\eta)}{\sin(2\eta_0)}. \tag{35}$$

Ниже на рисунке 11 представлены значения отношения $\sin(2\eta)/\sin(2\eta_0)$. Они построены по данным рисунка 5 для МСВ ДУ (η).

Рисунок 11: Эволюция отношения синусов

Из данных этого рисунка видно, что отношение синусов стало сильно уменьшаться после ≈1700 дня и достигло значения 0.53. В соответствии с уравнением (35) это привело к уменьшению модуля отрицательной скорости изменения наклонения и, в итоге, - к увеличению наклонения по сравнению с закономерностью его изменения на предшествующем интервале времени. Суммарный эффект изменения отношения синусов характеризуется площадью, которая выделена на рисунке розовым цветом. Площадь этой области равна S=180 дней. Соответствующее изменение наклонения составило

$$\delta i = -a_1^{(i)} \cdot S = 0.00013 \cdot 180 = 0.023\ ^\circ. \tag{36}$$

Эта величина фактически совпадает с оценкой отклонений наклонения от полинома, которая была приведена в комментариях к рисунку 2 (0.022°).

Таким образом, найдена причина отклонений значений наклонения от линейной зависимости, которые были выявлены по данным рисунка 2. Эта причина заключается во влиянии изменения МСВ ВУ на эволюцию наклонения, которая характеризуется дифференциальным уравнением (35). Из этого результата следует важный вывод, что в изменении наклонения имеется существенная нелинейная составляющая. При длительных сроках существования КА ее надо учитывать.

Имеется возможность дополнить уравнение (35) дифференциальным уравнением для отклонений МСВ ВУ от базового значения ($\delta\eta = \eta - \eta_0$), которое строится на основе соотношения (21). С использованием выражения (14) для частной производной это уравнение принимает вид

$$\frac{d\delta\eta}{dt} = \frac{d\delta\Omega}{dt} = \left(\partial\delta\dot{\Omega}/\partial i\right).\frac{di}{dt} = -\dot{\Omega}\cdot tg(i)\frac{di}{dt}. \qquad (37)$$

Здесь $\dot{\Omega}\approx 1°$ в сутки.

Таким образом, для наклонения орбиты и МСВ ВУ построена система из двух дифференциальных уравнений (35) и (37). Ее решение позволяет спрогнозировать значения МСВ ВУ. Эта система уравнений является исключительно простой. Она построена с учетом обоснованного выше вывода, что другие факторы не оказывают существенного влияния на МСВ ВУ. Ниже приведен фрагмент программы, которая выполняет решение построенной системы уравнений.

```
CONST
   a1=-0.000141;
   i0=98.77*pi/180;
   eta0=20.93;
   di0=0.108*pi/180;              {  radian  }
-----------------------------------------
di:=di0;
eta:=eta0*360/24;                 {  degree  }
for t:=1 to tmax do begin
sin2eta:=sin(2*eta*pi/180);
di:=di-a1*sin2eta*pi/180;         {  radian  }
it:=i0+di;
eta:=eta-tan(it)*di;              {  degree  }
                    end;
```

Исходными данными для решения упрощенной системы уравнений являются:

- Оценка коэффициента $a_1^{(i)}$ вековой составляющей наклонения;
- Базовое наклонение орбиты i_0;
- Базовое значение МСВ ВУ η_0;
- Поправка к базовому значению наклонения при запуске δi_0.

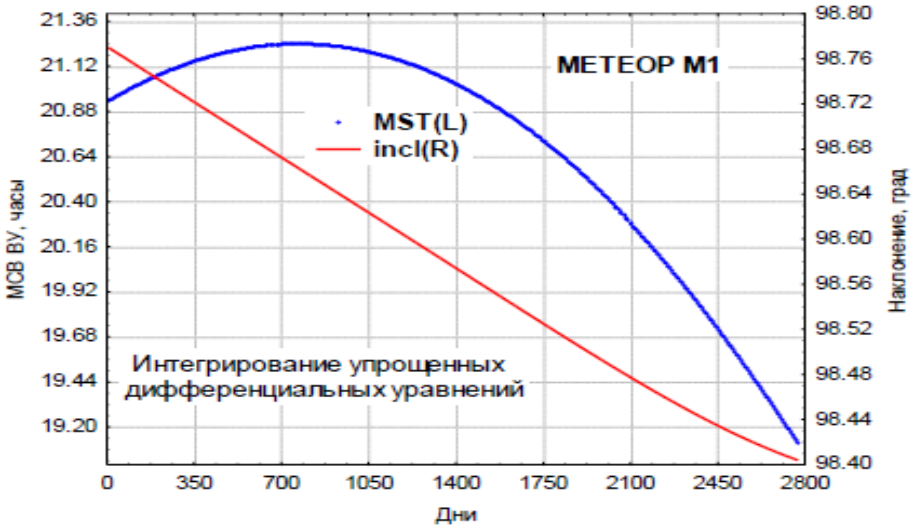

Рисунок 12: Прогноз МСВ ВУ и наклонения.

На рисунке 12 представлен пример прогноза МСВ ВУ и наклонения, полученного с использованием упрощенной системы уравнений. Из данных этого рисунка видно, что результаты интегрирования упрощенной системы уравнений хорошо согласуются с реальными данными об эволюции этих параметров, которые были представлены выше на рисунках 2 и 5.

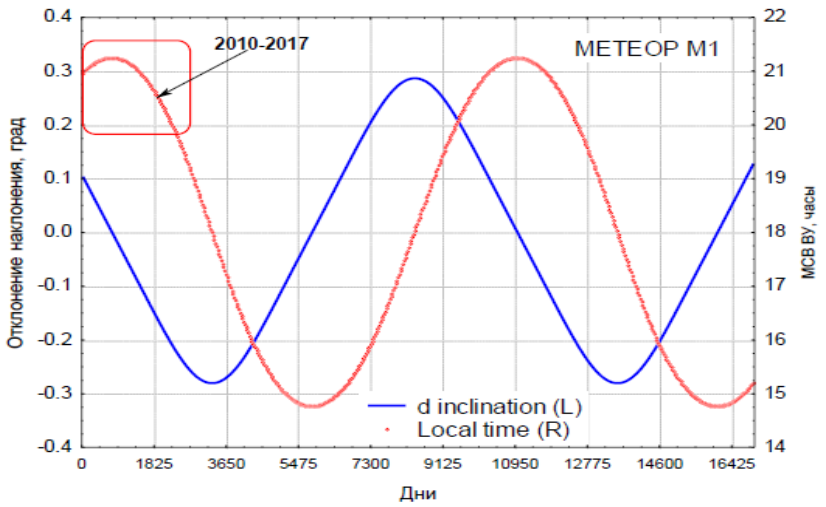

Рисунок 13: Долгосрочный прогноз наклонения и МСВ ВУ

Интересным является ответ на вопрос о закономерностях изменения наклонения и МСВ ВУ на больших интервалах времени. Результаты интегрирования упрощенной системы уравнений на 45-ти летнем интервале представлены на рисунке 13. Из этих данных четко виден долгопериодический характер отклонений наклонения и МСВ ВУ. Период составляет ≈28 лет, а амплитуды равны: ≈0.3° у наклонения и ≈3 часа у МСВ ВУ. Этот вывод согласуется с результатами применения современной компьютерной модели движения спутников, которые представлены на рисунке 14.

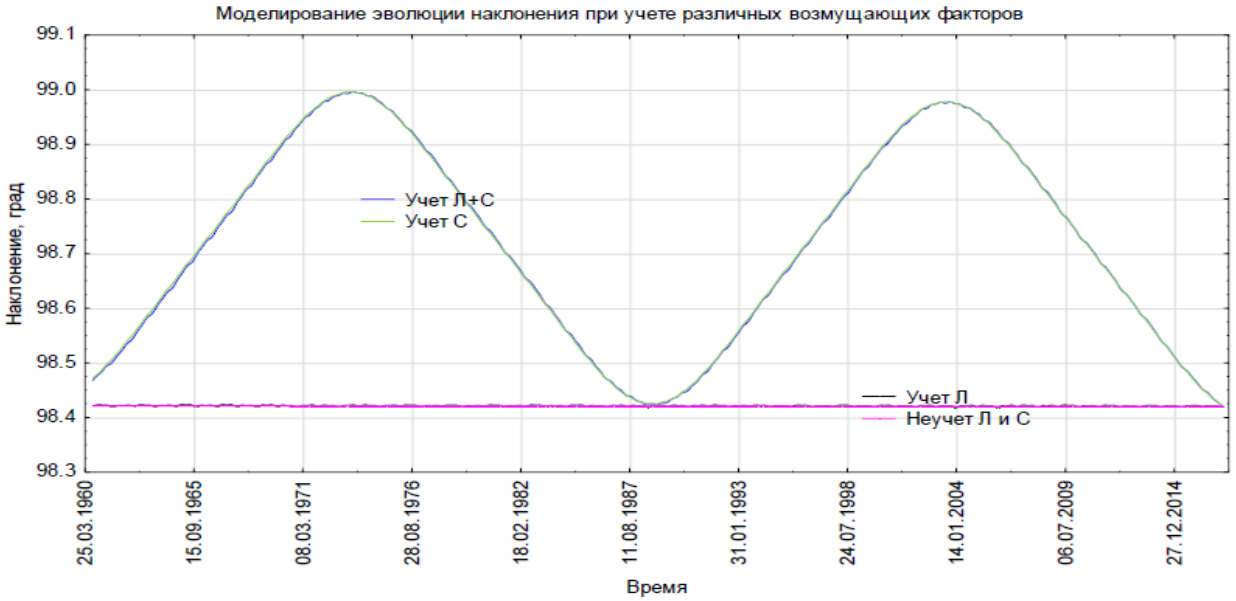

Рисунок 14: Долгосрочное прогнозирование наклонения с учетом и без учета лунно-солнечных возмущений.

Здесь оценки периода и амплитуды вариаций согласуются с данными предыдущего рисунка. Кроме того, видно, что единственной причиной долгопериодических вариаций наклонения являются солнечные гравитационные возмущения.

Выводы

1. На основе орбитальных данных КА МЕТЕОР М1 рассмотрено 5 возможных причин отклонений местного солнечного времени восходящего узла (МСВ ВУ) на интервале полета от начального значения:
   - погрешности начальных условий;
   - изменение большой полуоси орбиты;
   - изменение наклонения;
   - влияние погрешностей модели гравитационного поля Земли;
   - влияние лунно-солнечных возмущений.
2. Установлено, что основной причиной отклонений МСВ ВУ является изменение наклонения КА. Указанное изменение приводит в свою очередь к отклонению возмущений ДВУ первого порядка от заданного значения. Эти отклонения имеют второй порядок малости, но они на интервале полета КА накапливаются, что и приводит к существенным отклонениям МСВ ВУ от заданного значения.
3. Изменение наклонения орбиты КА происходит в результате действия солнечных гравитационных возмущений. Это приводит к тому, что отклонение МСВ ВУ от заданной величины изменяется нелинейно по времени и для КА МЕТЕОР М1 достигает значения 3часа 45 мин на 7-

ми летнем интервале времени. Это значение зависит от величины коэффициента при квадратичной составляющей ($a_2^{(\Omega)}$).

4. Простейшим способом уменьшения отклонений МСВ ВУ от заданного значения является внесение поправки в начальное наклонение орбиты при выводе КА на орбиту. Приведена формула для расчета этой поправки, которая зависит только от коэффициента $a_2^{(\Omega)}$. Применение данной поправки для КА МЕТЕОР М1 привело бы к уменьшению отклонений МСВ ВУ от заданного значения в 5-6 раз.
5. Расчет коэффициента $a_2^{(\Omega)}$ на основе корректного учета солнечных возмущений является необходимым этапом проектирования солнечно-синхронных орбит.
6. Выполнено сравнение результатов анализа эволюции орбиты КА МЕТЕОР М1 с соответствующими материалами статьи [7] «Обеспечение максимальной стабильности условий дистанционного зондирования Земли без коррекции орбиты». Установлено приемлемое согласие соответствующих результатов.
7. Опубликованная в статье [7] зависимость для возмущений наклонения применена для составления упрощенной системы дифференциальных уравнений, описывающих эволюцию наклонения и МСВ ВУ. Результаты интегрирования этой системы уравнений хорошо согласуются с реальными данными и результатами долгосрочного прогнозирования параметров орбиты КА МЕТЕОР М1. Показано, что вариации наклонения имеют долгопериодический характер с периодом ≈28 лет и амплитудой ≈0.3°.

Литература

1. А.А. Чернов, Г.М. Чернявский. Орбиты спутников дистанционного зондирования Земли. М.: Радио и связь, 2004, 200 с.
2. П.Е. Эльясберг. Введение в теорию полета искусственных спутников Земли. М.: Изд-во «НАУКА», 1965.
3. D.A. Vallado. Fundamentals of Astrodynamics and Applications. Published jointly by Microcosm Press and Kluwer Academic Publishers, 2004.
4. А.И. Назаренко и Б.С. Скребушевский. Эволюция и устойчивость спутниковых систем. Изд-во «*МАШИНОСТРОЕНИЕ*», 1981.
5. www.space-track.org.
6. В.И. Иванова, А.Д. Шептун. Минимизация ухода солнечного времени восходящего узла солнечносинхронной орбиты с учетом точности выведения. Авиационно-космическая техника и технология, 2015, № 2.

7. В.И. Иванова, А.Д. Шептун. Обеспечение максимальной стабильности условий дистанционного зондирования Земли без коррекции орбиты. *Космична наука і технология*. 2016. Т. 22, № 2.
8. Д.Ю. Виноградов, Е.А. Давыдов. Методика формирования устойчивых околокруговых солнечно-синхронных орбит при длительных сроках существования космического аппарата. Инженерный журнал: наука и инновации # 6·2017.
9. А.И. Назаренко. Погрешности прогнозирования движения спутников в гравитационном поле Земли, Москва, Институт космических исследований РАН, 2010.
10. Юрасов В.С. Применение универсального численно-аналитического метода для прогнозирования движения спутников в атмосфере. Труды совещания «Проблемы физики верхней атмосферы и динамики искусственных спутников Земли», проведенного в г. Ужгород 25-28 июня 1985 года, Сборник «Наблюдения искусственных небесных тел», №82. Астросовет АН СССР, Москва, 1987.
11. Юрасов В.С., Амелина Т.А. Применение универсального численно-аналитического метода для прогнозирования движения геостационарных спутников. Труды конференции «Программы наблюдения высокоорбитальных спутников и небесных тел солнечной системы», Санкт-Петербург, 1994.
12. Yurasov, V.S. ”Universal Semianalytic Satellite Motion Propagation Method,” Proceedings of the Second U.S.-Russian Space Surveillance Workshop, Poznan, Poland, July 1996.

Благодарность.

Автор признателен к.т.н. В.С. Юрасову и к.т.н. А.А. Чернову за участие в подготовке исходных данных в обсуждении полученных результатов.

This page is intentionally left blank

Global Journal of Researches in Engineering: I
Numerical Methods
Volume 20 Issue 1 Version 1.0 Year 2020
Type: Double Blind Peer Reviewed International Research Journal
Publisher: Global Journals
Online ISSN: 2249-4596 & Print ISSN: 0975-5861

Research of Airplane Waste Disposal System Tank Characteristics by Method of Numerical Simulation

By S.V. Medvediev

Abstract- The modern design enhances the role of preliminary research in aircraft development. Reducing iterations in the process of making conceptual decisions, along with the requirements for the project, and obtaining the most reliable models of the future system is one of the important tasks facing a design engineer. The article considers one of the life support systems designed to satisfy the physiological needs of the human body - a vacuum-type waste disposal system. One of the critical elements of the system is a waste storage tank. An important stage in the design of a tank is the determination of its weight and size characteristics in the early stages of development. The tank filling process has a significant influence on these characteristics which is crucial for the placement of equipment in it. The aim of the work presented in the article is to study the process of filling the tank with the help of numerical simulation methods. The results obtained in the process of numerical modeling make it possible, at the preliminary design stage, to evaluate the required air gap, to determine the total volume of the waste tank.

Keywords: vacuum, waste tank, waste disposal system, numerical methods, free surface model.

GJRE-I Classification: FOR Code: 091307

Strictly as per the compliance and regulations of:

Research of Airplane Waste Disposal System Tank Characteristics by Method of Numerical Simulation

S.V. Medvediev

Abstract- The modern design enhances the role of preliminary research in aircraft development. Reducing iterations in the process of making conceptual decisions, along with the requirements for the project, and obtaining the most reliable models of the future system is one of the important tasks facing a design engineer. The article considers one of the life support systems designed to satisfy the physiological needs of the human body - a vacuum-type waste disposal system. One of the critical elements of the system is a waste storage tank. An important stage in the design of a tank is the determination of its weight and size characteristics in the early stages of development. The tank filling process has a significant influence on these characteristics which is crucial for the placement of equipment in it. The aim of the work presented in the article is to study the process of filling the tank with the help of numerical simulation methods. The results obtained in the process of numerical modeling make it possible, at the preliminary design stage, to evaluate the required air gap, to determine the total volume of the waste tank.

Keywords: vacuum, waste tank, waste disposal system, numerical methods, free surface model.

I. Introduction

The modern design of any system on board an aircraft is a complex, multifactorial, ramified task consisting in finding the optimal ratio of parameters.

Continuous complication and, as a consequence, higher cost of aviation equipment entails a significant increase in costs from errors made at the design stage and, therefore, requires a sharp increase in the quality of design and development work.

Strengthening the systemic principle in the general approach to the creation of aviation technology has increased the role of external design in the development of aircraft, and raised the importance of the stages of preliminary and conceptual design. The role of pre-design studies related to the substantiation of the general concept and the technical appearance of the new aircraft planned to be created has also significantly increased [1].

In this regard, obtaining reliable results at these stages becomes an urgent task that the design engineer has to solve when developing the system.

Author: Life Support Systems Department, Antonov Design Bureau, Kyiv, Ukraine. e-mail: s.medvedev.v@gmail.com

To implement the requirements for ensuring safety and comfort, various life support systems are installed on board a modern aircraft, one of which is a waste disposal system designed to ensure the physiological needs of the human body. On board the aircraft, different types of action systems are used, but preference is given to a vacuum-type action system due to a number of factors (economy, environmental friendliness, comfort).

The development of vacuum-type systems on civilian aircraft begins its history in the mid-70s of the twentieth century. So, in 1975, inventor James Kemper patented a vacuum waste disposal system, the principle of which is used today in modern passenger aircraft [2]. The first vacuum toilet was installed on Boeing aircraft in 1982.

The principle of the system is that rarefied air is the driving force for moving waste from the toilet to the tank. When flying at low altitudes and on the ground, a vacuum generator is used that provides the pressure differential; at high altitude flight, a natural differential is used between the cabin and the atmosphere. The waste tank is connected to the atmosphere and in the system is present atmospheric pressure till the flush valve on the toilet, Fig. 1. Pressing the pushbutton opens the flush valve, and waste from the toilet bowl moves to the tank. The waste enters the tank and is stored there during the flight and does not enter the atmosphere. Tank service takes place on the ground.

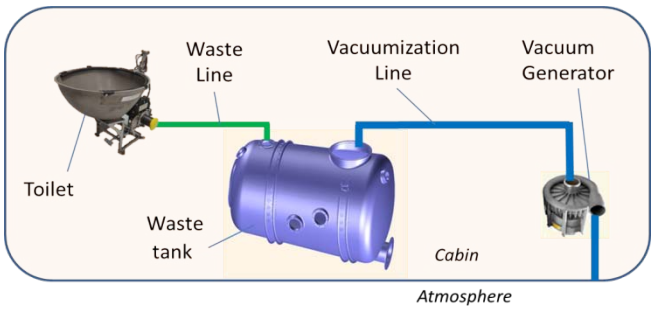

Fig. 1: Simplified waste disposal system

One of the important requirements for developing a waste disposal system is the requirement for tightness. The tightness of the system is determined not only by the tightness of the joints of the pipeline

network, but also by the requirement that the waste be stored in the tank without further movement along the vacuumization subsystem. If the developed system design does not comply with this requirement, the following negative consequences may occur:

- The formation of significant ice formation on the outer surface of the aircraft at the exit point of the vacuumization pipelines, which after separation can damage the structure of the aircraft;
- Waste getting onto the vacuum generator;
- Waste getting onto the surface of the airfield during parking, which entails the imposition of significant fines by the airport administration.

One of the system elements is a waste storage tank. When designing a tank, you must determine:

- Maximum amount of waste that will be stored in the tank;
- Configuration of the waste braking device (at the entrance to the tank);
- Tank configuration acceptable for placement on an airplane;
- Filling capacity of the waste tank (gas-dynamic calculation);
- Strength calculation of the tank.

The total tank volume consists of the waste volume and the air gap volume above the waste.

At the stage of research work, when conducting full-scale tests is extremely difficult and requires significant costs, the urgent task is to determine the volume of the tank that is needed to store a given amount of waste, as well as its configuration, taking into account the zonal distribution of equipment in the aircraft compartments. The required volume of the tank largely depends on the process of its filling, the study of which is presented below.

II. Research

The study of the tank filling process is performed by numerical methods. Non-stationary hydraulic processes are considered in the interaction of a two-phase waste-air environment, which are separated by a free surface.

a) Mathematical model of unsteady hydraulic processes with a free surface

An article [3] presents an analysis of existing mathematical models for free-flow flow modeling, which shows that the most widely used method is the Volume of Fluid method. This method uses the fluid volume fraction function α. This function takes a value of 0 if the medium is filled with gas and 1 if it is filled with liquid. At the boundary of the phase section, the value of the function lies in the range $0 < \alpha < 1$. The density, pressure and viscosity of the media under consideration are from the following equations:

$$\rho = \rho_1\alpha + (1-\alpha)\rho_2$$
$$p = p_1\alpha + (1-\alpha)p_2$$
$$\mu = \mu_1\alpha + (1-\mu)\rho_2$$

According to [4], taking into account [5] and using the SST turbulence model, the equations describing non-stationary gas-dynamic processes in two-dimensional formulation with the available free surface are as follows:

$$\frac{\partial Q_i}{\partial t} + \frac{\partial F_i}{\partial x} + \frac{\partial G_i}{\partial y} = \frac{\partial R_i}{\partial x} + \frac{\partial S_i}{\partial y} + M_i$$

where,

$$Q = \begin{bmatrix} \rho \\ \rho u \\ \rho v \\ e \\ \rho k \\ \rho \omega \\ \alpha \end{bmatrix}, \quad F = \begin{bmatrix} \rho u \\ \rho u^2 + p \\ \rho u v \\ u(e+p) \\ \rho u k \\ \rho u \omega \\ 0 \end{bmatrix}, \quad G = \begin{bmatrix} \rho v \\ \rho u v \\ \rho v^2 + p \\ v(e+p) \\ \rho v k \\ \rho v \omega \\ 0 \end{bmatrix},$$

$$M = \begin{bmatrix} 0 \\ 0 \\ \rho g \\ \rho F \cdot V \\ P_k - \beta^* \rho k \omega \\ \alpha_{SST} \rho S^2 - \beta \rho \omega^2 + A_x^\omega + A_y^\omega \\ 0 \end{bmatrix},$$

$$R = \begin{bmatrix} 0 \\ \tau_{xx} \\ \tau_{xy} \\ q_x + u\tau_{xx} + v\tau_{xy} \\ D_x^k \\ D_x^\omega \\ \alpha u \end{bmatrix}, \quad S = \begin{bmatrix} 0 \\ \tau_{xy} \\ \tau_{yy} \\ q_y + u\tau_{xy} + v\tau_{yy} \\ D_y^k \\ D_y^\omega \\ \alpha v \end{bmatrix} \quad (1)$$

where the coefficient i - number of the medium, ρ - density, u and v - projections of the velocity vector at the coordinates x and y, respectively, p - pressure, $V = (u, v)^T$ - velocity vector, $F = (f_x, f_y)^T$ - density distribution of bulk forces, τ - elements of the viscous stress tensor, k - kinetic energy of turbulence, ω - turbulence specific dissipation rate, P_k - the generation of kinetic energy of turbulence.

The first equation is the continuity equation, the second and third equation is the momentum conservation equation by x and y coordinates, the fourth equation is the energy conservation equation, the fifth

and sixth equation is the SST turbulence model, and the seventh is the transfer equation for the function α.

These equations completing the equation of state, as well as the equation of the condition of dynamic equilibrium at the interface:

$$p = \frac{R}{m}\rho T$$

$$(\tau_1 - \tau_2)e = (p_1 - p_2 + \sigma K)e$$

$$u_1 = u_2\,,\ v_1 = v_2$$

where,

e - single normal vector, K - surface curvature, and σ - surface tension coefficient.

The elements of the stress tensor are as follows:

$$\tau_{xx} = 2\mu_e \frac{\partial u}{\partial x} - \frac{2}{3}\mu_e\left(\frac{\partial u}{\partial x} + \frac{\partial v}{\partial y}\right)$$

$$\tau_{yy} = 2\mu_e \frac{\partial v}{\partial y} - \frac{2}{3}\mu_e\left(\frac{\partial u}{\partial x} + \frac{\partial v}{\partial y}\right)$$

$$\tau_{xy} = \mu_e\left(\frac{\partial u}{\partial y} + \frac{\partial v}{\partial x}\right)$$

Where μ_e - effective coefficient of viscosity:

$$\mu_e = \mu + \mu_t$$

μ - dynamic viscosity coefficient, μ_t - turbulent viscosity coefficient.

$$\mu_t = \rho C_\mu \frac{k^2}{\omega}$$

For turbulence model equations:

$$D_x^k = (\mu + \sigma_k \mu_t)\frac{\partial k}{\partial x},\ D_y^k = (\mu + \sigma_k \mu_t)\frac{\partial k}{\partial y}$$

$$D_x^\omega = (\mu + \sigma_\varepsilon \mu_t)\frac{\partial \omega}{\partial x},\ D_y^\omega = (\mu + \sigma_\varepsilon \mu_t)\frac{\partial \omega}{\partial y}$$

$$A_x^\omega = 2(1 - F_1)\rho\sigma_{\omega 2}\frac{1}{\omega}\frac{\partial k}{\partial x}\frac{\partial \omega}{\partial x},$$

$$A_y^\omega = 2(1 - F_1)\rho\sigma_{\omega 2}\frac{1}{\omega}\frac{\partial k}{\partial y}\frac{\partial \omega}{\partial y}$$

A detailed description of the coefficients included in the turbulence equation is given in [6 - 7].

Preparing and solving equation systems (1) is carried out with the help of software package numerical modeling Ansys CFX [8].

This software package is capable of solving complex problems with many effects. Two-phase flow studies using the numerical simulation method are considered in [9-11].

b) Investigation of the storage tank filling processes with numerical simulation

Since the design of aircraft systems is conducted in a confined space, the tanks of the waste disposal system can take many forms. The object of research is a conditional tank for storage of waste, cylindrical shape, Fig. 2. For research was proposed and developed tanks with a diameter of 0.5 to 10 m.
The three-dimensional tank model is made using NX 8.5 software.

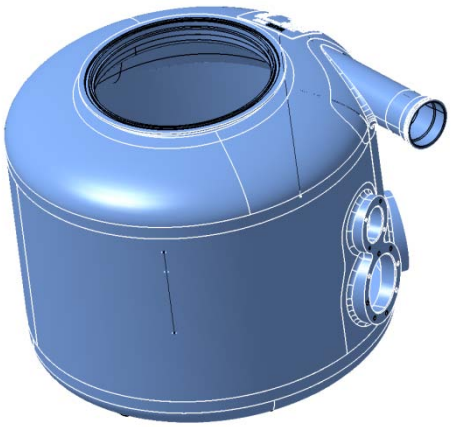

Fig. 2: Waste tank 3D model

Construction of the estimated grid made using ICEM software package. The tank volume is broken by an unstructured tetrahedral grid using the Robust (octree) method, Fig. 3. The maximum height of the grid element is 20 mm for the inlet and 7 mm for the outlet.

A two-phase air-water environment separated by a free surface is considered. The air is presented as perfect gas. Model of turbulence is SST.

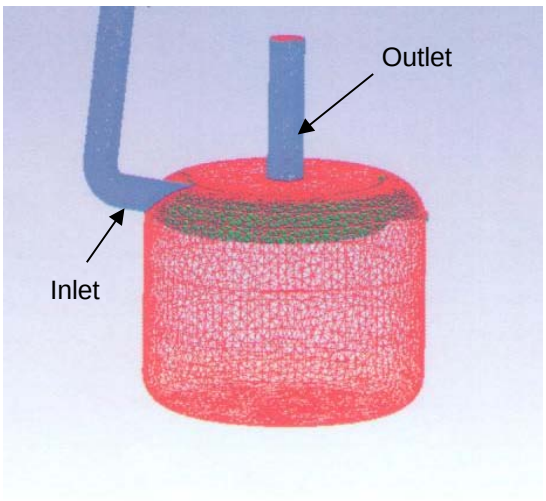

Fig. 3: Waste tank design grid

Flow simulation was performed in a non-stationary setting (Transient). The simulation time of the

tank filling process is 2 sec., and includes the following stages of the system units operation: operation of the vacuum generator from 0 to 1 s, opening of the waste receiver flap from 1 to 2 s, getting water to the tank.

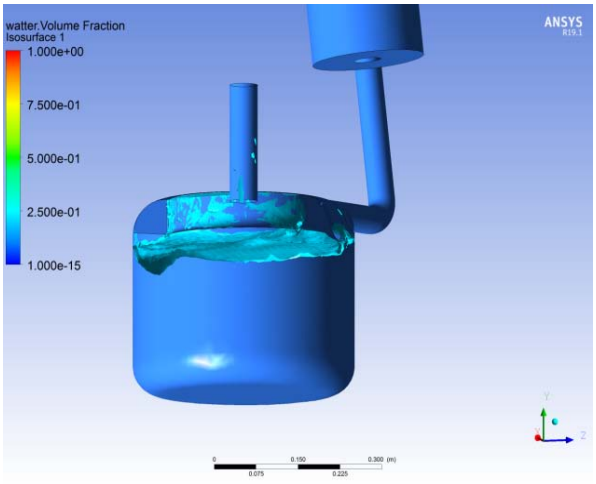

Fig. 4: The state of the mid-fracture surface after the end of the evacuation process

At the initial time in the tank there is a certain level of water (waste), the height of which is equal to y_h [12].

The purpose of the study is to determine the dependence of the amount of water in the outlet pipe on the amount of air gap between the water and the upper wall of the tank.

The initial values of the velocity vector are 0 m/s. The initial pressure value is given by the P_{ref} function:

$$P_{ref} = \begin{cases} P_w\_at\_y \prec y_h \\ P_{in}\_at\_y \geq y_h \end{cases}$$

where,

P_{in} = 1,0332 kg / cm^2 - air pressure;

P_w - water pressure, which is determined by the function:

$$P_w = P_{in} + (y_h - y) \cdot 1000 \cdot g$$

The initial temperature value of the two phases is t = 22 ° C. The volume ratio of each phase in the calculation region is determined by the WVF function:

$$WVF_{air} = \begin{cases} 0\_at\_y \prec y_h \\ 1\_at\_y \geq y_h \end{cases}$$

$$WVF_{water} = 1 - WVF_{air}$$

The results showed that the stability of the calculation is ensured at time step values of 0.001 sec. and less.

Fig. 5 presents the dependence of the volume of water in the outlet pipeline (maximum possible is 1) on the size of the gap between the waste surface and the upper wall of the tank (H) at different diameters of the waste tank (free surface area).

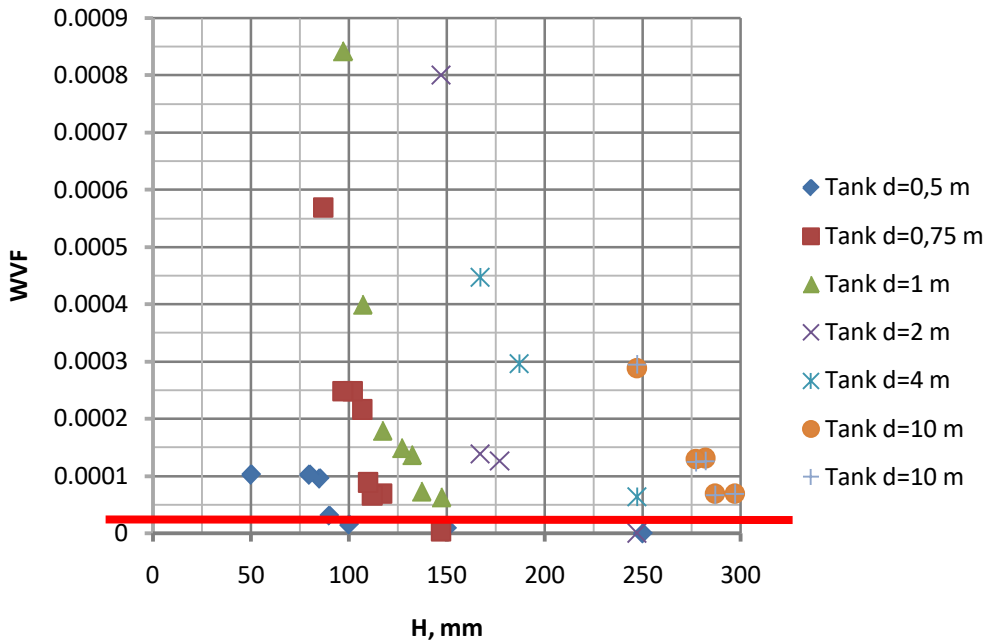

Fig. 5: Dependence of the volume amount of water in the outlet on the size of the air gap at different diameters of the waste tank

The study of the process of vacuumization of the system has made it possible to establish that with the reduction of the thickness of the air gap there is a significant intensification of the separation of water

particles (waste) from the surface due to the higher velocities of air flows in the gap, which occur during the process of vacuumization of the system. Further reduction of the thickness of the air gap leads to the formation of waves on the free surface, resulting in significant splashing of water and which can increase even when a new portion of waste enters the tank.

The results of numerical simulation of the process of filling the tank made it possible to determine the dependence of the coefficient of bulk water content in the outlet pipeline on different values of the initial water level in the tank.

If the concentration of the water particle is exceeded, we take 5 grams of fluid per drain (volume of water not more than 0.0001), in which the presence of water in the outlet channel becomes visually noticeable. The obtained numerical simulation data for tanks of different diameters made it possible to deduce the allowable minimum height of the air gap between the waste surface to the upper wall of the tank from the tank diameter, which is presented in Fig. 6, 7.

The first approximation dependency allows for the required tank dimensions (which are determined by taking into account the maximum amount of waste and the place of installation of the tank) to estimate the required additional volume of air gap, which will ensure no waste in the outlet.

The study of the process of vacuumization of the system has made it possible to establish that with the reduction of the thickness of the air gap there is a significant intensification of the separation of water particles (waste) from the surface due to the higher velocities of air flows in the gap, which occur during the process of vacuumization of the system. Further reduction of the thickness of the air gap leads to the formation of waves on the free surface, resulting in significant splashing of water and which can increase even when a new portion of waste enters the tank.

For a real aircraft, the range of tank diameters ranges from 0.5 m to 2 m, Fig. 6.

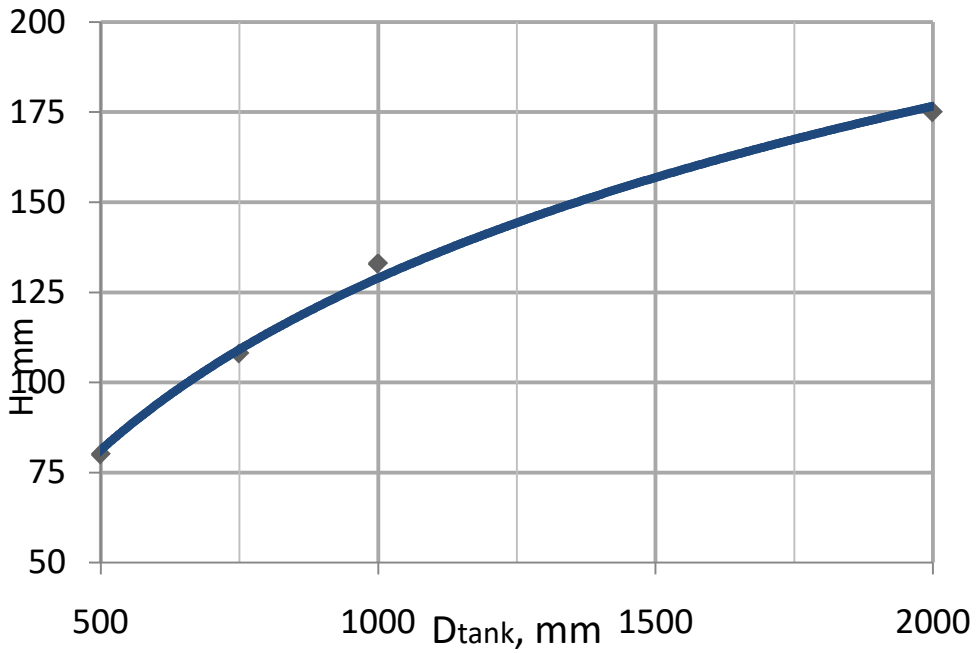

Fig. 6: Dependence of the volume amount of water in the outlet on the size of the air gap for diameters 0.5 m to 2 m

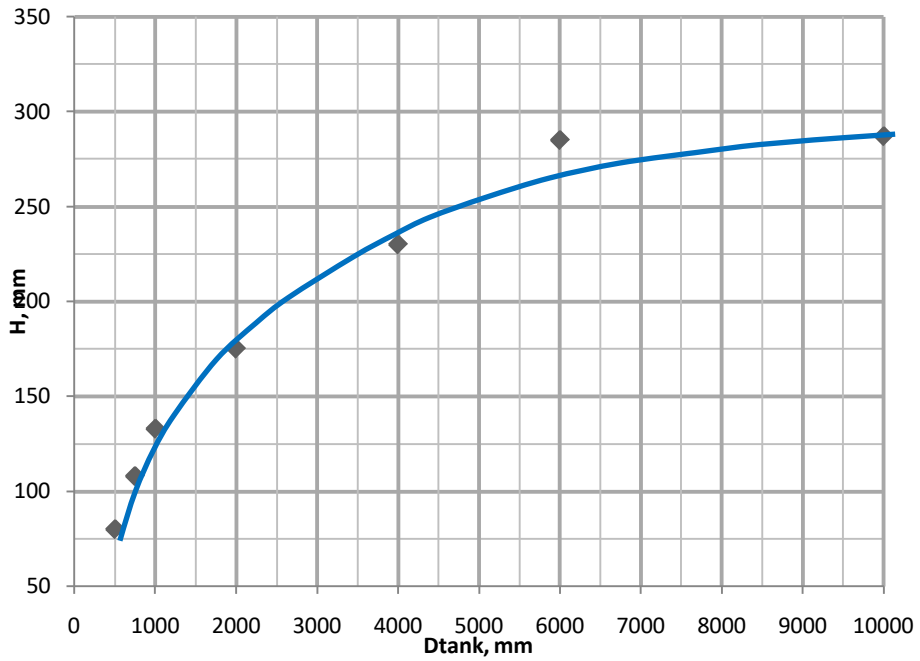

Fig. 7: Dependence of the volume amount of water in the outlet on the size of the air gap at different diameters of the waste tank

III. Conclusion

The study of the processes of evacuation and filling of the storage tank used of waste disposal system showed that the entry of waste into the vacuumization line is due to a significant intensification of the process of waste separation particles at a decrease in the thickness of the air gap during the process vacuumization.

According to the results of numerical studies, the minimum permissible value of the air gap thickness between the waste surface and the tank is determined for different tank diameters, at which the waste concentration in the vacuum line will not exceed critical values.

References Références Referencias

1. 1. Staack, I., Raghu Chaitanya.M.V, Berry, P., Melin, T., Amadori, K., Jouannet, C., Lundström, D., Petter Krus, P. (2012). Parametric aircraft conceptual design space. 28th Congress of the International Council of the Aeronautical Sciences, (1), 211-320.
2. Recirculating toilet system for use in aircraft or the like. https://patents.google.com/patent/US3922730A/en
3. Shalanin, V.A. (2010). Free surface flow modeling methods. Young Scientist, 2(106), 258-261. (in Russ.)
4. Glushko, G. S., Ivanov, I. E., Kryukov, I. A. (2010). Computational method for turbulent supersonic flows. Math Models Comput Simul, (2), 407–422. https://doi.org/10.1134/S2070048210040010
5. Minakov, A. V., Gavrilov, A. A., Dekterev, A. A. (2009). Numerical simulation unsteady flow with free surface by using of VOF method. Bulletin of the Siberian State Aerospace University named after Academician M.F. Reshetnev, (2), 9-13. (in Russ.)
6. Scherbakov, M. A., Yun, A.A., Krilov B.A. (2009). Comparative analysis of turbulence models using the scientific code "FASTEST-3D" and the commercial package ANSYS CFX. MAI Bulletin, (5), 116–122. (in Russ.)
7. Menter, F. R., Kuntz, M., Langtry, R. (2003). Ten Years of Industrial Experience with the SST Turbulence Model. Turbulence heat and mass transfer, (4), 625-632.
8. ANSYS CFX. http://www.ansys.com
9. Shams, M., Raeini, A.Q., Blunt, M.J., Bijeljic, B. (2018). A numerical model of two-phase flow at the micro-scale using the volume-of-fluid method. Journal of Computational Physics, (357), 159-182. https://doi.org/10.1016/j.jcp.2017.12.027
10. Hirt, C.W., Nichols, B.D. (1981). Volume of fluid (VOF) method for the dynamics of free boundaries. Journal of Computational Physics, 39(1), 201-225. https://doi.org/10.1016/0021-9991(81)90145-5
11. Menter, F.R. (1994). Two-Equation Eddy-Viscosity Turbulence Models for Engineering Applications. AIAA Journal, 32(8), 1598-1605. https://doi.org/10.2514/3.12149
12. Medvediev, S. V. (2019). Airplane waste disposal system tank designing using numerical modeling and experimental bench results. Journal of Engineering Sciences, 6(2), E41-E46, https://doi.org10.21272/jes.2019.6(2).e7

Global Journal of Researches in Engineering: I
Numerical Methods
Volume 20 Issue 1 Version 1.0 Year 2020
Type: Double Blind Peer Reviewed International Research Journal
Publisher: Global Journals
Online ISSN: 2249-4596 & Print ISSN: 0975-5861

Application of Numerical Methods for New Estimate of Rheology Constants in the 2D Computer Model of the Mantle Wedge Thermal Convection as a Possible Physical Mechanism of Hydrocarbons Transport

By S.V.Gavrilov & A.L.Kharitonov

Abstract- For both Newtonian and non-Newtonian mantle rheology laws, the numerical model of the 2D dissipationdriven mantle wedge thermal convection is constructed for the case of subduction of the Black sea micro-plate under the Crimea peninsula with the account taken of the phase transitions in the mantle. The horizontal extent of the positive 2D heat flux anomaly zone localized in the rear of the Crimea mountains is shown to correspond to the model subduction velocity ≥10 mm per year for the water content of one weight %. For Newtonian rheology upwelling convective flow transporting heat to the Earth's surface is formed at the subduction velocity of ~102 mm per year, which appears too excessive and probably evidence of that the non-Newtonian rheology dominates in the mantle wedge. In the case of non- Newtonian rheology, the velocity in convective vortices in the mantle wedge exceeds 10 m per year. The subduction velocity may be less than 10 mm a year for the water content in the mantle wedge over ~1 weight %. The upwelling convective flow is shown to transport mantle hydrocarbons to the Earth's surface since the zone of oil and gas accumulation coincides with the 2D one of heat flux anomaly.

Keywords: 2D thermal convection, Newtonian and non-newtonian rheology constants, phase transitions, hydrocarbons transport.

GJRE-I Classification: FOR Code: 090408

Strictly as per the compliance and regulations of:

Application of Numerical Methods for New Estimate of Rheology Constants in the 2D Computer Model of the Mantle Wedge Thermal Convection as a Possible Physical Mechanism of Hydrocarbons Transport

S.V.Gavrilov[α] & A.L.Kharitonov[σ]

Abstract- For both Newtonian and non-Newtonian mantle rheology laws, the numerical model of the 2D dissipation-driven mantle wedge thermal convection is constructed for the case of subduction of the Black sea micro-plate under the Crimea peninsula with the account taken of the phase transitions in the mantle. The horizontal extent of the positive 2D heat flux anomaly zone localized in the rear of the Crimea mountains is shown to correspond to the model subduction velocity ≥10 mm per year for the water content of one weight %. For Newtonian rheology upwelling convective flow transporting heat to the Earth's surface is formed at the subduction velocity of ~10^2 mm per year, which appears too excessive and probably evidence of that the non-Newtonian rheology dominates in the mantle wedge. In the case of non-Newtonian rheology, the velocity in convective vortices in the mantle wedge exceeds []10 m per year. The subduction velocity may be less than 10 mm a year for the water content in the mantle wedge over ~1 weight %. The upwelling convective flow is shown to transport mantle hydrocarbons to the Earth's surface since the zone of oil and gas accumulation coincides with the 2D one of heat flux anomaly.

Keywords: 2D thermal convection, Newtonian and non-Newtonian rheology constants, phase transitions, hydrocarbons transport.

I. Introduction

Interaction of the lithospheric plates in the Crimea-Caucasus region leads to the thrusting of the Black Sea micro-plate under the Crimea peninsula (under the Scythian plate) [Nimetulayeva, 2004]. As a consequence, the seismic focal plane is formed along which the Crimea ascends as the result of seismic jerks. The velocities of vertical uplift of the Crimea mountains and sinking of the near-Crimean area of the Black Sea micro-plate equal to ~4 mm per year and ~10 mm per year, respectively. Mountainous Crimea is a folded fault region being a part of the Alps-Himalaya-Indonesia belt [Yudin, 2001].

Author α: Schmidt Institute of Physics of the Earth, Russian Academy of Sciences, RAS, Troitsk, RF.
Author σ: Pushkov Institute of Terrestrial Magnetism, Ionosphere and Radio Wave Propagation, RAS, Troitsk, RF. e-mail: ahariton@izmiran.ru

In [Ushakov et al., 1977] the subduction velocity of the Black Sea micro-plate under the Crimea peninsula is estimated of ~1 mm per year as the best fit to the observed sedimentary layer distribution. Other estimations are unknown to the knowledge of the authors. However the obtained estimate of ~1 mm per year appears to be an underestimate, being not correspondent to the vertical velocities of ~4 and ~10 mm per year of Mountainous Crimea and the Black Sea micro-plate.

According to [Gavrilov, 2014; Gerya, 2011; Gerya et al., 2006] two types of dissipation driven small-scale thermal convection in the mantle wedge are possible, viz. 3D finger-like convective jets, raising to volcanic chain, and 2D transversal Karig vortices, aligned perpendicularly to subduction. These two types of convection are shown to be spatially separated due to the pressure and temperature dependence of mantle effective viscosity, the Karig vortices, if any of them formed, being located behind the volcanic arc [Gavrilov, 2014]. Despite the firmly established localization of the seismic focal plane there is just a single definite conclusion concerning the velocity of subduction of the Black Sea micro-plate [Ushakov et al., 1977]. It is not completely clear if volcanism played a substantial role in forming Mountainous Crimea, or the mountains are of a purely thrust-and-fold origin. [Nimetulayeva, 2004] indicates the contradictory statements on the Crimean volcanism to have been published, however in Fig.2.4 in [Nimetulayeva, 2004], the volcanic eruption in the Mountainous Crimea is depicted. The abovementioned picture is reproduced here in Fig.1 with the convective vortices drawn additionally. It is worth assuming the two heat flux anomaly maxima observed in the south of the Crimea peninsula [Smirnov, 1980; Nimetulayaeva, 2004, Fig.2.4] owe their origin to respectively 3D and 2D upward convective heat transfer from the mantle wedge to the Earth's surface (see Fig.1 of this paper). The latter 2D maximum located in the rear of the Mountainous Crimea is much greater as compared to the former 3D maximum located in the Mountainous Crimea. The 2D

heat flux anomaly maximum is associated with the 2D upward convective flow in the mantle wedge. Numerical modeling of 2D mantle wedge thermal convection occurring in the form of the Karig vortices and presumably transporting heat to the Earth's surface in the rear of the Mountainous Crimea allows judging about the mean velocity of subduction of the Black Sea micro-plate under the Crimea peninsula as well as about the rheological mantle parameters. The horizontal extent of the 2D heat flux anomaly in the rear of the Mountainous Crimea is shown to correspond to the mean subduction velocity >10 mm per year for the observed subduction angle 15°. Numerical convection models accounting for the effects of phase transitions as well as the pressure, temperature, and viscous stresses viscosity dependence fit in well with the heat flux observational data in the case of non-Newtonian mantle rheology at the mean concentration of water in the mantle wedge of ~1 wt. %.

II. Algorithm and Computation Complexity

Thermo-mechanical model of the mantle wedge between the base of the overlying Scythian plate and the upper surface of the Black Sea micro-plate subducting under the Scythian one with a velocity V at an angle β is obtained for the infinite Prandtl number fluid as the solution of non-dimensional 2D hydrodynamic equations in the Boussinesq approximation for the stream-function Ψ and temperature T.

$$(\partial_{zz}^2-\partial_{xx}^2)\eta(\partial_{zz}^2-\partial_{xx}^2)\psi+4\partial_{xz}^2\eta\partial_{xz}^2\psi=RaT_x-Ra^{(410)}\Gamma_x^{(410)}-Ra^{(660)}\Gamma_x^{(660)}, \quad (1)$$

$$\partial_t T=\Delta T-\psi_z T_x+\psi_x T_z+\frac{Di}{Ra}\times\frac{\tau_{ik}^2}{2\eta}+Q, \quad (2)$$

Here η is dynamic viscosity, ∂ and indices denote partial derivatives with respect to coordinates x (horizontal), z (vertical) and time t, Δ is the Laplace operator, $\Gamma^{(410)}$ and $\Gamma^{(660)}$ are volume ratios of the heavy phase at the 410 km and 660 km phase boundaries, the velocity components V_x and V_z are expressed through Ψ as

$$V_x=\psi_z,\ V_z=-\psi_x, \quad (3)$$

while non-dimensional Rayleigh number Ra, phase numbers $Ra^{(410)}$, $Ra^{(660)}$ and dissipative number Di are

$$Ra=\frac{\alpha\rho g d^3 T_1}{\bar{\eta}\chi}=5.55\times10^8,\ Ra^{(410)}=\frac{\delta\rho^{(410)}gd^3}{\bar{\eta}\chi}=6.6\times10^8,$$

$$Ra^{(660)}=\frac{\delta\rho^{(660)}gd^3}{\bar{\eta}\chi}=8.5\times10^8,\ Di=\frac{\alpha g d}{c_p}=0.165, \quad (4)$$

where $\alpha=3\cdot10^{-5}$ K^{-1} is the thermal expansion coefficient, $\rho=3.3$ g·cm^{-3} is the density, g is gravity acceleration, $c_p=1.2\times10^3$ J·kg^{-1}·K^{-1} is specific heat capacity at constant pressure, $T_1=1950$ K is the temperature at the base of the mantle transition zone (MTZ) at depth 660 km regarded the lower boundary of the model domain, $Q=6.25\cdot10^{-4}$ mW·m^{-3} is the volumetric heat generation in the crust, τ_{ik} is the viscous stress tensor, $d=660$ km is the vertical dimension of the modeled domain, $\bar{\eta}=10^{18}$ Pa·s is the viscosity scaling factor, $\chi=1$ mm^2·s^{-1} is thermal diffusivity, $\delta\rho^{(410)}=0.07\rho$ and $\delta\rho^{(660)}=0.09\rho$ are the density changes at the 410 km and 660 km phase boundaries respectively. In (1), (2) the scaling factors for time t, coordinates x and z, stresses τ_{ik}, and the stream-function Ψ are $d^2\cdot\chi^{-1}$, d, $\bar{\eta}\chi\cdot d^{-2}$, and χ respectively. Assuming rheology be linear for the diffusion creep deformation mechanism dominating in the mantle at depths over ~200 km [Billen & Hirth, 2005], we accept the temperature- and lithostatic pressure p dependent viscosity as [Zharkov, 2019]

$$\eta = \frac{\mu}{2A}\left(\frac{h}{b^*}\right)^m \exp\frac{E^* + pV^*}{RT}, \quad (5)$$

Where for "wet" olivine $A=5.3\times10^{15}$ s^{-1}, $m=2.5$, the grain size h $=10^{-1}$ – 10 mm, $b^*=5\times10^{-8}$ cm is the Burgers vector [Zharkov, 2003], $E^*=240$ kJ·mol^{-1} is activation energy, $V^*=5\times10^3$ mm^3·mol^{-1} is activation volume, μ $=300$ GPa is the shear modulus normalizing factor, R is the gas constant. At the chosen constants and the grain size $h=1.6$ mm, non-dimensional viscosity also denoted η is

$$\eta = 5.0\times10^{-7}\exp\frac{14.8 + 6.72(1-z)}{T}, \quad (6)$$

Where T is non-dimensional temperature, non-dimensional z normalized by d is pointing upwards from the MTZ base and x is pointing against subduction along the MTZ base. The aspect ratio of the model domain is 1:3.7 thus the subduction angle being $\beta \approx 15^o$ if subduction is assumed to take place along the model domain diagonal. Non-dimensional trial subduction velocity $V=45$ mm·a^{-1} normalized by $\chi \cdot d^{-1}$ equals $V=0.938\cdot10^3$, i.e. non-dimensional velocity components of subducting Black Sea micro-plate are $V_x = -0.898\cdot10^3$ and $V_z = -0.268\cdot10^3$.

To check as to how the estimate of the velocity of subduction of the Black Sea micro-plate is sensitive to the accepted linear rheological law here we make extra computations for non-Newtonian rheology, in which case the viscosity formulae (5)–

$$\eta = \frac{1}{2AC_w^r\tau^{n-1}}\left(\frac{h}{b^*}\right)^m \exp\frac{E^* + pV^*}{RT}, \quad (7)$$

Where according to [Trubitsyn, 2012] for "wet" olivine $n=3$, $r=1.2$, $m=0$, $\boxed{\tau = (\tau_{ik}^2)^{1/2}}$, $E^*=480$ kJ·mol^{-1}, $V^*=11\times10^3$ mm^3·mol^{-1}, $A=10^2$ c$^{-1}\times$(MPa)$^{-n}$, $C_w > 10^{-3}$ for "wet" olivine is the weight water concentration (in %%). It should be noted the constants in (7) vary considerably in the papers referred to by [Trubitsyn, 2012] and heretofore, we gave averaged values of constants. At $C_w = 10^{-3}$ on accounting for

$$\tau_{ik}^2 = 4\eta^2[(\psi_{zz} - \psi_{xx})^2/2 + 2\psi_{xz}^2] \quad (8)$$

non-dimensional viscosity is

$$\eta = \frac{1.00}{[(\psi_{zz} - \psi_{xx})^2/2 + 2\psi_{xz}^2]^{1/3}}\times\exp\frac{100 + 5.0\times(1-z)}{T}. \quad (9)$$

Following [Trubitsyn & Trubitsyn, 2014] we assume the phase functions $\Gamma^{(l)}$ as

$$\Gamma^{(l)} = \frac{1}{2}\left(1 - th\frac{z - z^{(l)}(T)}{w^{(l)}}\right),\ z^{(l)}(T) = z_0^{(l)} - \frac{\gamma^{(l)}}{\rho g}(T - T_0^{(l)}), \quad (10)$$

where the signs are changed as z-axis is pointing upwards, $z^{(l)}(T)$ is the depth of the l-th phase transition (l=410, 660), $z_0^{(l)}$ and $T_0^{(l)}$ are the averaged depth and temperature of the l-th phase transition, $\gamma^{(410)} = 3$ MPa×K^{-1} and $\gamma^{(660)} = -3$ MPa×K^{-1} are the slopes of the phase equilibrium curves, $w^{(l)}$ is the characteristic thickness of the l-th phase transition, $T_0^{(410)} = 1800$ K, $T_0^{(660)} = 1950$ K are the mean

mean phase transition temperatures. The heats of phase transitions are neglected in (2) as insignificant in the case of developed convection as in [Trubitsyn & Trubitsyn, 2014]. From (10) it follows

$$\Gamma_x^{(l)} = -\frac{\gamma^{(l)}}{2\rho g w^{(l)}} ch^{-2} \frac{z - z_0^{(l)} + \gamma^{(l)}(T - T_0^{(l)})/\rho g}{w^{(l)}} \times T_x , \quad (11)$$

Where from it is clear the phase transition with $\gamma^{(l)} > 0$ facilitates convection (at *l*=410), while the phase transition with $\gamma^{(l)} < 0$ hinders convection (at *l*=660). In non-dimensional form $z_0^{(410)}$ =0.38, $z_0^{(660)}$ =0, $w^{(l)}$ =0.05, $\gamma^{(410)}$ =2.5×10^9, $\gamma^{(660)}$ = –2.5×10^9, $T_0^{(410)}$ = 0.92, $T_0^{(660)}$ =1, and in (1).

$$\Gamma_x^{(l)} = -\frac{\delta\rho^{(l)}}{\rho Ra^{(l)}} \frac{\gamma^{(l)}}{2w^{(l)}} ch^{-2} \frac{z - z_0^{(l)} - \gamma^{(l)} \frac{\delta\rho^{(l)}}{\rho Ra^{(l)}} (T - T_0^{(l)})}{w^{(l)}} \times T_x . \quad (12)$$

Equations (1)–(2) are solved for the isothermal horizontal and insolated vertical boundaries regarded no-slip impenetrable ones except for the "windows" for in- and outgoing subducting plate, where the plate velocity is specified. Vertical boundary distant from subduction zone is assumed penetrable at right angle, the latter boundary condition appears not too imposing in the case of very flat subduction. *Q* in (2) is non-zero in the continental and oceanic crust 40 and 7 *km* thick. Initial vertical boundaries temperature is calculated for the half-space cooling model for 10^9 yr and 10^8 yr for Scythian (continental) and Black Sea (oceanic) plates respectively.

III. Results and Discussion

Assuming the second (more remote from the trench) heat flux *q* maximum in Fig.1 appears above the convective flow, ascending to C_2 point in Fig.1, and the convection cell dimension is equal to the two adjacent *q* minima separation (i.e. the *q* minima are located above the descending convective flows) we can estimate the convection cell dimension as ~250 km.

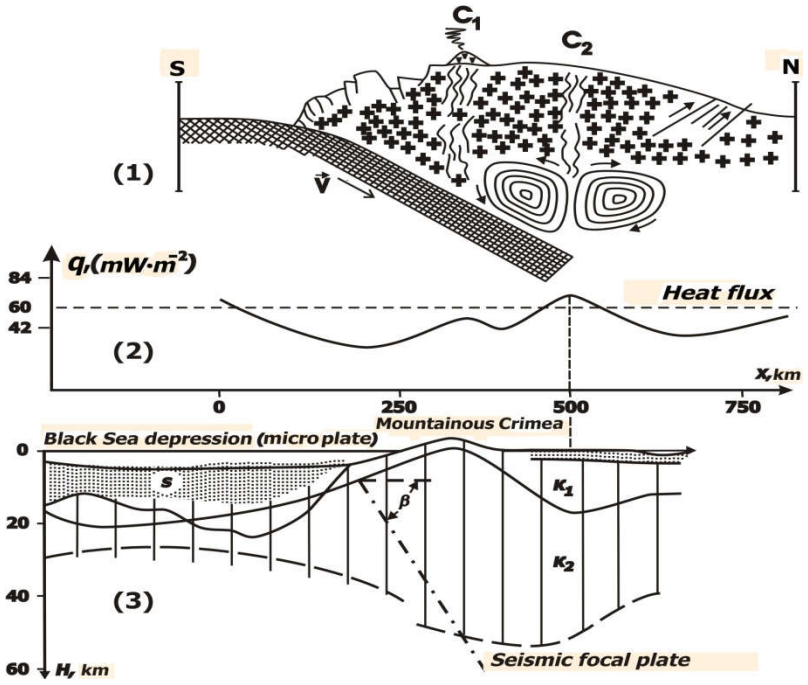

Fig. 1: Schematic cross section of the region of subduction of the Black Sea micro-plate under the Crimea peninsula (Scythian plate) C_1 and C_2 are the zones of 3D and 2D convective flows ascending to the heat flux *q* maxima, the whirls under C_2 are the 2D Karig convective flows. (2) – Heat flux *q* in the south of Crimea. (3) – The Black Sea micro-plate subducting under the Crimea peninsula and the seismic focal plane shown by the dotted line. (After [Nimetulayeva, 2006]).

To preliminarily access the mean velocity of subduction of the Black Sea micro-plate the coordinate x dependence of the growth rate $\gamma_\perp(x)$ of transversal convective rolls for the constant viscosity fluid model can be allowed for. In such the model the averaged temperature and pressure viscosity dependence is accounted for in an averaged manner, the factor describing the temperature- and pressure viscosity dependence being equal to its mean value [Gavrilov, 2014].

Analytical formulae in [Gavrilov, 2014] yield $\gamma_\perp(x)$ shown in Fig.2 for the subduction angle $\beta \approx 15^o$, convection cell dimension ~250 km and subduction velocities *V* given in Fig.2 in mm per year.

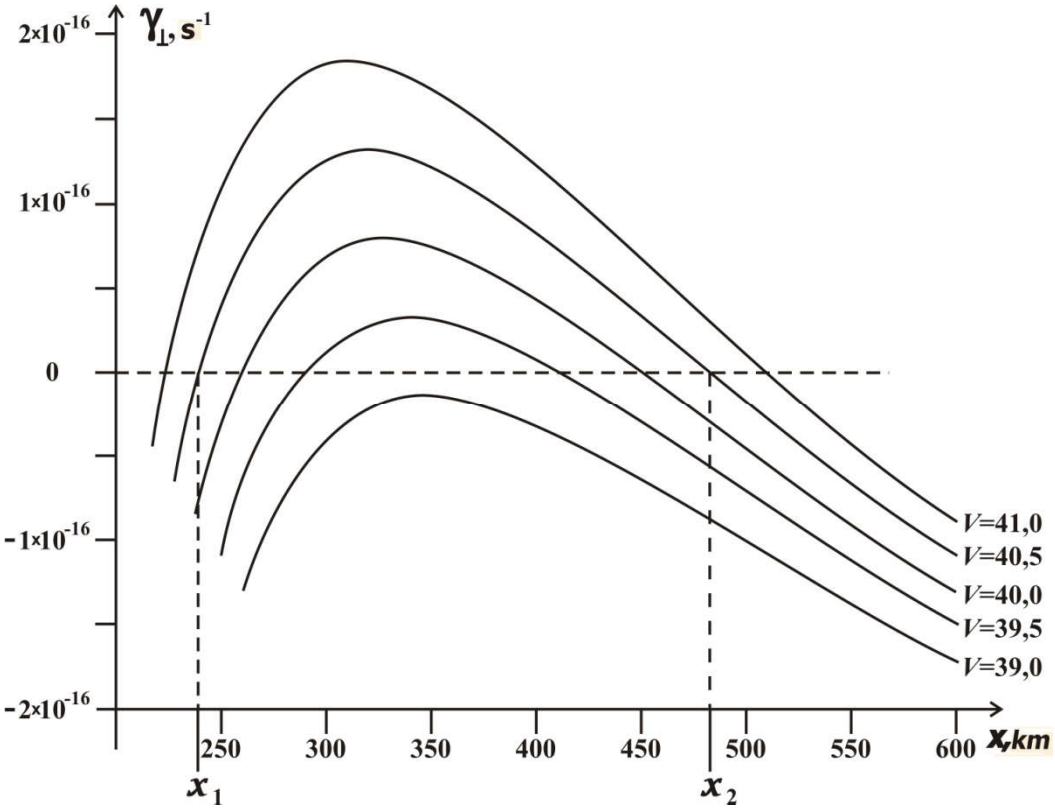

Fig. 2: Growth rate $\gamma_\perp(x)$ of convective instability vs. horizontal distance x for subduction velocities *V* in mm per year. In the zone $x_1 < x < x_2$ approximately 250 km long single 2D convection cell with $\gamma_\perp(x)>0$ is aroused at V=40.5 mm×yr^{-1} in the zone of heat flux maximum.

It should be noted the growth rates $\gamma_\perp(x)$ are viscosity independent as convection is driven by viscous heat release (which is directly proportional to viscosity), while, on the other hand, the greater is the viscosity the more difficult is to arouse the convection. Fig.2 clearly demonstrates the convective zone with $\gamma_\perp(x)>0$ amounts to $x_2 - x_1 \approx 250$ km (i.e. the single convective cell of ~250 size is actually aroused) at V=40.5 mm per year, the latter value being a preliminary estimate of the mean subduction velocity. The $\gamma_\perp(x)$ maximum is ~320 km distant from the trench which is very close to the distance from the trench to the observed 2D heat flux anomaly (~400 km, see Fig.1).

To compute more accurate consistent model of small-scale convection in the mantle wedge between the overriding Scythian plate and subducting Black Sea micro-plate it is necessary from the computational point of view first to specify vanishing non-dimensional numbers $Ra \to 0$, $Di = 0$ in (1)–(2), i.e. to ignore convection and viscous dissipation. This approach is applied as convection with Ra and Di (4) passes through very vigorous stages, and the time steps in integrating (1)–(2) become too small thus making it difficult to model the thermal structure of the plates. Solving (1)–(2) by the finite element method in space on the grid 104×104 and the 3-rd order Runge-Kutta method in time one obtains for $Ra \to 0$, $Di = 0$ and V=45 mm a year non-dimensional quasi steady-state Ψ and T shown in Figs.3, where the streamlines are depicted with step 0.25 and the isotherms with an interval of 0.05.

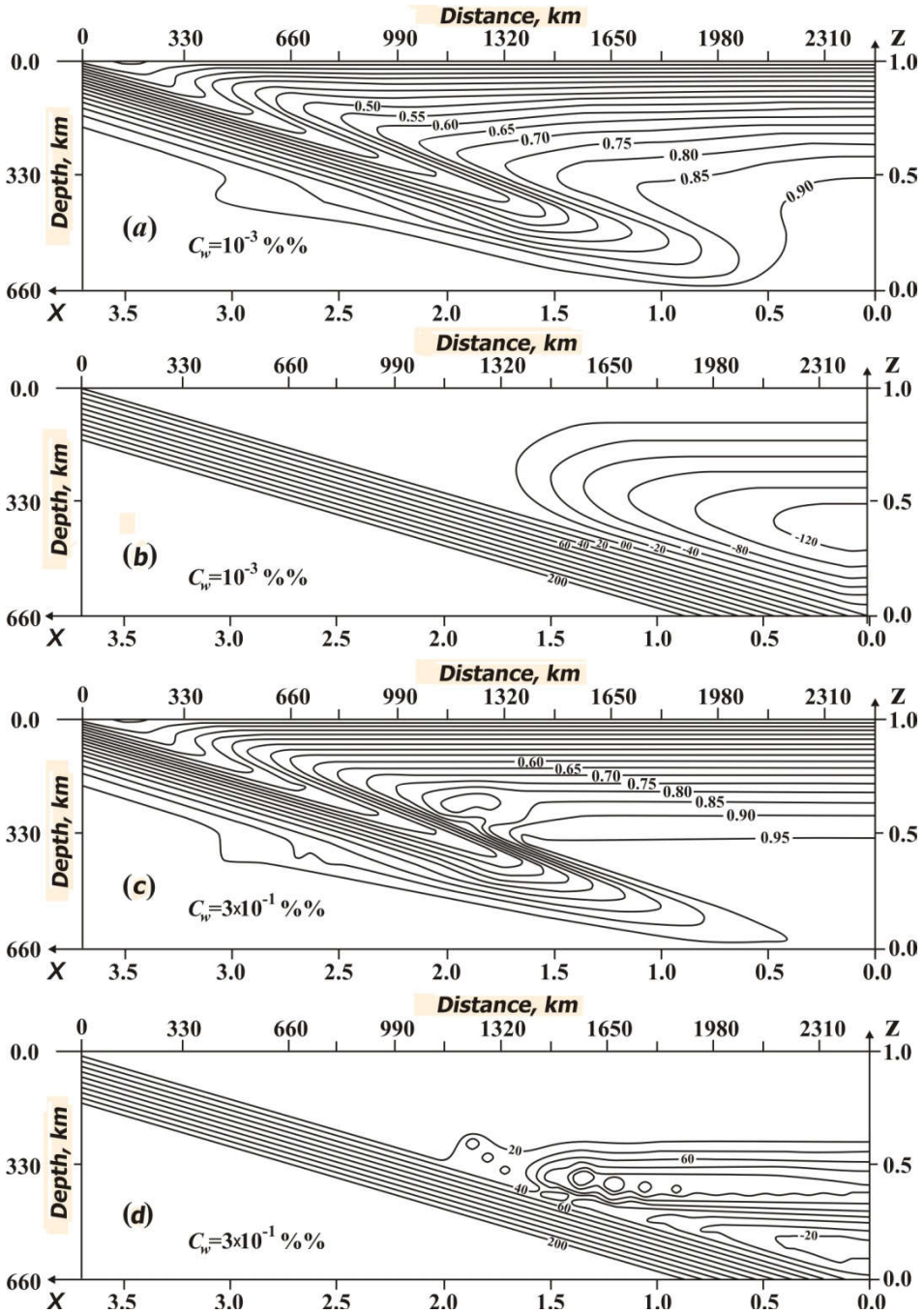

Fig. 3: Quasi steady-state non-dimensional stream-function and temperature distributions in the zone of subduction of the Black Sea micro-plate under the Scythian plate with no effects of dissipative heating and convection taken into account for non-Newtonian rheology: (*a*, *b*) for the water content $C_w=10^{-3}$ weight %% and (*c*, *d*) for the water content $C_w=3\square10^{-1}$ weight %%. Parallel equidistant streamlines represent subducting Black Sea micro-plate, the streamlines above correspond to the mantle wedge flow induced by subduction.

Subducting plate was considered rigid, while the viscosity at the zone of plates friction (at temperatures below 1200 *K*) was reduced by 2 orders of magnitude as compared to (5). The latter viscosity reduction at the plates contact zone accounts for lubrication effected by deposits partially entrained by the subducting plate. Such a lubrication prevents the overriding Scythian plate from gluing to the subducting one [Gerya, 2011]. It is worth noting the isotherm $T=0.15$ in Fig.3a,c approximately corresponding to the Earth's surface is depressed at subduction zone by~7 km which is of the order of a typical trench depth. Fig.3 shows the results of computation for formulae (7) – (9) for non-Newtonian rheology case for the water content $C_w=10^{-3}$ weight %% (Fig.3a, b) and $C_w=3\times10^{-1}$ weight %% (Fig.3c, d). The velocity $V=45$ mm per year is

chosen as resulting in the best convective zone size fitting in with the observed heat flux (positive and negative) anomaly size at the point C_2 in Fig.1, i.e. in the rear of the Mountainous Crimea. The Black Sea micro-plate subducting with a given velocity *V* is considered rigid and is shown in Fig.3b,d by the equidistant diagonal streamlines. The induced mantle wedge flow above the subducting plate is seen to occur in the form of a single vortex at $C_w=10^{-3}$ weight %% (Fig.3b) and in the form of the 2 vortices (located one above another) at $C_w=3\times10^{-1}$ weight %% (Fig.3d), the latter 2 vortices being considerably compressed in the vertical direction and the upper one (with $\psi > 0$) revolves clockwise while the lower one (with $\psi < 0$) revolves counterclockwise (Fig.3b,d). Micro-whirls ~10^2 km great are formed between the counter-flows inside the upper induced flow obviously due to the tangential discontinuity instability (Kelvin-Helmholtz instability).

Assuming $Ra = 5.55\times10^8$ and $Di = 0.165$, i.e. switching dissipation and convection on, and taking into account the effects of phase transitions, from (1)–(2) the convection is found not to arouse in the non-Newtonian rheology case at $C_w=10^{-3}$ weight %%. At $C_w=3\times10^{-1}$ weight %% the 2 induced mantle flows in the mantle wedge are destroyed during the time interval ~0.6×10^{-6} (in dimensional form ~0.1 Myr) by the convective vortices shown in Fig.4 with the streamlines depicted with the interval of 4~10^4.

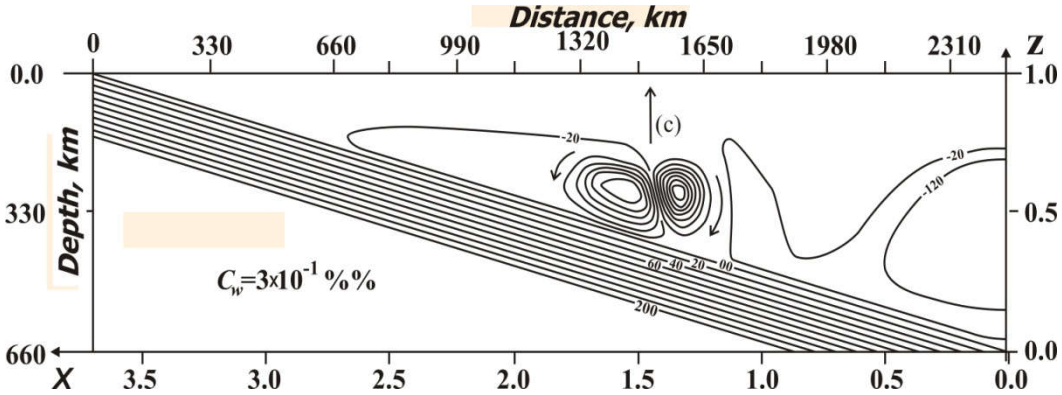

Fig. 4: Quasi steady-state stream-function in the mantle wedge with the effects of dissipative heating and convective instability for the case of non-Newtonian rheology and the water content $C_w=3\times10^{-1}$ weight %%. Arrow (*c*) shows ascending convective flow transporting mantle hydrocarbons to the Earth's surface at the point C_2 in Fig.1.

These convective vortices are seen actually to correspond to a single convection cell aroused at subduction velocity V=45 mm per year. The latter convection cell dimension is of the order of ~300 km, i.e., is very close to the observed minima *q* separation under the C_2 point in Fig.1.

Thus the for the non-Newtonian mantle wedge rheology case with the viscosity reduced by 3 orders of magnitude as compared to (7)– 9) the computation shows the convection in the mantle wedge to occur at $C_w=3\times10^{-1}$ weight %% in the form of two micro vortices at *V*=45 mm per year. Convection of this type can provide abnormal 2D heat flux *q* observed in the rear of the Mountainous Crimea and the upwelling of the mantle hydrocarbons to the Earth's surface along the arrow "c" [Yudin, 2003]. Considerable velocity in convective vortices in Fig.4 is due to the local viscous stresses increase resulting in the drop in viscosity in convective zone. In the case of Newtonian rheology the convection is aroused at the subduction velocity of over 10^2 mm×a^{-1}, which appears unrealistic.

According to [Zharkov, 2019, p.143], the water content in the mantle transition zone in the mantle wedge may amount to ~3 wt. %. To investigate the role of water infused into the mantle wedge from the subducting slab the above computations were carried out for the mean water content of 1 wt. % and subduction velocity of 30, 20, and 10 mm per year. The results of the convection computation are shown in Figs.5a and 5b for *V*=30 and 20 mm per year respectively, where the streamlines corresponding to subducting Black Sea micro-plate are shown with the interval of 10, and the streamlines, corresponding to convective vortices with the interval of 10^6. The mean non-dimensional velocity in the left micro-vortex are ~15.2×10^7, ~7.1×10^7 and ~0.05×10^7 for the velocity of subduction of *V* = 30, 20, and 10 mm per year respectively. Thus, the convection may be considered to arise at the subduction velocity over ~10 mm per year for the mean water content C_w~1 wt.%. Since the meant water content in the mantle wedge could hardly exceed ~1 wt.% even at the water content in the mantle transition zone of 3 wt%, the obtained subduction velocity of ~10 mm per year may be regarded the minimum estimate of that of subduction of the Black Sea micro-plate.

It is worth noting, that in the case of Newtonian rheology, the mantle wedge dissipation-driven convection in the form of transversal rolls, as in Fig.4, is characteristic of very small subduction angles, the

convection of this type being absent already at subduction angle β=30° [Gavrilov & Abbott, 1999]. At the subduction angle under consideration here, β=15°, the convective transversal rolls do not appear at $V<10$ cm×yr^{-1} for the Newtonian rheology case. Arrow (*c*) above the boundaries of the oppositely revolving convective vortices in Figs.4, 5 indicate a possible direction of transport of non-organic mantle hydrocarbons to the Earth's surface.

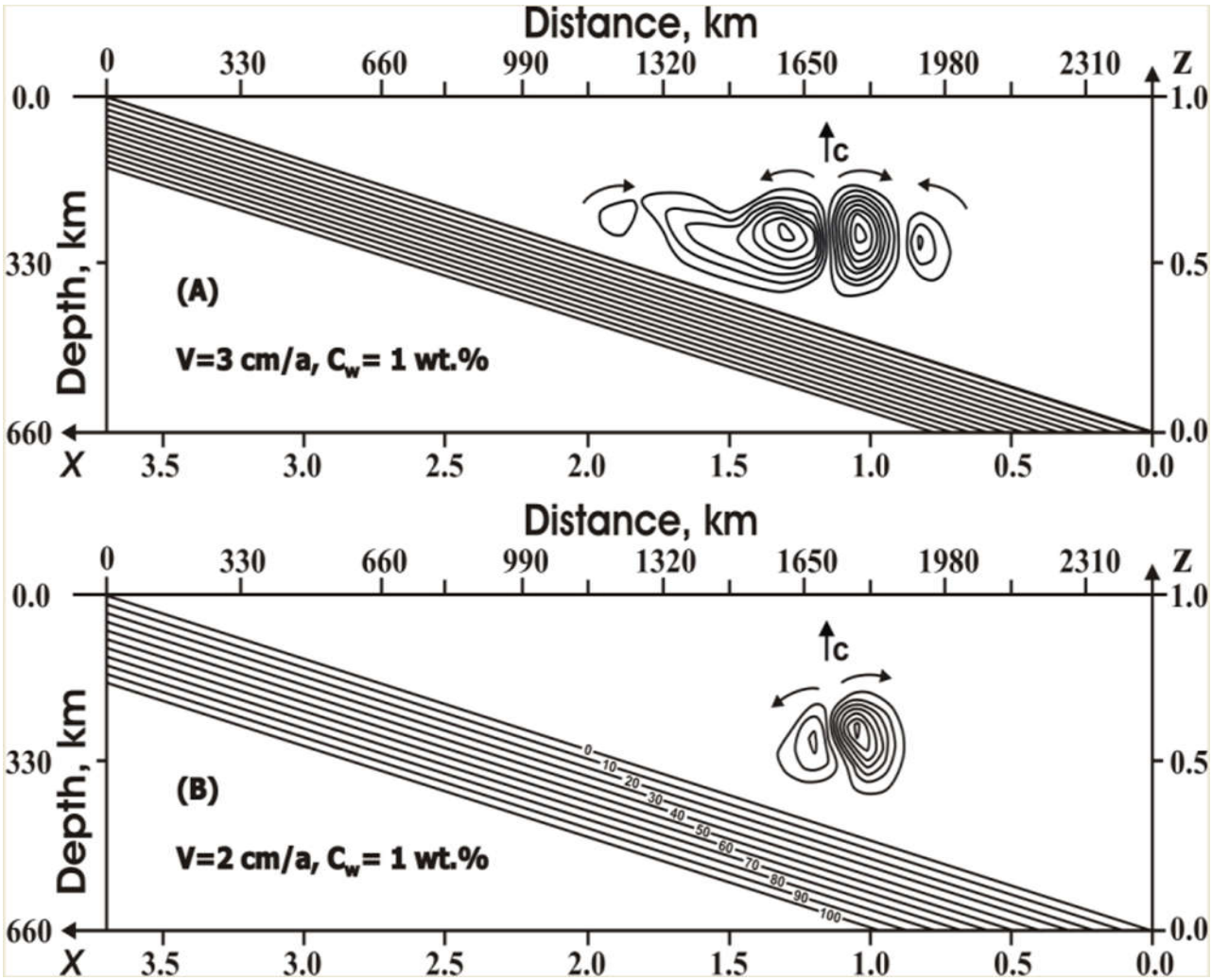

Fig. 5: Quasi steady-state stream-function in the mantle wedge with the effects of dissipative heating and convective instability for the case of non-Newtonian rheology and the water content C_w=1 wt. % at the subduction velocity of (a) – 30 mm per year and (b) – 20 mm per year. Arrow (*c*) shows ascending convective flow transporting mantle hydrocarbons to the Earth's surface at the point C_2 in Fig.1.

Computations for Newtonian mantle rheology with the viscosity (5)-(6) shows the transversal rolls to be aroused at far greater distance from the trench than the observed 2D heat flux anomaly. Thus the model constructed here favors the non-Newtonian mantle wedge rheology as better fitting in with the observed heat flux anomaly localization. It should be noted that numerous thermo-mechanical mantle models in the zones of subduction (see, e.g. [Gerya et al., 2006; Gerya, 2011] and the vast number of references there) showed convection in the form of transversal rolls never to occur as the models with extremely small subduction angle and sufficiently great subduction velocity were not investigated.

IV. Conclusions

The size of the cell of 2D mantle wedge dissipation-driven convection in the case of the realistic non-Newtonian rheology equals ~300 km at the subduction velocity 10 mm×yr^{-1} and the mean water content of ~1 wt.%, in which case a single convection cell is aroused. This explains the formation and horizontal extent (~250 km) of the only 2D heat flux anomaly observed in the rear of the Mountainous Crimea. The water content sufficient for the 2D convection to be aroused is ~1 wt. % at the velocity of a subduction of ~10 mm per year. The non-Newtonian model convection cell locates twice further from the

trench than the observed 2D heat flux anomaly. The velocity in convective vortices in the non-Newtonian rheology case is ~10 m per year which may be sufficient to provide upward transport of mantle wedge hydrocarbons to the Earth's surface.

References Références Referencias

1. *Billen M., Hirth G*. Newtonian versus non-Newtonian Upper Mantle Viscosity: Implications for Subduction Initiation // Geophys. Res. Lett. 2005. V.32. (L19304). Doi: 10.1029/2005GL023458.
2. *Gavrilov S.V. Issledovanie mehanizma formirovaniya ostrovnyh dug i tylovogo razdviganiya litosfery* (Investigation of the island arc formation mechanism and the back-arc lithosphere spreading) // *Geofizicheskie Issledovaniya* (Geophysical Researches). 2014. V.15. No.:4. pp. 35–43.
3. *Gavrilov S.V., Abbott D.H*. Thermo-mechanical model of heat- and mass-transfer in the vicinity of subduction zone // Physics of the Earth. 1999. V.35. No.: 12. pp. 967–976.
4. *Gavrilov S.V., Kharitonov A.L. Otsenka skorosti subduktsii Russkoy platformy pod Sibirskuyu v Paleozoe po raspredeleniyu zon vynosa mantiynykh uglevodorodov v Zapadnoy Sibiri* (Velocity of the subduction of the Russian platform under the Siberian one in the Paleozoic by the distribution of mantle hydro-carbon upwelling zones in Western Siberia) // *Geofizicheskie Issledovaniya* (Geophysical Researches). 2015. V.16. pp. 36–40.
5. *Gavrilov S.V., Kharitonov A.L*. Subduction velocity of the Russian plate under the Siberian one at Paleozoic: a constraint based on the mantle wedge convection model and the oil- and gas-bearing zones distribution in Western Siberia // Modern Science. 2016. No.:16. pp. 155-160.
6. *GeryaT.V., J.A.D.Connolly, D.A.Yuen, W.Gorczyk, A.M.Capel*. Seismic implications of mantle wedge plumes // Phys. Earth Planet. Inter. 2006. V.156. pp. 59-74.
7. *GeryaT.V.* Future directions in subduction modeling // J. of Geodynamics. 2011. V.52. pp. 344-378.
8. *Nimelulayeva G.Sh. Obespechenie ecologicheskoy bezopasnosti territirii Bakhchisarayskogo rayona Kryma pri opolznevykh yavleniyakh na osnove geodinamicheskogo rayonirovaniya nedr* (Provision of the ecological security of the territory of the Bahchisaray district of Crimea on the basis of geodynamical regionalization of interiors) // PhD thesis, Moscow, Moscow State University of Mines 2004. 200 p.
9. *Schubert G., Turcotte D.L., Olson P.* Mantle Convection in the Earth and Planets. New York: Cambridge University Press, 2001. 940 p.
10. *Trubutsyn V.P. Reologiya mantii i tektonika okeanicheskikh litosfernykh plit* (Mantle rheology and the oceanic lithospheric plate tectonics) // *Fizika Zemli* (Physics of the Earth). 2012. No.: 6. pp. 3-22.
11. *Trubutsyn V.P., Trubitsyn A.P. Chislennaya model' obrazovaniya sovokupnosti litosfernykh plit i ikh prokhozhdeniya cherez granitsu 660 km* (Numerical model of formation of the set of lithospheric plates and their penetration through the 660 km boundary) // *Fizika Zemli* (Physics of the Earth). 2014. No.: 6. pp. 138- 147.
12. *Ushakov S.A., Galushkin Yu.I., Ivanov O.P.* Priroda skladchatosti osadkov. na dne Chernogo morya v zone perekhoda k Krymu i Kavkazu (The nature of folding of the sediments at the Black Sea floor in the zone of transition to Crimea and Caucasus) // *Doklady Academii Nauk SSSR* (Reports of the USSR Academy of Sciences). 1977. V.233. No.:5. pp. 932 – 935.
13. *Yudin V.V.* Geologiya Kryma na geodinamicheskoy osnove (The Geology of Crimea on the Geodynamical Basis). Sympheropol. 2001. 46 p.
14. *Yudin V.V.* Potential oil- and gas-bearing structures at the foothills of the Mountainous Crimea. The collection of reports at the 4-th international symposium Crimea-2002 "Geodynamics and oil- and gas-bearing structures of the Black Sea – Caspian region". Sympheropol. 2003. pp.271 – 279.
15. *Zharkov V.N. Geofizicheskie issledovaniya planet I sputnikov* (Geophysical Researches of the Planets and Satellites). Moscow: Joint Institute of Physics of the Earth RAS. 2003. 102 p.
16. *Zharkov V.N*. Physics of the Earth's Interiors. Duesseldorf: Lambert Academic Publishing. 2019. 438 p.

This page is intentionally left blank

Global Journal of Researches in Engineering: I
Numerical Methods
Volume 20 Issue 1 Version 1.0 Year 2020
Type: Double Blind Peer Reviewed International Research Journal
Publisher: Global Journals
Online ISSN: 2249-4596 & Print ISSN: 0975-5861

Modeling Filters of Six Symmetrical Components of Controlled Self-compensating Power Transmission Lines

By Turturica Natalya
Pridnestrovian State University

Abstract- This article discusses the implementation of filters for six symmetrical components of currents (voltages) of a selfcompensating power line (SCPL) and a controlled selfcompensating power line with closely placed phases (CSCPL) Mathematical descriptions of these filters are provided. The principle of implementation of relay protection based on the allocation of six symmetrical components of currents (voltages) is proposed, which allows to increase its sensitivity and ensure the "survivability" of the SCPL (CSCPL) for various asymmetric short circuits. For this purpose, a structural model of the filter scheme of six symmetrical components is reproduced in the MATLAB & Simulink dynamic modeling environment.

Keywords: ***фильтр шести симметричных составляющих, самокомпенсирующейся линии электропередачи (СВЛ).***

GJRE-I Classification: *FOR Code: 010399*

Strictly as per the compliance and regulations of:

Modeling Filters of Six Symmetrical Components of Controlled Self-compensating Power Transmission Lines

Turturica Natalya

Abstract- This article discusses the implementation of filters for six symmetrical components of currents (voltages) of a self-compensating power line (SCPL) and a controlled self-compensating power line with closely placed phases (CSCPL) Mathematical descriptions of these filters are provided. The principle of implementation of relay protection based on the allocation of six symmetrical components of currents (voltages) is proposed, which allows to increase its sensitivity and ensure the "survivability" of the SCPL (CSCPL) for various asymmetric short circuits. For this purpose, a structural model of the filter scheme of six symmetrical components is reproduced in the MATLAB & Simulink dynamic modeling environment.

Results: The proposed mathematical MATLAB model of filters of six symmetrical components allows their mathematical implementation in the development of relay protection of SCPL (CSCPL).

Keywords: фильтр шести симметричных составляющих, самокомпенсирующейся линии электропередачи (СВЛ).

I. Введение

Один из способов повышения пропускной способности ЛЭП, является внедрение ЛЭП со сближенными одноимёнными фазами так называемые самокомпенсирующиеся ЛЭП (СВЛ) или управляемые самокомпенсирующиеся ЛЭП (УСВЛ), исследование которых были начеты в Московском Энергетическом Институте и Институте Энергетики Академии Наук Молдовы. [1-3]. Отличительная особенность от обычных двухцепных линий этих линий сводиться к тому, что самокомпенсирующаяся линия электропередачи представляет собой двухцепную линию, у которой сближены разноименные фазы разных цепей. Благодаря этому, усиливается электромагнитное влияние между сближенными фазами и обеспечивается естественный 120 градусный угол сдвига напряжений сближенных фаз. Внедрение указанных ЛЭП требует решения целого комплекса вопросов, в том числе расчёта токов коротких замыканий (к.з.) и релейной защиты. Проведенные исследования показали, что расчет различных несимметричных режимов и коротких замыканий.

Author: Turturica Natalya, Pridnestrovian State University.
e-mail: natalya_siti@mail.ru

наиболее целесообразно выполнить, используя шестифазные симметричные составляющие. Кроме того выявлено, что определенным видам к.з. соответствует «появление» определенных симметричных составляющих, что может послужить отличительным признаком данных видов к.з. для релейной защиты [4,5]. Для выявления данных симметричных составляющих необходимы соответствующие фильтры. До настоящего времени проведенные исследования касались только физического выполнения этих фильтров, что вполне приемлемо для традиционных защит. [6-9]. Для современных цифровых и микропроцессорных защит наиболее целесообразно математическое «выделение» данных симметричных составляющих при к.з

Целью данной работы являлось изучение работоспособности фильтров шести симметричных составляющих и выбор наиболее оптимального алгоритма их программного исполнения. Для этого предлагается реализация ниже приведенного алгоритма расчета коэффициентов данных фильтров, а в компьютерном пакете Matlab/Simulink [10,11] осуществлена имитационная модель с целью получения тех или иных симметричных составляющих УСВЛ (СВЛ) для релейной защиты и автоматики. В целом эта модель может быть распространена и применена в принципе к любым многофазным ЛЭП в частности двух цепным, рассматривая их как шестифазные линии.

II. Методика Исследования

Рассматривая УСВЛ(СВЛ) как шестифазные ЛЭП для расчета нессиметричных кз и сложных видов повреждений, включая обрывы фаз, можно использовать метод симметричных составляющих. Теоретические основы данного метода были изложены в работах C.L. Fortescue, а затем R. Evans и C. Wagner и детально рассмотрены в работах [12,13]. Метод основан на разложении несимметричных систем токов (напряжений) при различных повреждений на шесть симметричных составляющих 0,1,2,3,4,5 последовательностей.

В соответствии с разложением фазные напряжения (токи) в фазах A, A' ,B, B', C и C', могут быть выражены симметричными составляющими и наоборот следующим образом

$$\dot{F} = \dot{S}_6 \cdot \dot{F}_S;\ \dot{F} = \dot{S}_6^{-1} \cdot \dot{F}_S \qquad (1)$$

где

$$\dot{F} = \begin{vmatrix} \dot{F}_A \\ \dot{F}_B \\ \dot{F}_C \\ \dot{F}_D \\ \dot{F}_E \\ \dot{F}_F \end{vmatrix};\quad \dot{F}_S = \begin{vmatrix} \dot{F}_{A0} \\ \dot{F}_{A1} \\ \dot{F}_{A2} \\ \dot{F}_{A3} \\ \dot{F}_{A4} \\ \dot{F}_{A5} \end{vmatrix}$$

-матрицы векторов фазных напряжений (токов) в координатах шести симметричных составляющих

$$\dot{S}_6 = \begin{vmatrix} 1 & 1 & 1 & 1 & 1 & 1 \\ 1 & e^{j300} & e^{j240} & e^{j180} & e^{j120} & e^{j60} \\ 1 & e^{j240} & e^{j120} & 1 & e^{j240} & e^{j120} \\ 1 & e^{j180} & 1 & e^{j180} & 1 & e^{j180} \\ 1 & e^{j120} & e^{j240} & 1 & e^{j120} & e^{j240} \\ 1 & e^{j60} & e^{j120} & e^{j180} & e^{j240} & e^{j300} \end{vmatrix};$$

$$\dot{S}_6^{-1} = \frac{1}{6}\begin{vmatrix} 1 & 1 & 1 & 1 & 1 & 1 \\ 1 & e^{j60} & e^{j120} & e^{j180} & e^{j240} & e^{j300} \\ 1 & e^{j120} & e^{j240} & 1 & e^{j120} & e^{j240} \\ 1 & e^{j180} & 1 & e^{j180} & 1 & e^{j180} \\ 1 & e^{j240} & e^{j120} & 1 & e^{j240} & e^{j120} \\ 1 & e^{j300} & e^{j240} & e^{j180} & e^{j120} & e^{j60} \end{vmatrix} -$$

квадратные матрицы преобразования из симметричных составляющих 0,1,2,3,4,5 в фазные и обратная матрица S_6

Векторные диаграммы рисунок 1, иллюстрируют по фазное геометрическое разложение несимметричной шестифазной системы на шесть симметричных составляющих системы векторов токов (напряжения) УСВЛ $0^{\circ} \le \theta \le -120^{\circ}$, где θ это угол сдвига между системами векторов фазных напряжений, в общем, случаи от 0°до 360°

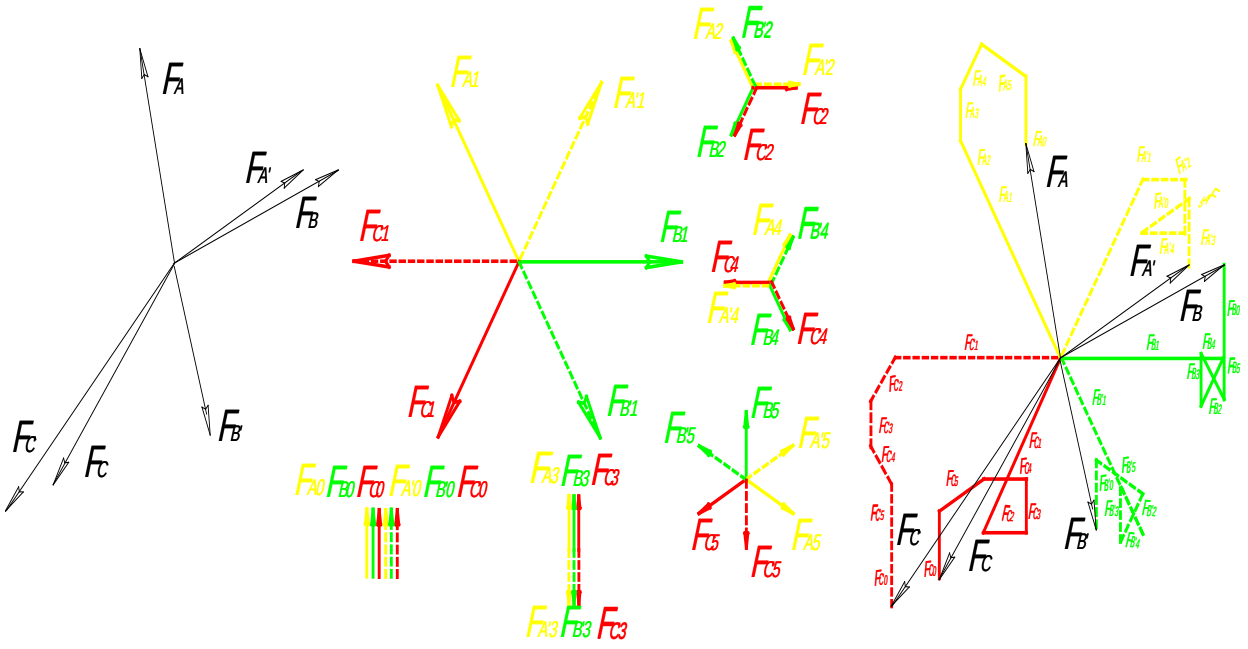

Рис. 1: Векторные диаграммы. а) несимметричная шестифазная система векторов б) вектора симметричных составляющих 0,1,2,3,4 и 5 последовательностей; в) по фазное сложение векторов симметричных составляющих.

При сложных видах повреждений УСВЛ (СВЛ) связанные с обрывом фаз или одновременный обрывом и кз присуще определённые симметричные составляющие 0, 1, 2, 3, 4 и 5 последовательности. Например граничные условия при обрыве фаз A и A' УСВЛ

$$\dot{U}_{LB} = \dot{U}_{LB'} = \dot{U}_{LC} = \dot{U}_{LC'} = 0;$$
$$\dot{I}_{LA} = 0;\ \dot{I}_{LA'} = 0. \qquad (2)$$

Согласно (1) переход от фазных координат к координатам шести симметричных составляющих УСВЛ и наоборот граничные условия примут вид:

$$\dot{I}_1 + \dot{I}_3 + \dot{I}_5 = 0;$$

$$\dot{U}_1 = \dot{U}_3 = \dot{U}_5 = \frac{1}{6}(\dot{U}_{LA} - \dot{U}_{LA'});$$

$$\dot{U}_0 = \dot{U}_2 = \dot{U}_4 = \frac{1}{6}(\dot{U}_{LA} + \dot{U}_{LA'}) \quad (3)$$

Аналогично можно найти последовательности токов и напряжений возникающих при различной несимметрий. Как было отмечено выше, релейная защита УСВЛ (СВЛ) может быть реализована на основе обнаружения тех или иных соответствующих симметричных составляющих. Для этого необходимы фильтры симметричных составляющих шестифазного разложения.

Фильтр симметричных составляющих напряжения (тока) подключён своими выходными зажимами к УСВЛ и выделяет на своих выходных зажимах напряжение (ток), пропорциональный одной или нескольким симметричным составляющим, подведённых к входным зажимам фильтра рисунок 2.

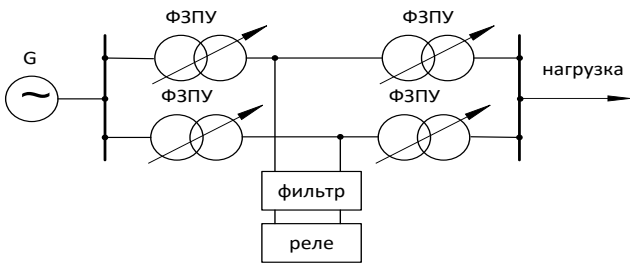

Рис.2. Условная схема подключение фильтра к УСВЛ

При разработке релейной защиты часто появляется задача выделения симметричных составляющих не из фазных величин, а из линейных, например, из линейных напряжений. Рассмотрим, как рассчитать напряжение второй последовательности $\dot{U}_2$, при фиксированном угле регулирования θ, из линейных напряжений $\dot{U}_{AB}, \dot{U}_{BC}, \dot{U}_{A'B'}, \dot{U}_{B'C'}$. Линейные напряжения связаны с фазными по следующим выражениям:

$$\begin{aligned} \dot{U}_{AB} &= \dot{U}_A - \dot{U}_B, \\ \dot{U}_{BC} &= \dot{U}_B - \dot{U}_C, \\ \dot{U}_{A'B'} &= \dot{U}_{A'} - \dot{U}_{B'}, \\ \dot{U}_{B'C'} &= \dot{U}_{B'} - \dot{U}_{C'} \end{aligned} \quad (4)$$

Расчёт напряжения второй последовательности согласно (1):

$$\begin{aligned} \dot{U}_2 &= \frac{1}{6}(\dot{U}_A + a\dot{U}_{C'} + a^2\dot{U}_B + \dot{U}_{A'} + a\dot{U}_C + a^2\dot{U}_{B'}) = \\ &= \frac{1}{6}(\dot{U} + a\dot{U}_{C'} + (-1-a)\dot{U}_B + \dot{U}_{A'} + a\dot{U}_C + (-1-a)\dot{U}_{B'}) = \\ &= \frac{1}{6}(\dot{U}_A + a\dot{U}_{C'} - \dot{U}_B - a\dot{U}_B + \dot{U}_{A'} + a\dot{U}_C - \dot{U}_{B'} - a\dot{U}_{B'}) = \\ &= \frac{1}{6}(\dot{U}_{AB} - a\dot{U}_{BC} + \dot{U}_{A'B'} - a\dot{U}_{B''}) = \\ &= \frac{1}{6}(\dot{U}_{AB} + \dot{U}_{BC}e^{j60^\circ} + \dot{U}_{A'B'} + \dot{U}_{B''}e^{j60^\circ}) \end{aligned} \quad (5)$$

Таким образом, задача построения фильтра напряжения второй последовательности сводится к использованию четырёх напряжений (вместо шести фазных), которые должны быть повёрнуты на соответствующие углы, а затем геометрически сложены.

Аналогичными преобразованиями из линейных напряжений можно получить фильтры 1,2,4 и 5 составляющих:

$$\begin{aligned} \dot{U}_1 &= \frac{1}{6}(\dot{U}_{AB} + \dot{U}_{BC}e^{-j60^\circ} - \dot{U}_{A'B'} - \dot{U}_{B'C'}e^{-j60^\circ}); \\ \dot{U}_2 &= \frac{1}{6}(\dot{U}_{AB} + \dot{U}_{BC}e^{j60^\circ} + \dot{U}_{A'B'} + \dot{U}_{B'C'}e^{j60^\circ}); \\ \dot{U}_4 &= \frac{1}{6}(\dot{U}_{AB} + \dot{U}_{BC}e^{-j60^\circ} + \dot{U}_{A'B'} + \dot{U}_{B'C'}e^{-j60^\circ}); \\ \dot{U}_5 &= \frac{1}{6}(\dot{U}_{AB} + \dot{U}_{BC}e^{j60^\circ} - \dot{U}_{A'B'} - \dot{U}_{B'C'}e^{j60^\circ}) \end{aligned} \quad (6)$$

Нулевую и третью составляющие выделить из линейных напряжений нельзя:

$$\begin{aligned} \dot{U}_0 &= \frac{1}{6}(\dot{U}_A + \dot{U}_{C'} + \dot{U}_B + \dot{U}_{A'} + \dot{U}_C + \dot{U}_{B'}) \\ \dot{U}_3 &= \frac{1}{6}(\dot{U}_A - \dot{U}_{C'} + \dot{U}_B - \dot{U}_{A'} + \dot{U}_C - \dot{U}_{B'}) \end{aligned} \quad (7)$$

Ориентация векторов токов нулевой и третьей последовательностей не зависит от угла θ сдвига между системами векторов фазных напряжений цепей, и поэтому угол θ не входит в уравнения для этих последовательностей.

Напряжение фильтра на вторичных зажимах находится в определённой зависимости от подведённых напряжений это одно из требований к фильтру симметричных составляющих. Должно выполняться условие

$$\dot{F}_p = \dot{k}_0\dot{F}_0 + \dot{k}_1\dot{F}_1 + \dot{k}_2\dot{F}_2 + \dot{k}_3\dot{F}_3 + \dot{k}_4\dot{F}_4 + \dot{k}_5\dot{F}_5 \quad (8)$$

где

$\dot{F}_0, \dot{F}_1, \dot{F}_2, \dot{F}_3, \dot{F}_4, \dot{F}_5$ -симметричные составляющие токов (напряжений);

Коэффициенты фильтра $\dot{k}_0, \dot{k}_1, \dot{k}_2, \dot{k}_3, \dot{k}_4, \dot{k}_5$, заданные комплексными или действительными значениями.

$$\dot{k}_{S\phi} = \dot{S}_6\eta \quad (9)$$

η_ϕ - коэффициенты, характеризующие амплитудные и фазные изменения токов (напряжений), подводимых к фильтру.

III. Реализация Методики в Matlab & Simulink

Решение уравнений и матричной математической модели осуществлялась в Matlab/Simulink. Одной из составных частей библиотеки SimPowerSystem пакета Matlab/Simulink является библиотека MathOperations. Она содержит функциональные блоки большинства математических преобразований. была создана Matlab-модель шестифазного фильтра, представленная на рисунок 3.

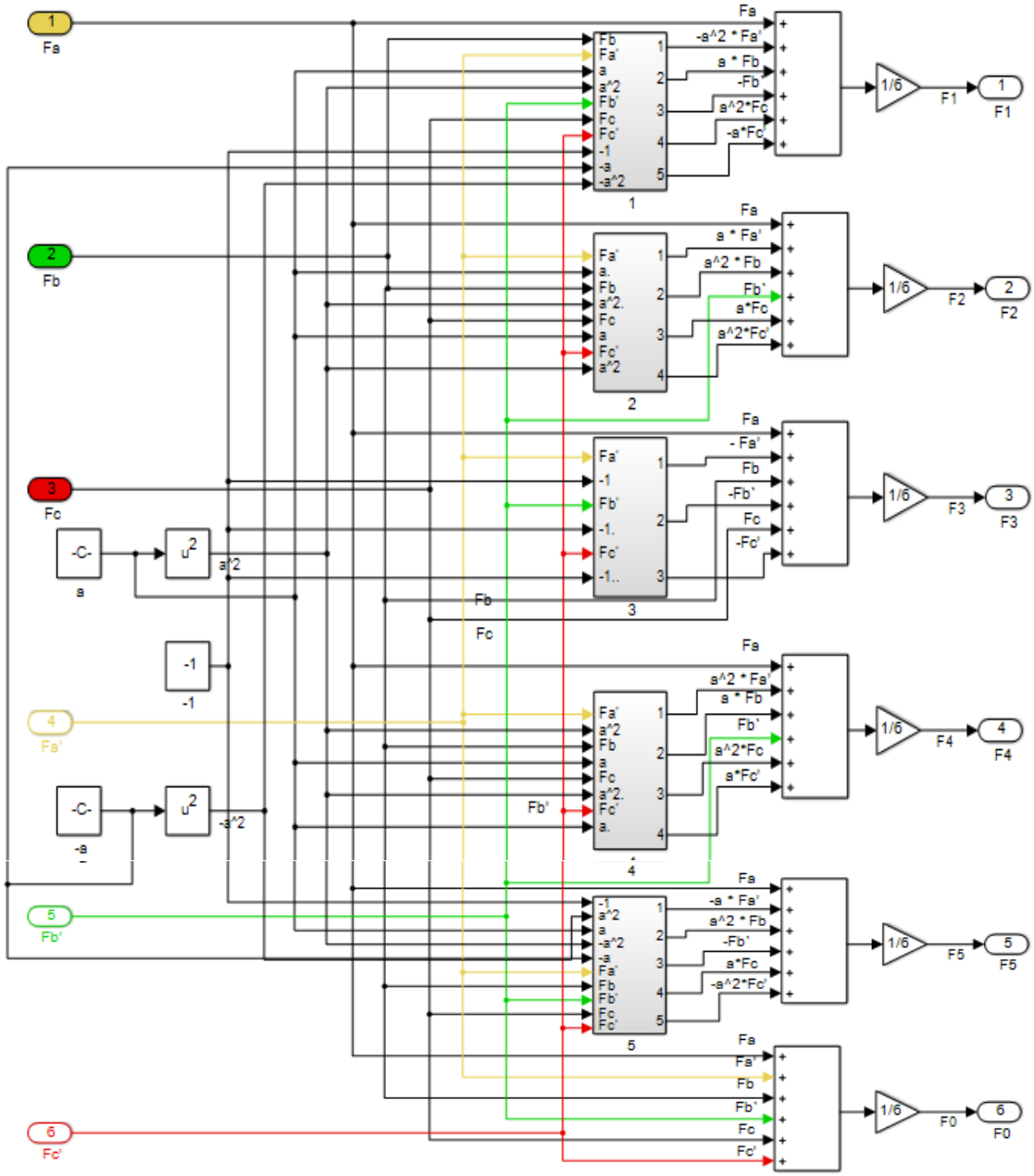

Рис. 3: Векторные диаграммы. а) несимметричная шестифазная система векторов б) вектора симметричных составляющих 0,1,2,3,4 и 5 последовательностей; в) по фазное сложение векторов симметричных составляющих.

Для реализации методики модели фильтра в библиотеке MathOperations использованы следующие блоки с их функциональными возможностями:

- Блок Constant – задание значений постоянных, например, оператор системы a=ej120;
- блок Math- общие математические функций;
- блок Product - выводит результат умножения двух входных данных, например, $a^2\dot{F}; -a^2\dot{F}; a\dot{F}; -a\dot{F}$ и т.д.
- Блок Sum - сложение или вычитание на своих входах.
- Блок Gain -умножает вход на постоянное значение (1/6).

Подсистемы 1,2,3,4 и 5 отвечают за обработку измерительной информации. Пример второй подсистемы представлен на рисунок 4.

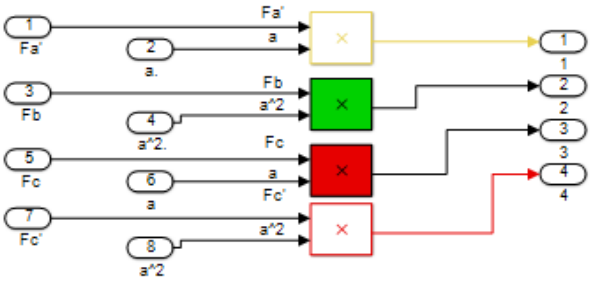

Рис.4. Подсистема расчёта составляющих .

Модуль Simulink (рис3.) вычисляет, исходя из заданных значений $\dot{F}_A, \dot{F}_{A'}, \dot{F}_B, \dot{F}_{B'}, \dot{F}_C, \dot{F}_{C'}$, симметричные составляющие $\dot{F}_0, \dot{F}_1, \dot{F}_2, \dot{F}_3, \dot{F}_4, \dot{F}_5$ по формуле (1). Matlab-модель может использоваться для анализа УСВЛ(СВЛ) при подключении к фильтра в любом из возможных режимах роботы.

IV. Выводы

Любую несимметричную систему токов (напряжений) можно разложить на шесть симметричных составляющих. Определённым несимметриям присущи свои симметричные составляющие что, может послужить отличительным признаком определённой несимметрии. Представленные формулы соотношений между напряжениями, позволяет получить фильтры шестифазных симметричных составляющих 0,1,2,3,4 и 5 и обнаружить на их основе любых комбинациях несимметричных коротких замыканий и обрывов фаз.

Исследование взаимосвязи фазных и симметричных составляющих, позволило построить в среде имитационного динамического моделирования MATLAB & Simulink их расчетную зависимость в виде фильтров соответствующих симметричных составляющих. Реализована возможность автоматизированного расчета, что более чем на порядок уменьшило время работы с моделью при исследовании режимов работы УСВЛ (СВЛ).

Разработана обобщённая методика моделирования на компьютере фильтров шести симметричных составляющих, что позволяет рассчитать и определить электрические величины не только простых, но и сложных видов повреждений для создания эффективной релейной защиты необходимой чувствительности, реагирующая не на фазные величины, а на их симметричные составляющие.

References Références Referencias

1. Веников В.А., Астахов Ю.Н., Постолатий В.М. Управляемые электропередачи переменного тока повышенной пропускной способности. – Электричество, 1969, № 12, с. 7-11.
2. V.M. Postolatii. Controllableflexible a.c. transmission systems. Conferinţa Naţională a Energiei,CNE'98. Energia mîine. Reconcilierea eficienţeişi competitivităţii cu dezvoltarea durabilă. 14-18 iunie, 1998, Neptun - Olimp, România. Report Nr. 61
3. Alexandrov G.N., Astakhov Y.N., Venikov V.A. et al. Electric transmission lines of increaset capacity and reduced ecological effect. – Paris, 1982.
4. L. A. Kojovic and J. F. Witte, "Improved protection systems using symmetrical components," 2001 IEEE/PES Transmission and Distribution Conference and Exposition. Developing New Perspectives (Cat. No.01CH37294), Atlanta, GA, USA, 2001, pp. 47-52 vol.1, doi: 10.1109/TDC.2001.971207.
5. I. A. Rizvi and G. Reeser, "Using symmetrical components for internal external fault discrimination in differential protection schemes," 2013 66th Annual Conference for Protective Relay Engineers, College Station, TX, 2013, pp. 68-79, doi: 10.1109/CPRE.2013.6822028.
6. Kiorsak M.V.,Postolatij V.M. Metod rascheta nesimmetrichnyh korotkih zamykanij na dvuh-cepnyh linijah jelektroperedachi so sblizhennymi fazami. «Informjenergo»,1984. (in Russian).
7. M. Chiorsac, Gh. Tertea, V. Sidelnicov, L. Turcuman Metoda componentelor simetrice în calculul circuitelor polifazate. Conferinţa tehnico-ştiinţifică a colaboratorilor, doctoranzilor şi studenţilor UTM, 19 noiembrie 2010, Chişinău
8. Kiorsak M., Turturica N. Methodology for Assessment the Possibility of Transfer Six-Phase Power Line into the Mode of Operation with Incomplete Number of Phases. Problemele Energeticii Regionale Nr. 1(45) / 2020
9. М.В. Киорсак, Ш. Фейгис, В.М. Постолатий. Определение электрических величин и

релейная защита УСВЛ. Монография. Кишинев, Штиинца, 1988, 222 стр
10. Hidaia M. A. Simulation of Some Power Electronics Case Studies In Matlab Simpowersystem Toolbox.,2018-47
11. Perelmuter V. Electrotechnical Systems: Simulation with Simulink and SimPowerSystems . CRC Press, 2012.
12. Вагнер К.Ф., Эванс Р.Д. Метод симметричных составляющих. – М., 1936. – 407 с.
13. Fortescue C.L. Method of symmetrical coordinates applied to solution pf poluphase network. “Transaction of AIEE”, 1918, vol. 33, Pt. 11. References must in APA Style.

Global Journal of Researches in Engineering: I
Numerical Methods
Volume 20 Issue 1 Version 1.0 Year 2020
Type: Double Blind Peer Reviewed International Research Journal
Publisher: Global Journals
Online ISSN: 2249-4596 & Print ISSN: 0975-5861

Finite and Numerical Simulations Applied in Tailor Welded Blank

By Wellington Augusto dos Santos, Etiene Pereira de Andrade,
Guilherme Souza Assunção & Gilmar Cordeiro da Silva
Pontifícia Universidade Católica de Minas Gerais

Abstract- The increase in economic and technological competitiveness means that the automobile industry seeks constant innovation in its production methods and processes, in order to produce lighter, safer and more efficient vehicles. Products with greater mechanical resistance, better conformability, thickness combinations of plates / materials are sought with a focus on reducing mass and increasing the rigidity of the vehicle body. In this scenario, Tailor Welded Blank (TWB), which is a top welding technique (by unconventional processes) of sheets of different specifications (materials, thicknesses and / or coatings), appears as a solution, as it allows localized distribution of mechanical properties, mass, optimizing the relationship between structural rigidity and the total weight of the vehicle body. The great challenge of this technique is to combine two processes with completely different demands, welding and mechanical forming. Due to the complexity of forming TWBs, the use of simulations has been widely adopted. In this review, different results of the numerical simulation methods used for a Tailor Welded Blank are compared, focusing on the details and the influence of the parameters used.

Keywords: *numerical simulation; tailor welded blank.*

GJRE-I Classification: *FOR Code: 010301*

Strictly as per the compliance and regulations of:

Finite and Numerical Simulations Applied in Tailor Welded Blank

Wellington Augusto dos Santos [α], Etiene Pereira de Andrade [σ], Guilherme Souza Assunção [ρ] & Gilmar Cordeiro da Silva [ω]

Abstract- The increase in economic and technological competitiveness means that the automobile industry seeks constant innovation in its production methods and processes, in order to produce lighter, safer and more efficient vehicles. Products with greater mechanical resistance, better conformability, thickness combinations of plates / materials are sought with a focus on reducing mass and increasing the rigidity of the vehicle body. In this scenario, Tailor Welded Blank (TWB), which is a top welding technique (by unconventional processes) of sheets of different specifications (materials, thicknesses and / or coatings), appears as a solution, as it allows localized distribution of mechanical properties, mass, optimizing the relationship between structural rigidity and the total weight of the vehicle body. The great challenge of this technique is to combine two processes with completely different demands, welding and mechanical forming. Due to the complexity of forming TWBs, the use of simulations has been widely adopted. In this review, different results of the numerical simulation methods used for a Tailor Welded Blank are compared, focusing on the details and the influence of the parameters used.

Keywords: numerical simulation; tailor welded blank.

I. Introduction

Tailor Welded Blank (TWB) is the combination of two or more metal sheets joined through the welding process, as shown in FIG. 1.There is possible to get a part with different materials, thicknesses, mechanical properties and coatings. This process leverages the global market in several sectors and especially the automotive market, due to the advantage of reducing production costs, weight and improving the structural performance of the vehicle. [1,2,3,8].

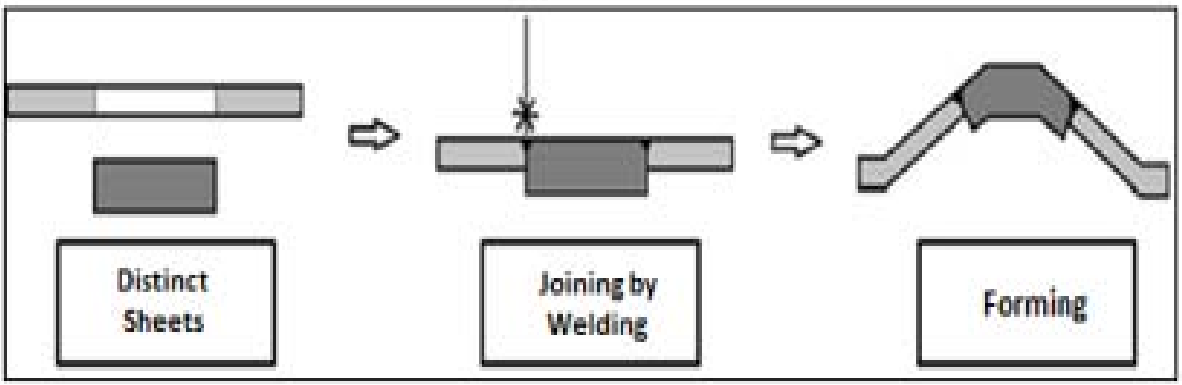

Source: (Adapted from ZHANG et al, 2016.)

Figure 1: Tailor Welded Blank principle

The patent this technique happened in 1964, been utilized on a large scale only in the late 1980s. In 1992, their application in the automotive industry stood out rightly, for its versatility [2,3,8]. The development of TWB technique shown in figure 2, enabled application in several parts in the car body, what that made possible the increment of resistance and mechanical rigidity according to the need of the vehicle and the behavior of the added part [1,2,3,8].

Author α: Pontifícia Universidade Católica de Minas Gerais, Belo Horizonte/MG, Brasil. e-mail: augustowellington@ymail.com
Author σ: Bolsista de Desenvolvimento Tecnológico Industrial-DTI - Conselho Nacional de Desenvolvimento Cientifico e Tecnológico-CNPQ, Belo Horizonte/MG, Brasil.
e-mail: andrade.etiene@hotmail.com
Author ρ: Universidade Federal de Minas Gerais, Belo Horizonte/MG, Brasil. e-mail: guilhermeassuncao@hotmail.com
Author ω: Pontifícia Universidade Católica de Minas Gerais, Belo Horizonte/MG, Brasil. e-mail: gilmarcord@gmail.com

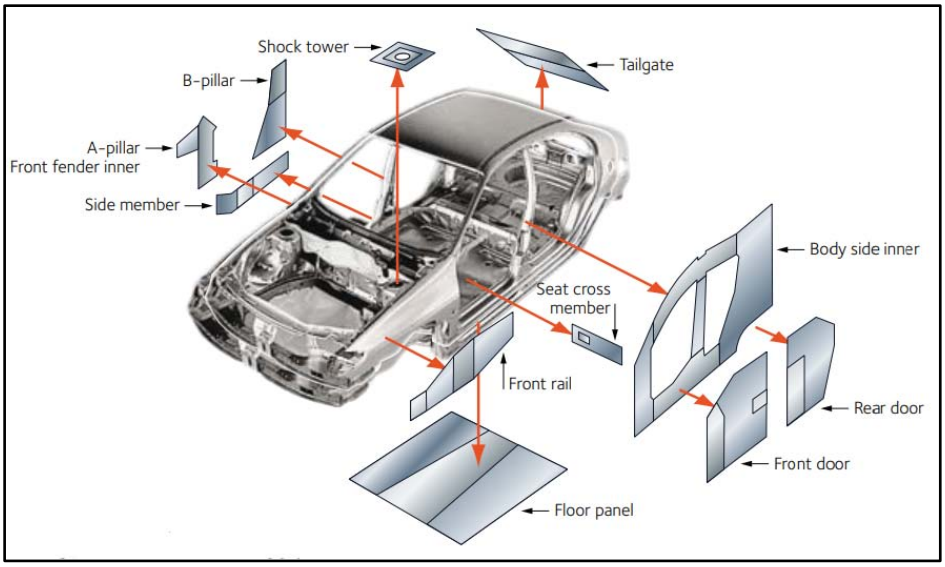

Source: (Adapted from the Arcelor Mittal Europe catalog, p.7).

Figure 2: Parts of a Car body with the application of Tailor Welded Blank

However, despite the advantages conferred by the use of TWB, their application can be considered complex, involving several variables and some complications. The most common problems are splits in the weld region, injurious levels of residual stresses, reduced formability in and displacement of the weld line during forming [2,3,8].

To avoid the occurrence of failures, some adjustments are made to the dies and recently was worked finite element analysis simulations in computer. However, given the complexities of modeling conventional of TWBs, the levels of correlation are not always the best. Numerical modeling of TWBs is more complicated than the modeling of conventional sheet metal forming processes. The great difficulty in performing the numerical modeling in the TWBs conformation is due to the mechanical properties caused by the welding process, and the non-uniformity of the base materials. [3,4,5].

This paper aims to provide an overview of the use of numerical modeling techniques for different simulations in TWBS, listing the advantages and disadvantages in industrial application, as well as the challenges and research activities.

II. Numerical Simulation Methods in Sheet Forming

The appearance of the finite element methods (FEM) occurred in the aerospace industry in the early 1950s, as a powerful numerical tool for solving mathematical engineering and physics problems, improvement the numerical resolution of a system of partial differential equations. One of the reasons why the FEM has been successful since the beginning of its formulation is its basic concept of discretization that produces many simultaneous algebraic equations that are generated and solved with the help of computers [6,7,8].

Due to the complexity of the sheet forming process, mainly in the deep-drawing operation, a fact, which led the engineers and designers, incorporate the FEM to development, seen the need to reduce the time and costs in the modelling of a new project. [6,8,55,62,63].

The representations of the effects of the contours of the elements in the sheets forming must be considered for permanent deformations and major changes in the geometry of the product. For this, it is necessary to use interpolation functions, which are curves built from known values, which in this case are the degrees of freedom of the element nodes. [6,7,9,55,62].

During the stamping of a product, the blank is subjected to a complex historical deformation and varied boundary conditions. Because of this loading history, the theory should describe the deformation of the blank that can be discretized as bi or three-dimensional. Three different classes of elements can be used in the printing simulation: MEMBRANE, SHELL and SOLID [6,9].

The membrane elements have three degrees of freedom of translation per node, in the direction that two nodes are tangent and a force is normal to knot. The orientation of the normal force at the node is determined by averaging the normal forces adjacent to the element. The geometry of the sheet is adjusted through the contact of the tools. However, this method is not recommended for calculating elastic return (spring back), as it does not accurately represent the simulated values [7,9].

The shell elements have a knot with five degrees of freedom: three of translation for the two tangent vectors and the normal vector, and two rotations with the tangent vectors on the axis of rotation. The shell element is an element capable of calculating bending and has membrane characteristics. Loading in flat and perpendicular directions is allowed. All shell element formulations have an arbitrary number of integration points along the thickness of the sheet. It is recommended for all stamping operations, but it does not express accuracy for sheets of high thickness [6,7,9].

The 3D or solid elements represent all degrees of freedom and the results of a simulation with this element allow an accurate visualization of stresses and strains through the thickness and with precise spring back data. Results of a simulation with solid elements help to visualize the material's behavior in problematic regions. The disadvantage of this method is the processing time, as there are solid elements in the thickness that generate a model with many more elements, which does not happen when we use the shell elements [7,9].

III. Numerical Modeling Methods in Tailor Welded Blanks

Numerical modeling in TWBs is more complicated than modeling of conventional sheet metal forming processes, mainly due to the change in mechanical and elastoplastic properties caused by the welding process and the difference in thickness between the base materials [5,10,11,12,61].

The modeling of TWBs by finite elements there are two methods: the first takes into account the weld line (TAZ - Thermally Affected Zone and WZ - Weld Zone), with a much more refined and precise mesh. The second neglects the effects of welding [13]. The first applies only in situations in which there is no localized strain of great intensity in the weld [5,11,14,61,62].

The simplification of the first method may cause a relative discrepancy between the practical and the simulated results. This is because in these models the Tailor Welded Blank Forming Limit Diagram (FLD) is not taken into account, but only the base materials. There is then another challenge to be overcome: prediction of the FLD of a TWB considering the local and global effects of the weld [15,59].

The conventional methods, using stamping software (such as PAMSTAMP®, for example), there is a level of accuracy higher than 94%, which is considered excellent. When working with the stamping of TWBs, this correlation is reduced to 78%, which explains the difficulty in predicting failures [16].

There are several parameters that directly influence the numerical modeling of TWBs. Welding processes can significantly change the mechanical properties of materials in weld zone (WZ) and Heat Affected Zone (HZA). However, materials should not be considered as uniform. To survey the parameters to be adopted in the numerical simulation, the results of experimental tests are necessary, revealing the localized mechanical behavior, such as the flow limit and the plasticity parameters of the regions affected by the welding process [10,11, 5].

The Plasticity is the area of mechanics that relates the calculation of stresses and strains in a body, which needs to be relatively ductile, permanently deformed by a set of applied forces. The theory is based on experimental observations on the macroscopic behavior of metals in uniform states of combined stresses. The results obtained are then idealized in mathematical equations that describe the behavior of metals under complex tensions [17,18,19,5,59].

However, it is necessary to develop more techniques that are experimental and analytical methods to quantitatively assess the mechanical characteristics of the welded metal and the formability of TWBs. Effects such as strain hardening during shaping and anisotropy of welded metal, for example, must be taken into account [20].

For mechanical characterization of Tailor Welded Blanks, tensile tests have been adopted, with specimens of different configurations, to feed numerical simulations and to be confronted with the so-called Mixture Rule [21,22]. In this case, we work with the ASTM E-8M standard [3].

The Mixtures Rule is used to extract properties from the weld, aiming to verify its influence on the mechanical properties and the elongation of the TWB. Thus, the load proportions supported by the weld and the base metal are calculated, assuming homogeneous deformation uniformity for the three materials [3,8].

Than those referred to mechanical effects, we also deal with micro structural issues related to welding in the Weld Zone. The changes, depending on the materials used, can be considerable. It is generated from a local softening of marten site to complex phase transformations in conditions imbalance, depending on the welded materials, the process and the welding parameters [21,23].

The two most used criteria in the numerical modeling of TWBs are based on the Theory of Plasticity: Yield and isotropic hardening. Different models of isotropic hardening in which the plastic deformation largely exceeds the yield, can be used in the modeling of Tailor Welded Blanks [10,11,7]. However, Holloman's equation is the simplest and most widely used model, and can be expressed as:

$$\overline{\sigma} = K\overline{\varepsilon}_p^n \quad (1)$$

Where:

- $\overline{\sigma}$= is the true stress
- K = is the resistance coefficient
- $\overline{\varepsilon}_p$ = is the true strain
- n = is the strain hardening coefficient

After the linearization of the Holloman equation, the strain-hardening coefficient can be determined, which is a key parameter to obtain the maximum deep drawing limit in the inlay operations. The higher the strain hardening coefficient, the greater the capacity of the material to strain, without the occurrence of necking down.

If there is a quantitative relationship between strain rate and yield stress, the Ludwik model can be used, which is a modification of the Holloman equation. In cold work, the yield stress is high at each strain level, mainly due to the strain-hardening phenomenon, so the yield stress is added to the equation [10,11,5]. Ludwik's law can be expressed as:

$$\overline{\sigma} = \sigma_y \; K\overline{\varepsilon}_p^{\,n} \tag{2}$$

Where:

- $\overline{\sigma}$= is the true stress
- σ_y = is the yield stress
- K = is the resistance coefficient
- $\overline{\varepsilon}_p$ = is the true strain
- n = is the strain hardening coefficient

The equations can be used so much to forming the TWBs how much for the base metal of the weld. If there is a need to consider the pre-strained material, the Ludwik model can also be modified [10,11,5]. Ludwik's law is modified and can be expressed as the Swift Equation:

$$\overline{\sigma} = \sigma_y \; \mathrm{K}\left(\overline{\varepsilon}_{p+}\overline{\varepsilon}_{0}\right)^{n} \tag{3}$$

Where:

- $\overline{\sigma}$= is the true stress
- σ_y = is the yield stress
- K = is the resistance coefficient
- $\overline{\varepsilon}_p$ = is the true strain
- $\overline{\varepsilon}_0$ = is the true strain rate
- n= is the strain hardening coefficient

A model widely used in the literature to describe the behavior of metals, such as aluminum, is the Voce equation, which takes into account the three parameters: initial yield stress, maximum stress and relaxation strain in the dynamic recovery regime. Such equation is described as:

$$\overline{\sigma} = \mathrm{A} - \mathrm{Bexp}(-\mathrm{C}\overline{\varepsilon}_{\mathrm{p}}) \tag{4}$$

Where:

- $\overline{\sigma}$= is the true stress
- A= is the steady-state flow stress voltage reached at high deformations
- $\overline{\varepsilon}_p$ = is the true strain
- C = is non-dimensional

For metals such as aluminum and ferritic stainless steels, once recovery is established, its effect is sufficiently efficient to contain hardening strain and the forming stress curve follows a horizontal line. Strains rates for both are omitted in FEM analysis of TWBs. However, one can simply take into account the effect of the strain rate, by multiplying the hardening strain law by a term like $\dot{\varepsilon}^m$ [10,18,24].

Steel sheets, due to the rolling process, have a very significant anisotropy. This can influence data entry for numerical simulation, so it is extremely important to analyze the best yield criterion to be used in experimental tests [24,10,25,26].

However, the importance of anisotropy in the process of forming TWBs, the isotropic criterion of Von Mises and Gurson - Tvergaard - Needleman (GTN) are still frequently used. Von Mises formulated a flow criterion suggesting that this phenomenon occurs when the second invariant of the deviation stresses reaches a critical value. [10,12,26,27]. The Von Mises model can be expressed as:

$$\sqrt{J}_{2\,-\frac{1}{\sqrt{2}}}\Phi\,(\alpha) \tag{5}$$

Where:

- Φ= depends on the hardening strain parameter
- α= is the radius of the yield surface

The second invariable tensor is given as:

$$\overline{\sigma} = \sqrt{J_2} \; = \sqrt{3/2}\,S{:}S = \sqrt{3/2\;S_{ij}\,S_{ij}} \; = \; S_{ij} \; = \sigma_{ij} \; - \; \sigma_m \delta_{ij} \tag{6}$$

Where:

- $\overline{\sigma}$= is the equivalent stress
- δ_{ij} = is the Kronecker delta, in matrix form, corresponds to the identity matrix

Hill's model is proposed for the yield of an anisotropic material and is assumed to be a quadratic function of the stress space. This is can be expressed as:

$$F(\sigma_{22-}\sigma_{23})^2 + G(\sigma_{33-}\sigma_{11})^2 + H(\sigma_{11-}\sigma_{22})^2 + 2L{\sigma_{23}}^2 + 2M{\sigma_{31}}^2 + 2N{\sigma_{12}}^2 = 1 \tag{7}$$

Where:

- F, G, H, L, M, N = are experimentally determined coefficients

The yield surface is defined using the three values r ($r_{0,}r_{45,}r_{90,}$) and the initial yield stress in the rolling direction [10,11,12,25,59]. If the biaxial factor is equal to 1 it is the classic Hill-48 model. Applied to flat tension the criterion can be used as:

$$\sigma_1{}^2 + \frac{R_0(1+R_{90})}{R_0(1+R_0)}\sigma_2{}^2 - \frac{2R_0}{1+R_0}\sigma_1\sigma_2 = \sigma_{y,1}{}^2 \quad (8)$$

Where:

- $\sigma_{y,1}{}^2$ = is the uniaxial yield stress
- $R_0 e\ R_{90}$ = are the coefficients of Lankford

Figure 3 shows how the experimentally extracted anisotropy parameters are related. The RD and TD are the directions in which the test samples of the steel plate are removed. With these parameters, the criteria for numerical simulation of the TWBs are modeled.

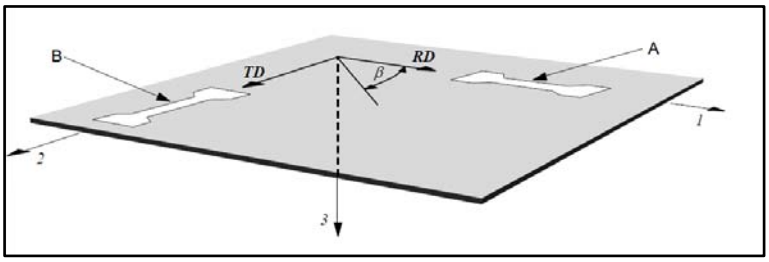

Source: (Adapted from Theory_of_Plasticity, p.11)

Figure 3: Orientations of the samples plans

The material constants present in the Hill criterion (F, G, H) are related to the parameters experimentally determined RD and TD. forR_0we have:

$$R_{\beta=0} = R_0 = \frac{d\varepsilon_{TD}^p}{d\varepsilon_{33}^p} = \frac{d\varepsilon_{22}^p}{d\varepsilon_{33}^p} - \frac{F\sigma_2 + H(\sigma_2 - \sigma_1)}{F\sigma_2 + G\sigma_1} = \frac{H}{G} \quad (9)$$

In case the mode is stretched in the second direction TD, we have the value ofR_{90}:

$$R_{\beta=90} = R_{90} = \frac{d\varepsilon_{RD}^p}{d\varepsilon_{33}^p} = \frac{d\varepsilon_{11}^p}{d\varepsilon_{33}^p} - \frac{G\sigma_1 + (H\sigma_1 - H\sigma_2)}{F\sigma_2 + G\sigma_1} = \frac{H}{F} \quad (10)$$

In the case of normal anisotropy, the flat stress version of Hill's 1948 yield criterion can be written as:

$$\sigma_1{}^2 + \sigma_2{}^2 - \frac{2R}{1+R}\sigma_1\sigma_2 = \sigma_{y,1}{}^2, R_{90} = R_0 = R_{45} \quad (11)$$

In 1979, Hill proposed a generalized non-quadratic criterion to explain an "anomalous" observation in some aluminum alloys, where the yield forces in biaxial stress were superior to the yield forces in uniaxial stress (which is not allowed by Hill's test 1948) [7,10,12,28]. The proposed model:

$$F|\sigma_2 + \sigma_3|^m + G|\sigma_3 - \sigma_1|^m + H|\sigma_1 - \sigma_2|^m + L|2\sigma_1 - \sigma_2 - \sigma_3|^m + M|2\sigma_2 - \sigma_3 - \sigma_1|^m + N|2\sigma_3 - \sigma_1 - \sigma_2| = \sigma_y{}^m \quad (12)$$

Where:

- F, G, H, L, M, N = are experimentally determined coefficients
- m = can be calculated from the non-linear relationship
- $\sigma_y{}^m$ = is the uniaxial yield stress

Other yield criteria can be derived from this model assuming combinations of experimental parameters [10]. Hosford elaborated his generalized criterion for Hill's yield and can be obtained considering L = N = 0. [10,28]. So for a flat isotropic material we get:

$$\frac{1}{1+R}(|\sigma_1|^m + |\sigma_2|^m) + \frac{R}{R+1}|\sigma_1 - \sigma_2|^m = \sigma_y{}^m \quad (13)$$

Where:

- $\sigma_y{}^m$ = is the uniaxial yield stress
- R = is the coefficient of Lankford

For a non-isotropic material, the Hosford criterion is treated by:

$$G|\sigma_2 - \sigma_3|^m + G|\sigma_3 - \sigma_1|^m + H|\sigma_1 - \sigma_2|^m = 1 \quad (14)$$

Where:

- F, G, H = are the coefficients of Lankford
- m = can be calculated from the non-linear relationship

The Barlat model is formulated in the stress space. The yield surface is defined using the Lankford coefficients ($r_{0,}r_{45,}r_{90,}$) and the exponent m. he Barlat model was specially developed for the description of aluminum alloys. [10.19.28]. It is also a generalization of the Hosford criterion for the case where the directions of the orthotropic axes:

$$\phi = (3I_2)^{\frac{m}{2}}\left\{\left|2\cos\left(\frac{2\theta+\pi}{6}\right)\right|^m + \left|2\cos\left(\frac{2\theta-3\pi}{6}\right)\right|^m + \left|2\cos\left(\frac{2\theta+5\pi}{6}\right)\right|^m\right\} = 2\bar{\sigma}^m \quad (15)$$

Where:

- θ = $\arccos\left(I2/I3^{3/2}\right)$ with the second and third stress determining invariant ($I_2 I_3$) re used using Bishop-Hill notation.
- m = represents the number of experimental r values

The yield model of Gurson Tvergaard Needleman (GTN) are generalizations of two models are the isotropic of Von Mises and Hill 1948 [10,19,26,27,28]. For the isotropic model, we have:

$$\Phi = \left(\frac{\sigma_{eq}}{\sigma_y}\right)^2 + 2q_1\varphi\cos h\left(-q_2\frac{3\sigma_H}{2\sigma_y}\right) - (1 + q_3\varphi^2) = 0 \quad (16)$$

Where:

- σ_{eq} = is the equivalent stress of Von Mises
- σ_y = is the yield stress of material
- σ_H = is the Hydrostatic stress of material
- q_1, q_2, q_{31} = are material parameters determined experimentally

For the modified criterion presenting the anisotropy parameters, we have:

$$\Phi = \left(\frac{\sigma_{eq}}{\sigma_y}\right)^2 + 2q_1\varphi \cos h\left(-q_2\sqrt{\frac{1+2R}{6(1+R)}}\frac{3\sigma_H}{\sigma_y}\right) - (1 + q_3\varphi^2) = 0 \quad (17)$$

Where:

- σ_{eq} = is the equivalent stress of Von Mises
- σ_y = is the yield stress of material
- σ_H = is the Hydrostatic stress of material
- q_1, q_2, q_{31} = are material parameters determined experimentally
- R = are the coefficients of Lankford

The numerical simulations used with this criterion are performed to describe the damage to the materials, which involves the triaxiality of the stress, that is, the law is based on the physical ductile fracture mechanism, that is, empty nucleation, growth and coalescence [5,7,10,19,26, 28].

IV. Finite Elements Method for Modeling of TWBs

One of the main objectives in applying a virtual analysis (figure 4) is to calculate the movement of the weld line and provide an ideal force balance between the punch and blankholder. The results of this combination aim to control the flow of the blank to be forming, avoiding the movement of the weld line and thus reducing the high tensile stresses perpendicular to the weld line [29,61,62,55].

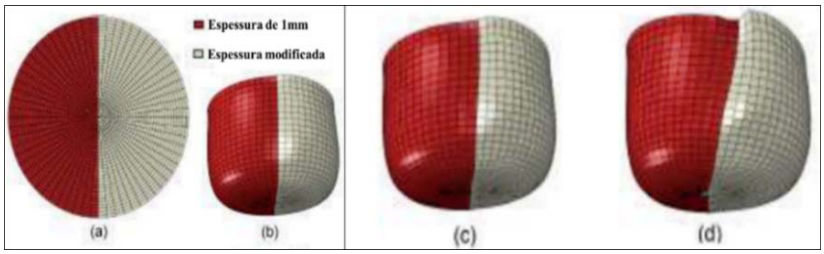

Source: (Adapted from FAZLI, 2016).

a) initial blank b) thicknesses of 0.85mm and 1mm c) thicknesses of 0.75mm and 1mm d) thicknesses of 0.5mm and 1mm.

Figure 4: Initial blank and three samples stamping with different thickness combinations

As the weld line moves to critical deep areas of inlay, the forming of the blank decreases. In some studies developed to control this situation, several tests have been carried out to decrease the strain in the thicker material, from increasing the flow of the thicker material and even reducing the stamping force on the thinner material. For that, the concept of draw beads was worked and pressure points were controlled in isolated quadrants of the blank holder [1,61,62].

Adony and Chen cited by Gautam found a strong correlation between the ductility of the weld and the limiting dome height for longitudinally welded TWBs, doing flat stretch, with original materials of similar thickness and different materials and coating combinations. The Limiting Drawing Ratio (LDR) for a TWB is between the values of the thinnest and thickest sheet if the thickness ratio is different from the unit [30,31].

According to research carried out by R. Safdarian and M. J. Torkamany, he describes that after the experimental tests carried out; the different thicknesses of the TWBs were modeled in the ABAQUS® program. The Finite Elements Method (FEM) was used to construct Forming Limit Diagram (FLD) based on the Hecker principle. In the physical cupping tests, the Limit Dome Height parameter was used, as shown in figure 5 [25].

For simulation, the following data were collected from the materials that make up the TWB: Yield Strength (YS), Ultimate Tensile Strength (UTS), hardening exponent (n), hardening coefficient (K) , total elongation and anisotropy coefficient (R_0, R_{45}, R_{90}) [25].

In the modeling, the Punch, Die and blankholder were considered as rigid items. The TWBs were modeled as a shell element with S4R elements, maintaining the left and right side weld line inclination between 20 ° and 45 °. The calculation of stresses and strains was based on the Hill criterion (1948) and a flat state of strain was sought. To perform the tests, the use of a 20-ton hydraulic press is suggested [25].

The experimental results show that the greater the difference in thickness and mechanical strength between the materials that make up the TWB, the greater the movement of the weld line. As a consequence, the lower the stamping of the TWB will be, which is reflected in a lower Limit Dome Height (LDH), as shown in figure 5 [25].

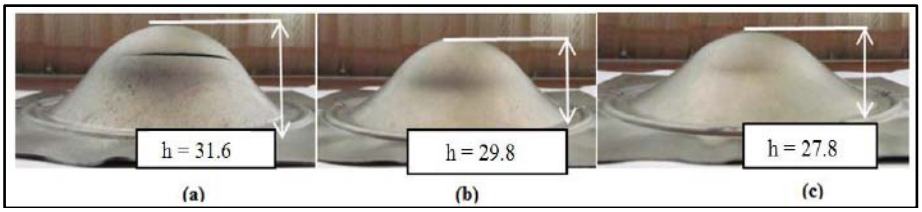

Source: Safdarian; Torkamany, 2016

Figure 5: Limit Dome Height for different thickness ratios (A) 1.25 (B) 1.7 and (C) 2.13

Figure 6 shows the movement of the weld line in mm, due to the reason for different thicknesses after the experiments.

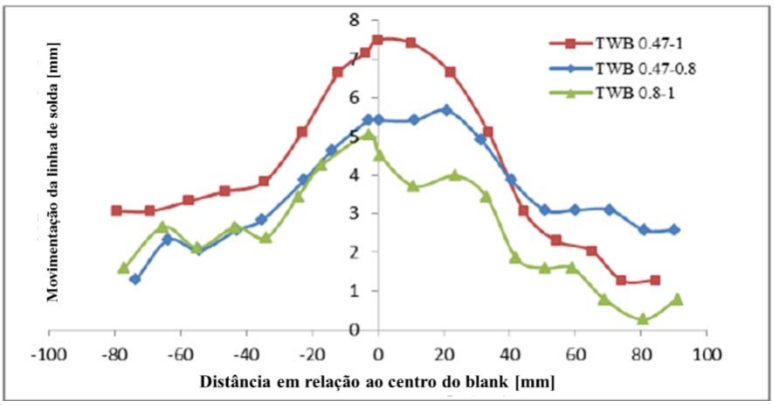

Source: Safdarian; Torkamany, 2016

Figure 6: Movement of the weld line for different thickness ratios of the plates that make up the TWB

In general, the greater the difference in thickness and mechanical strength between the materials that make up the TWB, the greater the movement of the weld line. Consequently, less tends to be its conformability [25].

According to research by Masumi, Nakajimacupping tests, tensile tests and simulations were performed to correlate the values obtained experimentally. In the simulations, the effects of welding on WZ and HAZ were not considered. The weld line was referred to only as the dividing point between the two materials that made up the TWB. For a better correlation, it was necessary to use the anisotropy criteria and parameters [5,32].

In the work developed by Gautam, for the TWB, the simulation was performed on half the blank, being obtained for a complete blank using the principle of symmetry on the X-Y plane, this is technique was applied to reduce the size of the problem and the time of the simulation. The FEM analysis of the base material sheet was also performed to compare the LDH values obtained in each case [30,31].

Hill's plasticity model, also known as Hill's yield potential, which is an extension of the Von Mises function for anisotropic materials, was used in finite element modeling to incorporate sheets anisotropy.

Figure 7 shows the mesh and elements used for simulation in Gautam's work.

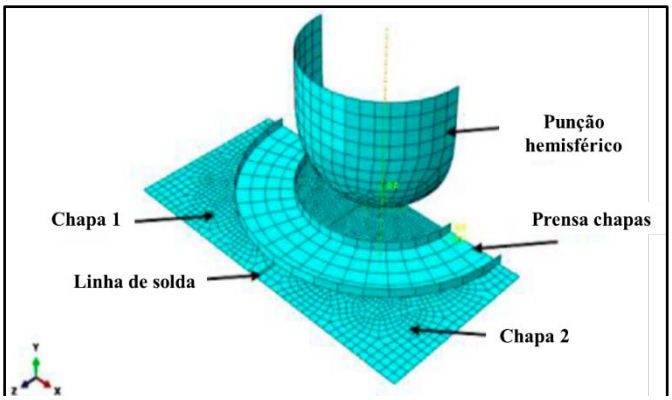

Source: Adapted from Gautam et al (2019).

Figure 7: Mesh and elements used for simulating a TWB

Gautam's experimental results showed that LDH is higher in the thicker sheet than in the less thick sheet, indicating greater formability of the thicker sheet. Similar results were observed in the simulations, although higher LDH values were obtained in a simulated manner [30,31].

The refinement of simulations through experimental tests is of fundamental importance. The failure points predicted for the FLD were captured in the DYNAFORM® software. These points were plotted as major and minor strains for a comparison with the actual stress data obtained from the LDH experiments [30,31].

Gautam's results showed that the simulation predicts a maximum displacement value of the weld line of 2.45mm, which is lower than the experimental values of 2.57mm. This deviation in the results of the displacement of the weld line obtained by experiments and the numerical results can be attributed to the friction between the punch and the blank [30,31].

In another study, developed by Korouyeh in interstitial free steel sheets (IF - Interstitial Free) were used to compose a TWB. The numerical investigation of the TWBs forming was done using a commercially available finite element code ABAQUS 6.10® [60].

The model consisted of a hemispherical punch, blankholder, die and blank. This model was based on the Hecker Forming Limit Diagram (FLD) test. Eight specimens of size 25mmx200mm to 200mmx200mm were cut from the laser-welded sample, so that the weld line was perpendicular to the stretch direction (cross-sectional samples) [33].

In the standard cupping tests, the check also took place on the thinner side of the TWB and parallel to the weld line. Figure 8 shows the FLD of the TWB made. It is noticed that the numerical criteria cannot predict the right side of the FLD, being suitable only for the left side, under condition of plane strain.

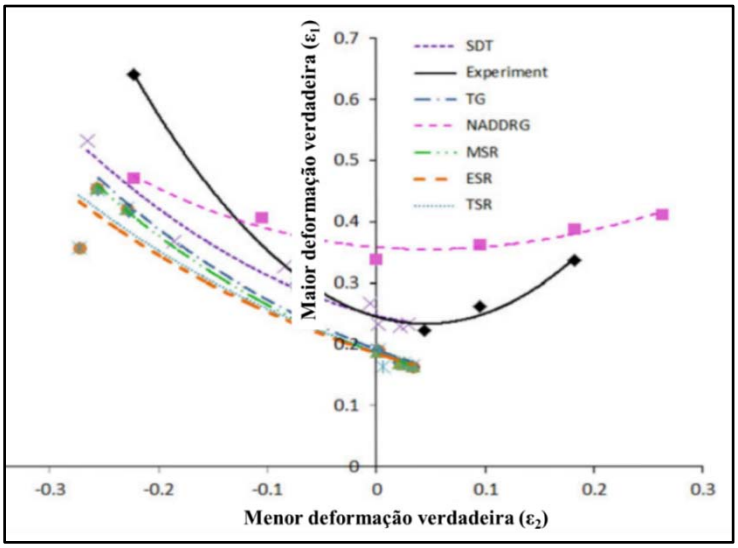

Source: Korouyeh et al, 2012.

Figure 8: Different FLDs from the same TWB, obtained from different methods

Figure 9 shows the results for samples of different widths, showing that there are different heights of LDH. For experiments and numerical criteria, the LDH height was smaller for the 125mm wide sample.

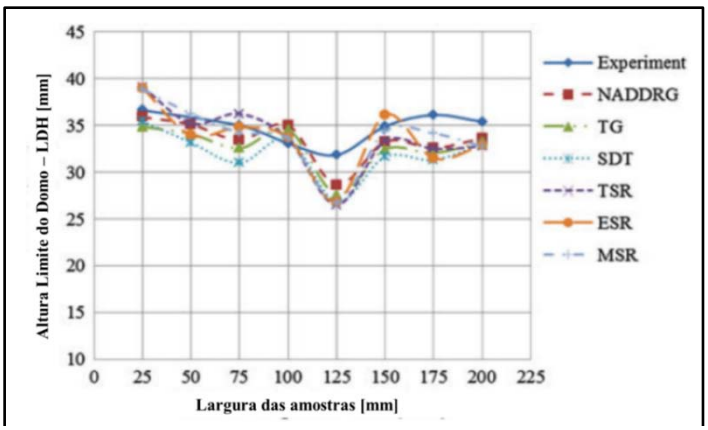

Source: Korouyeh et al, 2012.

Figure 9: Results of the LDH test, for samples of different widths, working with different evaluation criteria

TWB samples with different widths produce different LDH values, so the dispersion of the LDH test depends on the variation of the stress path at the fracture site. For experiments and numerical criteria, the LDH value is minimum for a 125mm wide sample that is in the plane stress condition [33].

The comparison of the fracture position of the FEM and the experiment shows that there is good agreement for the fracture position predicted by the SDT criterion and experiment. The results show that, due to the increase of the sample width or in the condition of biaxial elongation, the fracture occurs closer to the weld line.

In research carried out by Andrade and Santos, the conditions found to be optimal in the tensile test (relative inclination of the 30º and 60º weld line) were simulated. In this work, it was evidenced that the total relative elongation of the weld line would support a maximum strain for an angle of 30 ° in relation to the rolling direction of the base materials. The AutoForm® forming software, from the AutoForm ®Company with triangular meshes, Shell model, friction coefficient 0.15 was used. The materials considered were FEE 210 with 1.10mm and FeP05 0.65mm, both IF. The yield criterion used was based on the Hill 1948 and the Hollomon model [2,3,8,34].

Figure 10 Represents the maximum elongation graph extracted in the tensile test for an angle of 30 °

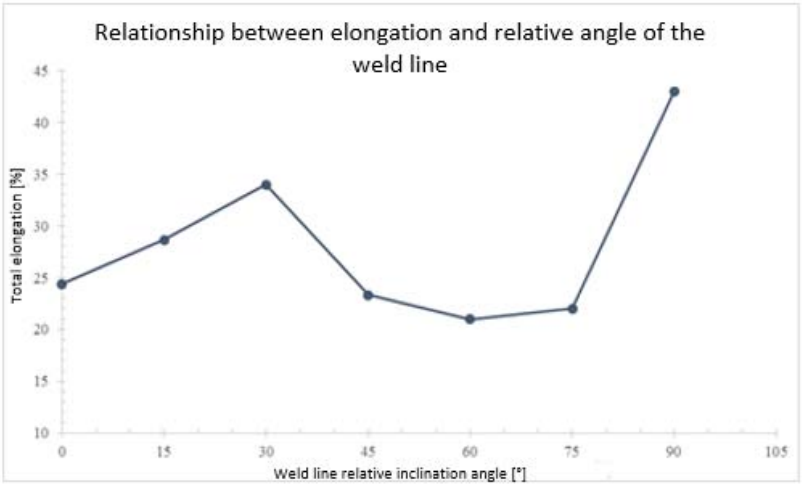

Source: Andrade, Etiene Pereira de; Santos, Wellington Augusto dos, 2019.

Figure 10: Relationship between the total elongation and the relative inclination angle of the weld line

After the experimental test, the Door Inner was simulated as shown in figure 10. That product always presented several stamping problems, such for example as localized splits in deep-drawn part.

Figure 11 Result of the stamping simulation, showing strain deviation curve as a function of the relative inclination angle of the weld line

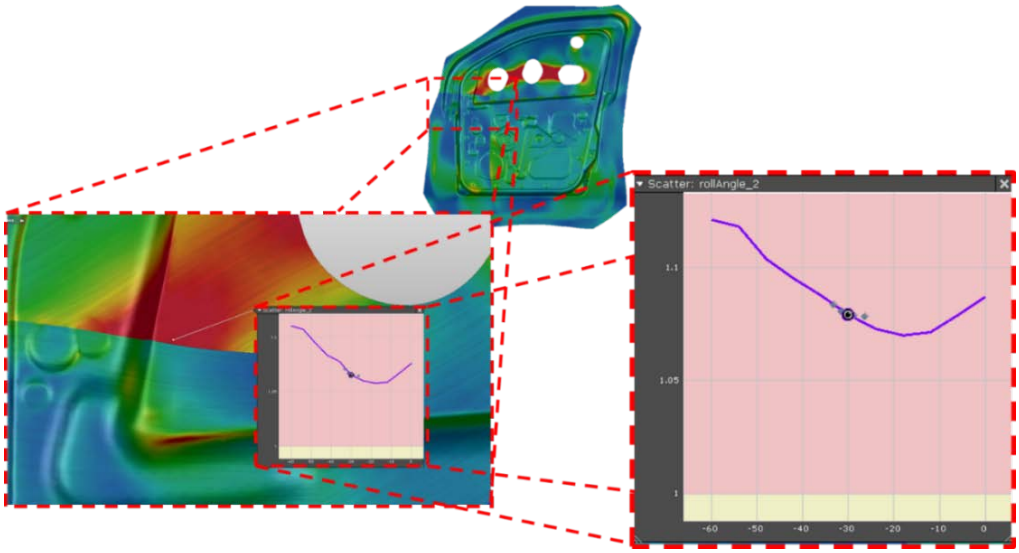

Source: Andrade, Etiene Pereira de Santos, Wellington Augusto dos, 2019.

Figure 11: Result of the stamping simulation

According to the highlighted strain curve, it turns out that the maximum stress peak tends to decrease, indicating that the purely tensile stresses are attenuated. Even that happen the weld line fractures, efforts will are reduced. This indicates the relative improvement in mechanical behavior when tilting the weld line. However, the simulation does not take into account the weld (HAZ and WZ), nor their mechanical properties [2,3,5,8,34].

In summary, there is then a lack of methods and processes that more accurately determine the effects of the forming about the TWB. It is therefore necessary to develop more experimental techniques and analytical methods to quantitatively evaluate the mechanical characteristics of the welded metal and the formability of TWBs. Effects such as hardening strain during shaping and anisotropy of welded metal, for example, must be taken into account. In this respect, the use of simulations is will growing and aims to overcome the challenges mentioned above.

V. Conclusions

A review of the TWBs was elaborate and in most of the work done, researchers always adopt a numerical model in their studies that disregards the WZ and the HAZ. This parameter is often adopted due to the limitations of the software's used, due to the high computational cost or the lack of experimental data for the mechanical and micro structural behavior of the weld.

Usually the elements of numerical analysis used are the shell, due to its speed of data processing and good precision. However, the inclusion of the Heat-Affected Zone (modeled also by the shell element) does not represent an improvement in the results forming and the localized Springback\ effect. The reason is that due greater resistance to yield and Heat-Affected Zone modulus of the weld has an opposite effect to the elastic return.

An alternative likely would be to model the weld in 3D solid elements and the base materials by the shell element. Where the movements of the dependent nodes will be interpolated from the movement of independent nodes in the base metal mesh. The solid formulation in the region is the case where the elastic portion of the deformation is not neglected.

However, to that, there is a good approximation for numerical modeling, some conclusions are recommended:

- ✓ Previous qualification and analysis of the weld, by means of microscopy, either optical or electron beam scanning;
- ✓ The weld line must not be worked entirely parallel to the rolling direction (relative inclination of 0°), nor entirely perpendicular (relative inclination of 90°), as it tends to facilitate the propagation of cracks, splits and worsen the mechanical behavior of the TWB;
- ✓ It is necessary that the base materials work in a balance of forces (FA = FB) and, to satisfy these conditions, disregarding the metallurgical effects. This thickness ratio, the greater than the unit (1.0), the worse the forming, the threshold can be obtained by the equation: $\mathrm{LSR} = \left(\frac{\sigma_{YB}}{\sigma_{TA}}\right) = \left(\frac{t_{0A}}{t_{0B}}\right)$(18)
- ✓ The tensile tests, once the weld is qualified, proved to be useful for surveying the mechanical properties of the TWB and the influence of the relative inclination of the weld line on its performance during forming;
- ✓ Determination of an optimized curve (FLD) for the three materials, including here the weld region , which is extremely important for the development of TWBs, because with the obtaining of the curve it is possible to previously identify conditions that would lead to plastic instability or even to material failure.

The validation of the numerical model requires constant comparison with experimental results, in order to identify possible deviations in the simulation results. Thus, the validation of numerical simulation has a fundamental role in this field of investigation.

Acknowledgments

The authors would like to thank FIAT Chrysler do Brazil for the technical contribution to this research, Capes (Coordination for the Improvement of Higher Weight) and PUC Minas (Pontifical Catholic University of Minas Gerais) for financially supporting this research and for assisting in the publication of this article.

References Références Referencias

1. MEINDERS, T; BERG, A Van Den; HUÉTINK, J. Deep drawing simulations of Tailor Blanks and experimental verification. Journal of Materials Processing Technology, [s.l.], v. 103, n. 1, p.65-73, jun. 2000. Elsevier BV.
2. ASSUNÇÃO, Guilherme Souza; ANDRADE, Etiene Pereira de; SANTOS, Wellington Augusto dos; FELIZARDO, Ivanilza Felizardo; BRACARENSE, Alexandre Queiroz Bracarense. Caracterização Mecânica da Região Soldada de Tailor Welded Blanks (TWB) a Partir do Perfil de Microdureza. Soldagem & Inspeção, [s.l.], v. 24, p.1-10, 2019. FapUNIFESP (SciELO). http://dx.doi.org/10.1590/0104-9224/si24.32.
3. ANDRADE, Etiene Pereira de; ASSUNÇÃO, Guilherme Souza; SANTOS, Wellington Augusto dos; FELIZARDO, Ivanilza Felizardo; BRACARENSE, Alexandre Queiroz Bracarense. Caracterização Mecânica e Análise Microestrutural de Chapas Obtidas pelo Processo de Tailor Welded Blank (TWB). Soldagem & Inspeção, [s.l.], v. 24, p.1-11, nov. 2019. FapUNIFESP (SciELO). http://dx.doi.org/10.1590/0104-9224/si24.25

4. ZADPOOR, A. A., Sinke , J. and Benedictus , R. (2008 a) ' Experimental and numerical study of machined aluminum tailor made blanks ', Journal of Materials Processing Technology ,200 , 288 – 299.
5. M. Shehryar Khan, M. H. Razmpoosh, E. Biro & Y. Zhou (2020): A review on the laser welding of coated 22MnB5 press-hardened steel and its impact on the production of tailor-welded blanks, Science and Technology of Welding and Joining, 26 Mar 2020.https://doi.org/10.1080/13621718.2020.1742472.
6. DOS REIS, L.C.: Estudo dos Parâmetros de Influência na simulação numérica de estampagens de Chapas. Dissertação de Mestrado. Curso de Pós-Graduação em Engenharia Metalúrgica e de Minas. UFMG. 2002.
7. Amit Kumar Rana; Suchibrata Datta; Sanjib Kundu. Deformation behaviour during deep drawing operation under simple loading path: A simulation study, [s.1], V. 2; n.3, p. 1–6, 31 December 2019. Elsevier BV. https://doi.org/10.1016/j.matpr.2019.12.413
8. ANDRADE, Etiene Pereira de SANTOS, Wellington Augusto dos; BRACARENSE, Alexandre Queiroz. Caracterização mecânica e análise de falhas de chapas fabricadas pelo processo de Tailor Welded Blank submetidas a estampagem profunda. ABM Proceedings, [s.l.], p.293-301, out. 2017. Editora Blucher.
9. AUTOFORM PLUS R3.1®: Software for Sheet Metal Forming. AutoForm Engineering GmbH.2011.
10. ZADPOOR, A. A,; SINKE, J,; BENEDICTUS,R. Woodhead Publishing Limited, 2011 Numerical simulation modeling of tailor welded blank forming. Materials Innovation Institute (M2i) and Delft University of Technology, the Netherlands:p.68-94, 2011Woodhead Publishing Limited.
11. Yong Chan Hur; Yong Chan Hur; Byung Min Kim; Myoung-Gyu; Ji Hoon Kim. MEASUREMENT OF WELD ZONE PROPERTIES OF LASER-WELDED TAILOR-WELDED BLANKS AND ITS APPLICATION TO DEEP DRAWING. 2020 KSAE/ 115–08 pISSN, [s.1], V. 21; n.3, p. 615–622, 30 January 2019. International Journal of Automotive Technology. https://DOI 10.1007/s12239–020–0058.
12. Hossein Moayedi; Roya Darabi; Aria Ghabussi; Mostafa Habibi; Loke Kok Foong h. Weld orientation effects on the formability of tailor welded thin steel sheets, ScienceDirect ,[s.1],V. 21; n.3, p. 615–622 15 February 2020. Elsevier BV. https://doi.org/10.1016/j.tws.2020.106669.
13. WANG, H.; ZHOU, J.; ZHAO, T.S.; LIU, L.Z.; LIANG, Q. et al. Multiple-iteration spring back compensation of tailor welded blanks during stamping forming process. Materials & Design, [s.l.], v. 102, p.247-254, jul. 2016.
14. SHI, Ming F.; PICKETT, Ken M.; BHATT, Kumar K.. Formability Issues in the Application of Tailor Welded Blank Sheets. Sae Technical Paper Series, [s.l.], p.1-11, 1 mar. 1993. SAE International.
15. PANDA, Sushanta Kumar; KUMAR, D. Ravi; KUMAR, Harish; NATH, A.K.. Characterization of tensile properties of tailor welded IF steel sheets and their formability in stretch forming. Journal Of Materials Processing Technology, [s.l.], v. 183, n. 2-3, p.321-332, mar. 2007. Elsevier BV.
16. KARAJIBANI, Ehsan; HASHEMI, Ramin; SEDIGHI, Mohammad. Determination of forming limit curve in two-layer metallic sheets using the finite element simulation. Proceedings of the Institution of Mechanical Engineers, Part L: Journal of Materials, [s.l.], v. 230, n. 6, p.1018-1029, 3 ago. 2016. SAGE Publications.
17. BRESCIANI FILHO, Ettore et al. Conformação Plástica Dos Metais. 6. ed. Campinas: Epusp, 2011. 254p.
18. DIETER, G. E. Mechanical metallurgy. 3 Ed. Boston: McGraw-Hill, 1988.
19. https://www.researchgate.net/publication/329680368_Theory_of_Plasticity [accessed Dec 08 2019]
20. KIM, Jaehun; KIM, Sanseo; KIM, Keunug; JUNG, Wonyeong; YOUN, Deokhyun; LEE, Jangseok; KI, Hyungson. Effect of beam size in laser welding of ultra-thin stainless steel foils. Journal Of Materials Processing Technology, [s.l.], v. 233, p.125-134, jul. 2016. Elsevier BV
21. KHAN, Arman; SURESH, V.V.N.Satya; REGALLA, Srinivasa Prakash. Effect of Thickness Ratio on Weld Line Displacement in Deep Drawing of Aluminium Steel Tailor Welded Blanks. Procedia Materials Science, [s.l.], v. 6, p.401-408, 2014. Elsevier BV.
22. SURESH, V. V. N. Satya; REGALLA, Srinivasa Prakash; GUPTA, Amit Kumar. Combined effect of thickness ratio and selective heating on weld line movement in stamped tailor-welded blanks. Materials And Manufacturing Processes, [s.l.], v. 32, n. 12, p.1363-1367, 10 nov. 2016. Informa UK Limited.
23. CALLISTER, William D.; RETHWISCH, David G.. Ciência e Engenharia de Materiais: Uma Introdução. 9. ed. São Paulo: LTC: GEN - Grupo Editorial Nacional, 2016. 912 p.
24. CETLIN, PR; HELMAN, H. Fundamentos da conformação: mecânica dos metais. 2. ed. São Paulo: Artliber; 2005. 265 p.
25. SAFDARIAN, R. The effects of strength ratio on the forming limit diagram of tailor-welded blanks. Ironmaking & Steelmaking, [s.l.], v. 45, n. 1, p.17-24, 27 set. 2016. Informa UK Limited.
26. Abdelkader, Slimane,; Benattou Bouchouicha,; Mohamed Benguediab,; Sid-Ahmed Slimaneb, 2015 Parametric study of the ductile damage by the

Gurson–Tvergaard–Needleman model of structures in carbon steel A48-AP. Brazilian Metallurgical, Materials and Mining Association: v. 4, n. , p.2017-223, 2015. Elsevier BV.
27. Safdarian, R., "Forming Limit Diagram Prediction of AISI 304–St 12.Tailor Welded Blanks Using GTN Damage Model," Journal of Testing and Evaluation, [s.1], V.2, n.1, p.1-16, January 15, 2019. ASTM International. https:// doi.org/10.1520/JTE20180069.
28. HOSFORD, William F.; CADDELL, Robert M.. Metal Forming: Mechanics and Metallurgy. 3. ed. Nova Iorque: Cambridge University Press, 2007. 312 p.
29. KINSEY, Brad L.; WU, Xin. Tailor welded blanks for advanced manufacturing. Cambridge: Woodhead Publishing Limited, 2011. 217 p.
30. GAUTAM, Vijay; RAUT, Vinayak Manohar; KUMAR, D Ravi. Analytical prediction of spring back in bending of tailor-welded blanks incorporating effect of anisotropy and weld zone properties. Proceedings of the Institution of Mechanical Engineers, Part L: Journal of Materials, [s.l.], v. 232, n. 4, p.294-306, 4 jan. 2016. SAGE Publications.
31. GAUTAM, Vijay; KUMAR, Arvind. Experimental and Numerical Studies on Formability of Tailor Welded Blanks of High Strength Steel. Procedia Manufacturing, [s.l.], v. 29, p.472-480, 2019. Elsevier BV.
32. MAMUSI, Hossein; MASOUMI, Abolfazl; HASHEMI, Ramin; MAHDAVINEJAD, Ramazanali. A Novel Approach to the Determination of Forming Limit Diagrams for Tailor-Welded Blanks. Journal of Materials Engineering and Performance, [s.l.], v. 22, n. 11, p.3210-3221, 27 jun. 2013. Springer Nature
33. KOROUYEH, R. Safdarian; NAEINI, H. Moslemi; TORKAMANY, M.J.; LIAGHAT, Gh.. Experimental and theoretical investigation of thickness ratio effect on the formability of tailor welded blank. Optics & Laser Technology, [s.l.], v. 51, p.24-31, out. 2013. Elsevier BV.
34. ANDRADE, Etiene Pereira de. Caracterização mecânica e análise microestrutural de chapas obtidas pelo processo de Tailor Welded Blank (TWB). 2019. 115 f. Dissertação (Mestrado) - Curso de Engenharia Mecânica, PPGMEC, Universidade Federal de Minas Gerais, Belo Horizonte, 2019.
35. ABDULLAH, K.; WILD, P.M.; JESWIET, J.J.; GHASEMPOOR, A. Tensile testing for weld deformation properties in similar gage tailor welded blanks using the rule of mixtures. Journal Of Materials Processing Technology, [s.l.], v. 112, n. 1, p.91-97, maio 2001. Elsevier BV.
36. AFFONSO, Luiz Otávio Amaral. Ductile and Brittle Fractures. In: AFFONSO, Luiz Otávio Amaral. Machinery Failure Analysis Handbook: Sustain Your Operations and Maximize Uptime. Houston: Gulf Publishing Company, 2007. Cap. 4. p. 33-42.
37. AMERICAN SOCIETY FOR TESTING AND MATERIALS. ASTM E8/E8M: Standard Test Methods for Tension Testing of Metallic Materials. 16 ed. West Conshohocken: ASTM International, 2016. 30 p.
38. ANDRADE, Etiene Pereira de: Estudo do Efeito das Condições de Processamento Mecânico na Transformação de fases do aço inoxidável AISI - Centro Federal de Educação Tecnológica de Minas Gerais, Belo Horizonte, 2015.
39. ASSUNÇÃO, Eurico; QUINTINO, Luisa; MIRANDA, Rosa. Comparative study of laser welding in tailor blanks for the automotive industry. The International Journal of Advanced Manufacturing Technology, [s.l.], v. 49, n. 1-4, p.123-131, 17 nov. 2009. Springer Nature.
40. BROWN, Arthur A.; BAMMANN, Douglas J.. Validation of a model for static and dynamic recrystallization in metals. International Journal of Plasticity, [s.l.], v. 32-33, p.17-35, maio 2012. Elsevier BV. http://dx.doi.org/10.1016/j.ijplas.2011.12.006.
41. CASTRO, Frederico de Magalhães: Estudo Numérico e Analítico das Evoluções da Força e da Espessura em Chapas de Aço Livre de Intersticiais Durante Processamento por Embutimento e Ironing. 2005. 63 f. Dissertação (Mestrado) – Universidade Federal de Minas Gerais, Belo Horizonte, 2005.
42. DHARAN, C. K. H.; KANG, B. S.; FINNIE, Iain. Cleavage and Ductile Fracture Mechanisms: The Microstructural Basis of Fracture Toughness. In: DHARAN, C. K. H.; KANG, B. S.; FINNIE, Iain. Finnie's Notes on Fracture Mechanics: Fundamental and Practical Lessons. Nova Iorque: Springer, 2016. Cap. 7. p. 201-213.
43. DUAN, Libin; XIAO, Ning-Cong; LI, Guangyao; XU Fengxiang; CHEN, Tao; CHENG, Aiguo. Bending analysis and design optimization of tailor-rolled blank thin-walled structures with top-hat sections. International Journal Of Crashworthiness, [s.l.], v. 22, n. 3, p.227-242, 8 nov. 2016. Informa UK Limited.
44. FAZLI, Ali. Investigation of The Effects of Process Parameters on The Welding Line Movement in Deep Drawing of Tailor Welded Blanks. International Journal of Advanced Design and Manufacturing Technology, [s.l.], v. 9, n. 2, p.45-52, abr. 2016. TWB.
45. GONG, Hongying; WANG, Sifan; KNYSH, Paul; KORKOLIS, Yannis P.. Experimental investigation of the mechanical response of laser-welded dissimilar blanks from advanced- and ultra-high-strength steels. Materials & Design, [s.l.], v. 90, p.1115-1123, jan. 2016. Elsevier BV.
46. HE, Sijun; WU, Xin; HU, S. Jack. Formability Enhancement for Tailor-Welded Blanks Using Blank Holding Force Control. Journal of Manufacturing

Science and Engineering, [s.l.], v. 125, n. 3, p.461-467, 2003. ASME International.
47. INTERNATIONAL ORGANIZATION FOR STANDARDIZATION. 6892-1: Metallic materials — Tensile testing — Part 1: Method of test at room temperature. 2 ed. Geneva: ISO, 2016. 79 p.
48. KOROUYEH, R. Safdarian; NAEINI, H. Moslemi; TORKAMANY, M.J.; LIAGHAT, Gh.. Experimental and theoretical investigation of thickness ratio effect on the formability of tailor welded blank. Optics & Laser Technology, [s.l.], v. 51, p.24-31, out. 2013. Elsevier BV.
49. LEE, Dong Nyung; KIM, Yoon Keun. On the rule of mixtures for flow stresses in stainless-steel-clad aluminium sandwich sheet metals. Journal Of Materials Science, [s.l.], v. 23, n. 2, p.558-564, fev. 1988. Springer Science and Business Media LLC. http://dx.doi.org/10.1007/bf01174685.
50. LI, J.; NAYAK, S.S.; BIRO, E.; PANDA, S.K.; GOODWIN, F.; ZHOU, Y. Effects of weld line position and geometry on the formability of laser welded high strength low alloy and dual-phase steel blanks. Materials & Design (1980-2015), [s.l.], v. 52, p.757-766, dez. 2013. Elsevier BV
51. LI, Guangyao; XU, Fengxiang; HUANG, X.; SUN, Guangyong. Topology Optimization of an Automotive Tailor-Welded Blank Door. Journal Of Mechanical Design, [s.l.], v. 137, n. 5, p.055001-055008, 5 mar. 2015. ASME International.
52. LI, Yanhua; LIN, Jianping. Experimental and Numerical Investigations of Constraint Effect on Deformation Behavior of Tailor-Welded Blanks. Journal of Materials Engineering and Performance, [s.l.], v. 24, n. 8, p.2957-2969, 30 jun. 2015. Springer Nature.
53. LIU, Jun; WANG, Li-Liang; LEE, Junyi; CHEN, Ruili; EL-FAKIR, Omer; CHEN, Li; LIN, Jianguo; DEAN, Trevor A.. Size-dependent mechanical properties in AA6082 tailor welded specimens. Journal of Materials Processing Technology, [s.l.], v. 224, p.169-180, out. 2015. Elsevier BV.
54. MERKLEIN, Marion; JOHANNES, Maren; LECHNER, Michael; KUPERT, Andreas. A review on tailor blanks—Production, applications and evaluation. Journal of Materials Processing Technology, [s.l.], v. 214, n. 2, p.151-164, fev. 2014. Elsevier BV.
55. Miguel A. Sanz,; K. Nguyen,; Marcos Latorre,; Manuel Rodríguez,; Francisco J. Montáns. Sheet metal forming analysis using a large strain anisotropic multiplicative plasticity formulation, based on elastic correctors, which preserves the structure of the infinitesimal theory. Finite Elements in Analysis and Design v. 164, n. 1, p.1-17, 2019. Elsevier BV.
56. MIYAZAK, Yasunobu; SAKIYAMA, Tatsuya; KODAMA, Shinji. NIPPON Steel Technical Report: Welding Techniques for Tailor Blanks. 95. ed. Japão (Tóquio): NSSM, 2007. 7 p.
57. NALLI, F.; SPENA, P. Russo; CORTESE, L.; REITERER, D.. Global-local characterization and numerical modeling of TWB laser welded joints. In: International Mechanical Engineering Congress and Exposition - IMECE, 5., 2017, Flórida (Tampa). Proceedings of the ASME 2017 International Mechanical Engineering Congress and Exposition. Flórida (Tampa): ASME, 2017. p. 1 - 8.
58. RIAHI, M; AMINI, A.; SABBAGHZADEH, J.; TORKAMANI, M.J.. Analysis of weld location effect and thickness ratio on formability of tailor welded blank. Science and Technology of Welding and Joining, [s.l.], v. 17, n. 4, p.282-287, maio 2012. Informa UK Limited.
59. SCHREK, A.; ŠVEC, P.; BRUSILOVÁ, A.. Formability of Tailor-Welded Blanks From Dual-Phase and Bake-Hardened Steels with a Planar Anisotropy Influence. Strength Of Materials, [s.l.], v. 49, n. 4, p.550-554, jul. 2017. Springer Nature.
60. SINGH, Mayank Kumar. Application of Steel in Automotive Industry. International Journal of Emerging Technology and Advanced Engineering, [s.l.], v. 6, n. 7, p.246-253, jul. 2016
61. VIJAY, GAUTAM.; ARVIND KUMAR. Experimental and Numerical Studies on Formability of Tailor Welded Blanks of High Strength Steel. 18th International conference on Sheet Metal, v.29, n.1, p472-480, feb.2019. Elsevier BV.
62. Won-Ik, CHO.; PEER WOIZESCHKE.; VILLADS SCHULTZ. Simulation of molten pool dynamics and stability analysis in laser buttonhole welding.10th CIRP conference on Photonic Technologies, v. 74, n. 1,p.687-690, 2018.Elsevier BV.
63. Yanhong Um,; Jing Zhou,; Baoyu Wang,; Qiaoling Wang,; Andrea Ghiotti,; Stefania Bruschi,; Numerical simulation of hot stamping by partition heating based on advanced constitutive modelling of 22MnB5 behaviour. Finite Elements in Analysis and Design, v. xxx, n. 1, p.1-11, 2018. Elsevier BV.
64. ZADPOOR, Amir Abbas; SINKE; Jos; BENEDICTUS, Rinze; PIETERS, Raph. Mechanical properties and microstructure of friction stir welded tailor-made blanks. Materials Science And Engineering: A, [s.l.], v. 494, n. 1-2, p.281-290, out. 2008. Elsevier BV.
65. ZHAO, K.M; CHUN, B.K; LEE, J.K. Finite element analysis of tailor-welded blanks. Finite Elements in Analysis and Design, [s.l.], v. 37, n. 2, p.117-130, fev. 2001. Elsevier BV.
66. G.D. Huynh; X. Zhuang; H.G. Bui; G. Meschke; H. Nguyen-Xuan.Elasto-plastic large deformation analysis of multi-patch thin shells by is geometric approach. Finite Elements in Analysis and Design, [s.l.], v. 3, n. 2, p.1-12, fev. 2020. Elsevier BV. https://doi.org/10.1016/j.finel.2020.103389.

Global Journals Guidelines Handbook 2020

www.GlobalJournals.org

Memberships

Fellows/Associates of Engineering Research Council

FERC/AERC Memberships

Introduction

FERC/AERC is the most prestigious membership of Global Journals accredited by Open Association of Research Society, U.S.A (OARS). The credentials of Fellow and Associate designations signify that the researcher has gained the knowledge of the fundamental and high-level concepts, and is a subject matter expert, proficient in an expertise course covering the professional code of conduct, and follows recognized standards of practice. The credentials are designated only to the researchers, scientists, and professionals that have been selected by a rigorous process by our Editorial Board and Management Board.

Associates of FERC/AERC are scientists and researchers from around the world are working on projects/researches that have huge potentials. Members support Global Journals' mission to advance technology for humanity and the profession.

FERC

Fellow of Engineering Research Council

FELLOW OF ENGINEERING RESEARCH COUNCIL is the most prestigious membership of Global Journals. It is an award and membership granted to individuals that the Open Association of Research Society judges to have made a 'substantial contribution to the improvement of computer science, technology, and electronics engineering.

The primary objective is to recognize the leaders in research and scientific fields of the current era with a global perspective and to create a channel between them and other researchers for better exposure and knowledge sharing. Members are most eminent scientists, engineers, and technologists from all across the world. Fellows are elected for life through a peer review process on the basis of excellence in the respective domain. There is no limit on the number of new nominations made in any year. Each year, the Open Association of Research Society elect up to 12 new Fellow Members.

Benefit

To the institution

Get letter of appreciation

Global Journals sends a letter of appreciation of author to the Dean or CEO of the University or Company of which author is a part, signed by editor in chief or chief author.

Exclusive Network

Get access to a closed network

A FERC member gets access to a closed network of Tier 1 researchers and scientists with direct communication channel through our website. Fellows can reach out to other members or researchers directly. They should also be open to reaching out by other.

Career | Credibility | Exclusive | Reputation

Certificate

Certificate, LoR and Laser-Momento

Fellows receive a printed copy of a certificate signed by our Chief Author that may be used for academic purposes and a personal recommendation letter to the dean of member's university.

Career | Credibility | Exclusive | Reputation

Designation

Get honored title of membership

Fellows can use the honored title of membership. The “FERC” is an honored title which is accorded to a person’s name viz. Dr. John E. Hall, Ph.D., FERC or William Walldroff, M.S., FERC.

Career | Credibility | Exclusive | Reputation

Recognition on the Platform

Better visibility and citation

All the Fellow members of FERC get a badge of "Leading Member of Global Journals" on the Research Community that distinguishes them from others. Additionally, the profile is also partially maintained by our team for better visibility and citation. All fellows get a dedicated page on the website with their biography.

Career | Credibility | Reputation

Future Work

Get discounts on the future publications

Fellows receive discounts on the future publications with Global Journals up to 60%. Through our recommendation programs, members also receive discounts on publications made with OARS affiliated organizations.

Career | Financial

GJ Account

Unlimited forward of Emails

Fellows get secure and fast GJ work emails with unlimited storage of emails that they may use them as their primary email. For example, john [AT] globaljournals [DOT] org.

Career | Credibility | Reputation

Premium Tools

Access to all the premium tools

To take future researches to the zenith, fellows receive access to all the premium tools that Global Journals have to offer along with the partnership with some of the best marketing leading tools out there.

Financial

Conferences & Events

Organize seminar/conference

Fellows are authorized to organize symposium/seminar/conference on behalf of Global Journal Incorporation (USA). They can also participate in the same organized by another institution as representative of Global Journal. In both the cases, it is mandatory for him to discuss with us and obtain our consent. Additionally, they get free research conferences (and others) alerts.

Career | Credibility | Financial

Early Invitations

Early invitations to all the symposiums, seminars, conferences

All fellows receive the early invitations to all the symposiums, seminars, conferences and webinars hosted by Global Journals in their subject.

Exclusive

Publishing Articles & Books

Earn 60% of sales proceeds

Fellows can publish articles (limited) without any fees. Also, they can earn up to 70% of sales proceeds from the sale of reference/review books/literature/publishing of research paper. The FERC member can decide its price and we can help in making the right decision.

Exclusive | Financial

Reviewers

Get a remuneration of 15% of author fees

Fellow members are eligible to join as a paid peer reviewer at Global Journals Incorporation (USA) and can get a remuneration of 15% of author fees, taken from the author of a respective paper.

Financial

Access to Editorial Board

Become a member of the Editorial Board

Fellows may join as a member of the Editorial Board of Global Journals Incorporation (USA) after successful completion of three years as Fellow and as Peer Reviewer. Additionally, Fellows get a chance to nominate other members for Editorial Board.

Career | Credibility | Exclusive | Reputation

And Much More

Get access to scientific museums and observatories across the globe

All members get access to 5 selected scientific museums and observatories across the globe. All researches published with Global Journals will be kept under deep archival facilities across regions for future protections and disaster recovery. They get 10 GB free secure cloud access for storing research files.

AERC

ASSOCIATE OF ENGINEERING RESEARCH COUNCIL

ASSOCIATE OF ENGINEERING RESEARCH COUNCIL is the membership of Global Journals awarded to individuals that the Open Association of Research Society judges to have made a 'substantial contribution to the improvement of computer science, technology, and electronics engineering.

The primary objective is to recognize the leaders in research and scientific fields of the current era with a global perspective and to create a channel between them and other researchers for better exposure and knowledge sharing. Members are most eminent scientists, engineers, and technologists from all across the world. Associate membership can later be promoted to Fellow Membership. Associates are elected for life through a peer review process on the basis of excellence in the respective domain. There is no limit on the number of new nominations made in any year. Each year, the Open Association of Research Society elect up to 12 new Associate Members.

Benefit

To the institution

Get letter of appreciation

Global Journals sends a letter of appreciation of author to the Dean or CEO of the University or Company of which author is a part, signed by editor in chief or chief author.

Exclusive Network

Get access to a closed network

A AERC member gets access to a closed network of Tier 1 researchers and scientists with direct communication channel through our website. Associates can reach out to other members or researchers directly. They should also be open to reaching out by other.

Career | Credibility | Exclusive | Reputation

Certificate

Certificate, LoR and Laser-Momento

Associates receive a printed copy of a certificate signed by our Chief Author that may be used for academic purposes and a personal recommendation letter to the dean of member's university.

Career | Credibility | Exclusive | Reputation

Designation

Get honored title of membership

Associates can use the honored title of membership. The “AERC” is an honored title which is accorded to a person’s name viz. Dr. John E. Hall, Ph.D., AERC or William Walldroff, M.S., AERC.

Career | Credibility | Exclusive | Reputation

Recognition on the Platform

Better visibility and citation

All the Associate members of AERC get a badge of "Leading Member of Global Journals" on the Research Community that distinguishes them from others. Additionally, the profile is also partially maintained by our team for better visibility and citation. All associates get a dedicated page on the website with their biography.

Career | Credibility | Reputation

Future Work

Get discounts on the future publications

Associates receive discounts on the future publications with Global Journals up to 60%. Through our recommendation programs, members also receive discounts on publications made with OARS affiliated organizations.

Career | Financial

GJ Account

Unlimited forward of Emails

Associates get secure and fast GJ work emails with unlimited storage of emails that they may use them as their primary email. For example, john [AT] globaljournals [DOT] org..

Career | Credibility | Reputation

Premium Tools

Access to all the premium tools

To take future researches to the zenith, associates receive access to all the premium tools that Global Journals have to offer along with the partnership with some of the best marketing leading tools out there.

Financial

Conferences & Events

Organize seminar/conference

Associates are authorized to organize symposium/seminar/conference on behalf of Global Journal Incorporation (USA). They can also participate in the same organized by another institution as representative of Global Journal. In both the cases, it is mandatory for him to discuss with us and obtain our consent. Additionally, they get free research conferences (and others) alerts.

Career | Credibility | Financial

Early Invitations

Early invitations to all the symposiums, seminars, conferences

All associates receive the early invitations to all the symposiums, seminars, conferences and webinars hosted by Global Journals in their subject.

Exclusive

Publishing Articles & Books

Earn 30-40% of sales proceeds

Associates can publish articles (limited) without any fees. Also, they can earn up to 30-40% of sales proceeds from the sale of reference/review books/literature/publishing of research paper.

Exclusive | Financial

Reviewers

Get a remuneration of 15% of author fees

Associate members are eligible to join as a paid peer reviewer at Global Journals Incorporation (USA) and can get a remuneration of 15% of author fees, taken from the author of a respective paper.

Financial

And Much More

Get access to scientific museums and observatories across the globe

All members get access to 2 selected scientific museums and observatories across the globe. All researches published with Global Journals will be kept under deep archival facilities across regions for future protections and disaster recovery. They get 5 GB free secure cloud access for storing research files.

Associate	Fellow	Research Group	Basic
$4800 **lifetime designation**	$6800 **lifetime designation**	$12500.00 **organizational**	APC **per article**
Certificate, LoR and Momento **2** discounted publishing/year **Gradation** of Research **10** research contacts/day **1 GB** Cloud Storage **GJ** Community Access	**Certificate,** LoR and Momento **Unlimited** discounted publishing/year **Gradation** of Research **Unlimited** research contacts/day **5 GB** Cloud Storage **Online Presense** Assistance **GJ** Community Access	**Certificates,** LoRs and Momentos **Unlimited** free publishing/year **Gradation** of Research **Unlimited** research contacts/day **Unlimited** Cloud Storage **Online Presense** Assistance **GJ** Community Access	**GJ** Community Access

We accept the manuscript submissions in any standard (generic) format.

We typeset manuscripts using advanced typesetting tools like Adobe In Design, CorelDraw, TeXnicCenter, and TeXStudio. We usually recommend authors submit their research using any standard format they are comfortable with, and let Global Journals do the rest.

Alternatively, you can download our basic template from https://globaljournals.org/Template.zip

Authors should submit their complete paper/article, including text illustrations, graphics, conclusions, artwork, and tables. Authors who are not able to submit manuscript using the form above can email the manuscript department at submit@globaljournals.org or get in touch with chiefeditor@globaljournals.org if they wish to send the abstract before submission.

Before and during Submission

Authors must ensure the information provided during the submission of a paper is authentic. Please go through the following checklist before submitting:

1. Authors must go through the complete author guideline and understand and *agree to Global Journals' ethics and code of conduct,* along with author responsibilities.
2. Authors must accept the privacy policy, terms, and conditions of Global Journals.
3. Ensure corresponding author's email address and postal address are accurate and reachable.
4. Manuscript to be submitted must include keywords, an abstract, a paper title, co-author(s') names and details (email address, name, phone number, and institution), figures and illustrations in vector format including appropriate captions, tables, including titles and footnotes, a conclusion, results, acknowledgments and references.
5. Authors should submit paper in a ZIP archive if any supplementary files are required along with the paper.
6. Proper permissions must be acquired for the use of any copyrighted material.
7. Manuscript submitted *must not have been submitted or published elsewhere* and all authors must be aware of the submission.

Declaration of Conflicts of Interest

It is required for authors to declare all financial, institutional, and personal relationships with other individuals and organizations that could influence (bias) their research.

Policy on Plagiarism

Plagiarism is not acceptable in Global Journals submissions at all.

Plagiarized content will not be considered for publication. We reserve the right to inform authors' institutions about plagiarism detected either before or after publication. If plagiarism is identified, we will follow COPE guidelines:

Authors are solely responsible for all the plagiarism that is found. The author must not fabricate, falsify or plagiarize existing research data. The following, if copied, will be considered plagiarism:

- Words (language)
- Ideas
- Findings
- Writings
- Diagrams
- Graphs
- Illustrations
- Lectures

- Printed material
- Graphic representations
- Computer programs
- Electronic material
- Any other original work

Authorship Policies

Global Journals follows the definition of authorship set up by the Open Association of Research Society, USA. According to its guidelines, authorship criteria must be based on:

1. Substantial contributions to the conception and acquisition of data, analysis, and interpretation of findings.
2. Drafting the paper and revising it critically regarding important academic content.
3. Final approval of the version of the paper to be published.

Changes in Authorship

The corresponding author should mention the name and complete details of all co-authors during submission and in manuscript. We support addition, rearrangement, manipulation, and deletions in authors list till the early view publication of the journal. We expect that corresponding author will notify all co-authors of submission. We follow COPE guidelines for changes in authorship.

Copyright

During submission of the manuscript, the author is confirming an exclusive license agreement with Global Journals which gives Global Journals the authority to reproduce, reuse, and republish authors' research. We also believe in flexible copyright terms where copyright may remain with authors/employers/institutions as well. Contact your editor after acceptance to choose your copyright policy. You may follow this form for copyright transfers.

Appealing Decisions

Unless specified in the notification, the Editorial Board's decision on publication of the paper is final and cannot be appealed before making the major change in the manuscript.

Acknowledgments

Contributors to the research other than authors credited should be mentioned in Acknowledgments. The source of funding for the research can be included. Suppliers of resources may be mentioned along with their addresses.

Declaration of funding sources

Global Journals is in partnership with various universities, laboratories, and other institutions worldwide in the research domain. Authors are requested to disclose their source of funding during every stage of their research, such as making analysis, performing laboratory operations, computing data, and using institutional resources, from writing an article to its submission. This will also help authors to get reimbursements by requesting an open access publication letter from Global Journals and submitting to the respective funding source.

Preparing your Manuscript

Authors can submit papers and articles in an acceptable file format: MS Word (doc, docx), LaTeX (.tex, .zip or .rar including all of your files), Adobe PDF (.pdf), rich text format (.rtf), simple text document (.txt), Open Document Text (.odt), and Apple Pages (.pages). Our professional layout editors will format the entire paper according to our official guidelines. This is one of the highlights of publishing with Global Journals—authors should not be concerned about the formatting of their paper. Global Journals accepts articles and manuscripts in every major language, be it Spanish, Chinese, Japanese, Portuguese, Russian, French, German, Dutch, Italian, Greek, or any other national language, but the title, subtitle, and abstract should be in English. This will facilitate indexing and the pre-peer review process.

The following is the official style and template developed for publication of a research paper. Authors are not required to follow this style during the submission of the paper. It is just for reference purposes.

Manuscript Style Instruction (Optional)

- Microsoft Word Document Setting Instructions.
- Font type of all text should be Swis721 Lt BT.
- Page size: 8.27" x 11'", left margin: 0.65, right margin: 0.65, bottom margin: 0.75.
- Paper title should be in one column of font size 24.
- Author name in font size of 11 in one column.
- Abstract: font size 9 with the word "Abstract" in bold italics.
- Main text: font size 10 with two justified columns.
- Two columns with equal column width of 3.38 and spacing of 0.2.
- First character must be three lines drop-capped.
- The paragraph before spacing of 1 pt and after of 0 pt.
- Line spacing of 1 pt.
- Large images must be in one column.
- The names of first main headings (Heading 1) must be in Roman font, capital letters, and font size of 10.
- The names of second main headings (Heading 2) must not include numbers and must be in italics with a font size of 10.

Structure and Format of Manuscript

The recommended size of an original research paper is under 15,000 words and review papers under 7,000 words. Research articles should be less than 10,000 words. Research papers are usually longer than review papers. Review papers are reports of significant research (typically less than 7,000 words, including tables, figures, and references)

A research paper must include:

a) A title which should be relevant to the theme of the paper.
b) A summary, known as an abstract (less than 150 words), containing the major results and conclusions.
c) Up to 10 keywords that precisely identify the paper's subject, purpose, and focus.
d) An introduction, giving fundamental background objectives.
e) Resources and techniques with sufficient complete experimental details (wherever possible by reference) to permit repetition, sources of information must be given, and numerical methods must be specified by reference.
f) Results which should be presented concisely by well-designed tables and figures.
g) Suitable statistical data should also be given.
h) All data must have been gathered with attention to numerical detail in the planning stage.

Design has been recognized to be essential to experiments for a considerable time, and the editor has decided that any paper that appears not to have adequate numerical treatments of the data will be returned unrefereed.

i) Discussion should cover implications and consequences and not just recapitulate the results; conclusions should also be summarized.
j) There should be brief acknowledgments.
k) There ought to be references in the conventional format. Global Journals recommends APA format.

Authors should carefully consider the preparation of papers to ensure that they communicate effectively. Papers are much more likely to be accepted if they are carefully designed and laid out, contain few or no errors, are summarizing, and follow instructions. They will also be published with much fewer delays than those that require much technical and editorial correction.

The Editorial Board reserves the right to make literary corrections and suggestions to improve brevity.

Format Structure

It is necessary that authors take care in submitting a manuscript that is written in simple language and adheres to published guidelines.

All manuscripts submitted to Global Journals should include:

Title

The title page must carry an informative title that reflects the content, a running title (less than 45 characters together with spaces), names of the authors and co-authors, and the place(s) where the work was carried out.

Author details

The full postal address of any related author(s) must be specified.

Abstract

The abstract is the foundation of the research paper. It should be clear and concise and must contain the objective of the paper and inferences drawn. It is advised to not include big mathematical equations or complicated jargon.

Many researchers searching for information online will use search engines such as Google, Yahoo or others. By optimizing your paper for search engines, you will amplify the chance of someone finding it. In turn, this will make it more likely to be viewed and cited in further works. Global Journals has compiled these guidelines to facilitate you to maximize the web-friendliness of the most public part of your paper.

Keywords

A major lynchpin of research work for the writing of research papers is the keyword search, which one will employ to find both library and internet resources. Up to eleven keywords or very brief phrases have to be given to help data retrieval, mining, and indexing.

One must be persistent and creative in using keywords. An effective keyword search requires a strategy: planning of a list of possible keywords and phrases to try.

Choice of the main keywords is the first tool of writing a research paper. Research paper writing is an art. Keyword search should be as strategic as possible.

One should start brainstorming lists of potential keywords before even beginning searching. Think about the most important concepts related to research work. Ask, “What words would a source have to include to be truly valuable in a research paper?” Then consider synonyms for the important words.

It may take the discovery of only one important paper to steer in the right keyword direction because, in most databases, the keywords under which a research paper is abstracted are listed with the paper.

Numerical Methods

Numerical methods used should be transparent and, where appropriate, supported by references.

Abbreviations

Authors must list all the abbreviations used in the paper at the end of the paper or in a separate table before using them.

Formulas and equations

Authors are advised to submit any mathematical equation using either MathJax, KaTeX, or LaTeX, or in a very high-quality image.

Tables, Figures, and Figure Legends

Tables: Tables should be cautiously designed, uncrowned, and include only essential data. Each must have an Arabic number, e.g., Table 4, a self-explanatory caption, and be on a separate sheet. Authors must submit tables in an editable format and not as images. References to these tables (if any) must be mentioned accurately.

Figures

Figures are supposed to be submitted as separate files. Always include a citation in the text for each figure using Arabic numbers, e.g., Fig. 4. Artwork must be submitted online in vector electronic form or by emailing it.

Preparation of Eletronic Figures for Publication

Although low-quality images are sufficient for review purposes, print publication requires high-quality images to prevent the final product being blurred or fuzzy. Submit (possibly by e-mail) EPS (line art) or TIFF (halftone/ photographs) files only. MS PowerPoint and Word Graphics are unsuitable for printed pictures. Avoid using pixel-oriented software. Scans (TIFF only) should have a resolution of at least 350 dpi (halftone) or 700 to 1100 dpi (line drawings). Please give the data for figures in black and white or submit a Color Work Agreement form. EPS files must be saved with fonts embedded (and with a TIFF preview, if possible).

For scanned images, the scanning resolution at final image size ought to be as follows to ensure good reproduction: line art: >650 dpi; halftones (including gel photographs): >350 dpi; figures containing both halftone and line images: >650 dpi.

Color charges: Authors are advised to pay the full cost for the reproduction of their color artwork. Hence, please note that if there is color artwork in your manuscript when it is accepted for publication, we would require you to complete and return a Color Work Agreement form before your paper can be published. Also, you can email your editor to remove the color fee after acceptance of the paper.

Tips for Writing a Good Quality Engineering Research Paper

Techniques for writing a good quality engineering research paper:

1. Choosing the topic: In most cases, the topic is selected by the interests of the author, but it can also be suggested by the guides. You can have several topics, and then judge which you are most comfortable with. This may be done by asking several questions of yourself, like "Will I be able to carry out a search in this area? Will I find all necessary resources to accomplish the search? Will I be able to find all information in this field area?" If the answer to this type of question is "yes," then you ought to choose that topic. In most cases, you may have to conduct surveys and visit several places. Also, you might have to do a lot of work to find all the rises and falls of the various data on that subject. Sometimes, detailed information plays a vital role, instead of short information. Evaluators are human: The first thing to remember is that evaluators are also human beings. They are not only meant for rejecting a paper. They are here to evaluate your paper. So present your best aspect.

2. Think like evaluators: If you are in confusion or getting demotivated because your paper may not be accepted by the evaluators, then think, and try to evaluate your paper like an evaluator. Try to understand what an evaluator wants in your research paper, and you will automatically have your answer. Make blueprints of paper: The outline is the plan or framework that will help you to arrange your thoughts. It will make your paper logical. But remember that all points of your outline must be related to the topic you have chosen.

3. Ask your guides: If you are having any difficulty with your research, then do not hesitate to share your difficulty with your guide (if you have one). They will surely help you out and resolve your doubts. If you can't clarify what exactly you require for your work, then ask your supervisor to help you with an alternative. He or she might also provide you with a list of essential readings.

4. Use of computer is recommended: As you are doing research in the field of research engineering then this point is quite obvious. Use right software: Always use good quality software packages. If you are not capable of judging good software, then you can lose the quality of your paper unknowingly. There are various programs available to help you which you can get through the internet.

5. Use the internet for help: An excellent start for your paper is using Google. It is a wondrous search engine, where you can have your doubts resolved. You may also read some answers for the frequent question of how to write your research paper or find a model research paper. You can download books from the internet. If you have all the required books, place importance on reading, selecting, and analyzing the specified information. Then sketch out your research paper. Use big pictures: You may use encyclopedias like Wikipedia to get pictures with the best resolution. At Global Journals, you should strictly follow here.

6. Bookmarks are useful: When you read any book or magazine, you generally use bookmarks, right? It is a good habit which helps to not lose your continuity. You should always use bookmarks while searching on the internet also, which will make your search easier.

7. Revise what you wrote: When you write anything, always read it, summarize it, and then finalize it.

8. Make every effort: Make every effort to mention what you are going to write in your paper. That means always have a good start. Try to mention everything in the introduction—what is the need for a particular research paper. Polish your work with good writing skills and always give an evaluator what he wants. Make backups: When you are going to do any important thing like making a research paper, you should always have backup copies of it either on your computer or on paper. This protects you from losing any portion of your important data.

9. Produce good diagrams of your own: Always try to include good charts or diagrams in your paper to improve quality. Using several unnecessary diagrams will degrade the quality of your paper by creating a hodgepodge. So always try to include diagrams which were made by you to improve the readability of your paper. Use of direct quotes: When you do research relevant to literature, history, or current affairs, then use of quotes becomes essential, but if the study is relevant to science, use of quotes is not preferable.

10. Use proper verb tense: Use proper verb tenses in your paper. Use past tense to present those events that have happened. Use present tense to indicate events that are going on. Use future tense to indicate events that will happen in the future. Use of wrong tenses will confuse the evaluator. Avoid sentences that are incomplete.

11. Pick a good study spot: Always try to pick a spot for your research which is quiet. Not every spot is good for studying.

12. Know what you know: Always try to know what you know by making objectives, otherwise you will be confused and unable to achieve your target.

13. Use good grammar: Always use good grammar and words that will have a positive impact on the evaluator; use of good vocabulary does not mean using tough words which the evaluator has to find in a dictionary. Do not fragment sentences. Eliminate one-word sentences. Do not ever use a big word when a smaller one would suffice.

Verbs have to be in agreement with their subjects. In a research paper, do not start sentences with conjunctions or finish them with prepositions. When writing formally, it is advisable to never split an infinitive because someone will (wrongly) complain. Avoid clichés like a disease. Always shun irritating alliteration. Use language which is simple and straightforward. Put together a neat summary.

14. Arrangement of information: Each section of the main body should start with an opening sentence, and there should be a changeover at the end of the section. Give only valid and powerful arguments for your topic. You may also maintain your arguments with records.

15. Never start at the last minute: Always allow enough time for research work. Leaving everything to the last minute will degrade your paper and spoil your work.

16. Multitasking in research is not good: Doing several things at the same time is a bad habit in the case of research activity. Research is an area where everything has a particular time slot. Divide your research work into parts, and do a particular part in a particular time slot.

17. Never copy others' work: Never copy others' work and give it your name because if the evaluator has seen it anywhere, you will be in trouble. Take proper rest and food: No matter how many hours you spend on your research activity, if you are not taking care of your health, then all your efforts will have been in vain. For quality research, take proper rest and food.

18. Go to seminars: Attend seminars if the topic is relevant to your research area. Utilize all your resources.

19. Refresh your mind after intervals: Try to give your mind a rest by listening to soft music or sleeping in intervals. This will also improve your memory. Acquire colleagues: Always try to acquire colleagues. No matter how sharp you are, if you acquire colleagues, they can give you ideas which will be helpful to your research.

20. Think technically: Always think technically. If anything happens, search for its reasons, benefits, and demerits. Think and then print: When you go to print your paper, check that tables are not split, headings are not detached from their descriptions, and page sequence is maintained.

21. Adding unnecessary information: Do not add unnecessary information like "I have used MS Excel to draw graphs." Irrelevant and inappropriate material is superfluous. Foreign terminology and phrases are not apropos. One should never take a broad view. Analogy is like feathers on a snake. Use words properly, regardless of how others use them. Remove quotations. Puns are for kids, not grunt readers. Never oversimplify: When adding material to your research paper, never go for oversimplification; this will definitely irritate the evaluator. Be specific. Never use rhythmic redundancies. Contractions shouldn't be used in a research paper. Comparisons are as terrible as clichés. Give up ampersands, abbreviations, and so on. Remove commas that are not necessary. Parenthetical words should be between brackets or commas. Understatement is always the best way to put forward earth-shaking thoughts. Give a detailed literary review.

22. Report concluded results: Use concluded results. From raw data, filter the results, and then conclude your studies based on measurements and observations taken. An appropriate number of decimal places should be used. Parenthetical remarks are prohibited here. Proofread carefully at the final stage. At the end, give an outline to your arguments. Spot perspectives of further study of the subject. Justify your conclusion at the bottom sufficiently, which will probably include examples.

23. Upon conclusion: Once you have concluded your research, the next most important step is to present your findings. Presentation is extremely important as it is the definite medium though which your research is going to be in print for the rest of the crowd. Care should be taken to categorize your thoughts well and present them in a logical and neat manner. A good quality research paper format is essential because it serves to highlight your research paper and bring to light all necessary aspects of your research.

Informal Guidelines of Research Paper Writing

Key points to remember:

- Submit all work in its final form.
- Write your paper in the form which is presented in the guidelines using the template.
- Please note the criteria peer reviewers will use for grading the final paper.

Final points:

One purpose of organizing a research paper is to let people interpret your efforts selectively. The journal requires the following sections, submitted in the order listed, with each section starting on a new page:

The introduction: This will be compiled from reference matter and reflect the design processes or outline of basis that directed you to make a study. As you carry out the process of study, the method and process section will be constructed like that. The results segment will show related statistics in nearly sequential order and direct reviewers to similar intellectual paths throughout the data that you gathered to carry out your study.

The discussion section:

This will provide understanding of the data and projections as to the implications of the results. The use of good quality references throughout the paper will give the effort trustworthiness by representing an alertness to prior workings.

Writing a research paper is not an easy job, no matter how trouble-free the actual research or concept. Practice, excellent preparation, and controlled record-keeping are the only means to make straightforward progression.

General style:

Specific editorial column necessities for compliance of a manuscript will always take over from directions in these general guidelines.

To make a paper clear: Adhere to recommended page limits.

Mistakes to avoid:

- Insertion of a title at the foot of a page with subsequent text on the next page.
- Separating a table, chart, or figure—confine each to a single page.
- Submitting a manuscript with pages out of sequence.
- In every section of your document, use standard writing style, including articles ("a" and "the").
- Keep paying attention to the topic of the paper.

- Use paragraphs to split each significant point (excluding the abstract).
- Align the primary line of each section.
- Present your points in sound order.
- Use present tense to report well-accepted matters.
- Use past tense to describe specific results.
- Do not use familiar wording; don't address the reviewer directly. Don't use slang or superlatives.
- Avoid use of extra pictures—include only those figures essential to presenting results.

Title page:

Choose a revealing title. It should be short and include the name(s) and address(es) of all authors. It should not have acronyms or abbreviations or exceed two printed lines.

Abstract: This summary should be two hundred words or less. It should clearly and briefly explain the key findings reported in the manuscript and must have precise statistics. It should not have acronyms or abbreviations. It should be logical in itself. Do not cite references at this point.

An abstract is a brief, distinct paragraph summary of finished work or work in development. In a minute or less, a reviewer can be taught the foundation behind the study, common approaches to the problem, relevant results, and significant conclusions or new questions.

Write your summary when your paper is completed because how can you write the summary of anything which is not yet written? Wealth of terminology is very essential in abstract. Use comprehensive sentences, and do not sacrifice readability for brevity; you can maintain it succinctly by phrasing sentences so that they provide more than a lone rationale. The author can at this moment go straight to shortening the outcome. Sum up the study with the subsequent elements in any summary. Try to limit the initial two items to no more than one line each.

Reason for writing the article—theory, overall issue, purpose.

- Fundamental goal.
- To-the-point depiction of the research.
- Consequences, including definite statistics—if the consequences are quantitative in nature, account for this; results of any numerical analysis should be reported. Significant conclusions or questions that emerge from the research.

Approach:

- Single section and succinct.
- An outline of the job done is always written in past tense.
- Concentrate on shortening results—limit background information to a verdict or two.
- Exact spelling, clarity of sentences and phrases, and appropriate reporting of quantities (proper units, important statistics) are just as significant in an abstract as they are anywhere else.

Introduction:

The introduction should "introduce" the manuscript. The reviewer should be presented with sufficient background information to be capable of comprehending and calculating the purpose of your study without having to refer to other works. The basis for the study should be offered. Give the most important references, but avoid making a comprehensive appraisal of the topic. Describe the problem visibly. If the problem is not acknowledged in a logical, reasonable way, the reviewer will give no attention to your results. Speak in common terms about techniques used to explain the problem, if needed, but do not present any particulars about the protocols here.

The following approach can create a valuable beginning:

- Explain the value (significance) of the study.
- Defend the model—why did you employ this particular system or method? What is its compensation? Remark upon its appropriateness from an abstract point of view as well as pointing out sensible reasons for using it.
- Present a justification. State your particular theory(-ies) or aim(s), and describe the logic that led you to choose them.
- Briefly explain the study's tentative purpose and how it meets the declared objectives.

Approach:

Use past tense except for when referring to recognized facts. After all, the manuscript will be submitted after the entire job is done. Sort out your thoughts; manufacture one key point for every section. If you make the four points listed above, you will need at least four paragraphs. Present surrounding information only when it is necessary to support a situation. The reviewer does not desire to read everything you know about a topic. Shape the theory specifically—do not take a broad view.

As always, give awareness to spelling, simplicity, and correctness of sentences and phrases.

Procedures (methods and materials):

This part is supposed to be the easiest to carve if you have good skills. A soundly written procedures segment allows a capable scientist to replicate your results. Present precise information about your supplies. The suppliers and clarity of reagents can be helpful bits of information. Present methods in sequential order, but linked methodologies can be grouped as a segment. Be concise when relating the protocols. Attempt to give the least amount of information that would permit another capable scientist to replicate your outcome, but be cautious that vital information is integrated. The use of subheadings is suggested and ought to be synchronized with the results section.

When a technique is used that has been well-described in another section, mention the specific item describing the way, but draw the basic principle while stating the situation. The purpose is to show all particular resources and broad procedures so that another person may use some or all of the methods in one more study or referee the scientific value of your work. It is not to be a step-by-step report of the whole thing you did, nor is a methods section a set of orders.

Materials:

Materials may be reported in part of a section or else they may be recognized along with your measures.

Methods:

- Report the method and not the particulars of each process that engaged the same methodology.
- Describe the method entirely.
- To be succinct, present methods under headings dedicated to specific dealings or groups of measures.
- Simplify—detail how procedures were completed, not how they were performed on a particular day.
- If well-known procedures were used, account for the procedure by name, possibly with a reference, and that's all.

Approach:

It is embarrassing to use vigorous voice when documenting methods without using first person, which would focus the reviewer's interest on the researcher rather than the job. As a result, when writing up the methods, most authors use third person passive voice.

Use standard style in this and every other part of the paper—avoid familiar lists, and use full sentences.

What to keep away from:

- Resources and methods are not a set of information.
- Skip all descriptive information and surroundings—save it for the argument.
- Leave out information that is immaterial to a third party.

Results:

The principle of a results segment is to present and demonstrate your conclusion. Create this part as entirely objective details of the outcome, and save all understanding for the discussion.

The page length of this segment is set by the sum and types of data to be reported. Use statistics and tables, if suitable, to present consequences most efficiently.

You must clearly differentiate material which would usually be incorporated in a study editorial from any unprocessed data or additional appendix matter that would not be available. In fact, such matters should not be submitted at all except if requested by the instructor.

Content:

- Sum up your conclusions in text and demonstrate them, if suitable, with figures and tables.
- In the manuscript, explain each of your consequences, and point the reader to remarks that are most appropriate.
- Present a background, such as by describing the question that was addressed by creation of an exacting study.
- Explain results of control experiments and give remarks that are not accessible in a prescribed figure or table, if appropriate.
- Examine your data, then prepare the analyzed (transformed) data in the form of a figure (graph), table, or manuscript.

What to stay away from:

- Do not discuss or infer your outcome, report surrounding information, or try to explain anything.
- Do not include raw data or intermediate calculations in a research manuscript.
- Do not present similar data more than once.
- A manuscript should complement any figures or tables, not duplicate information.
- Never confuse figures with tables—there is a difference.

Approach:

As always, use past tense when you submit your results, and put the whole thing in a reasonable order.

Put figures and tables, appropriately numbered, in order at the end of the report.

If you desire, you may place your figures and tables properly within the text of your results section.

Figures and tables:

If you put figures and tables at the end of some details, make certain that they are visibly distinguished from any attached appendix materials, such as raw facts. Whatever the position, each table must be titled, numbered one after the other, and include a heading. All figures and tables must be divided from the text.

Discussion:

The discussion is expected to be the trickiest segment to write. A lot of papers submitted to the journal are discarded based on problems with the discussion. There is no rule for how long an argument should be.

Position your understanding of the outcome visibly to lead the reviewer through your conclusions, and then finish the paper with a summing up of the implications of the study. The purpose here is to offer an understanding of your results and support all of your conclusions, using facts from your research and generally accepted information, if suitable. The implication of results should be fully described.

Infer your data in the conversation in suitable depth. This means that when you clarify an observable fact, you must explain mechanisms that may account for the observation. If your results vary from your prospect, make clear why that may have happened. If your results agree, then explain the theory that the proof supported. It is never suitable to just state that the data approved the prospect, and let it drop at that. Make a decision as to whether each premise is supported or discarded or if you cannot make a conclusion with assurance. Do not just dismiss a study or part of a study as "uncertain."

Research papers are not acknowledged if the work is imperfect. Draw what conclusions you can based upon the results that you have, and take care of the study as a finished work.

- You may propose future guidelines, such as how an experiment might be personalized to accomplish a new idea.
- Give details of all of your remarks as much as possible, focusing on mechanisms.
- Make a decision as to whether the tentative design sufficiently addressed the theory and whether or not it was correctly restricted. Try to present substitute explanations if they are sensible alternatives.
- One piece of research will not counter an overall question, so maintain the large picture in mind. Where do you go next? The best studies unlock new avenues of study. What questions remain?
- Recommendations for detailed papers will offer supplementary suggestions.

Approach:

When you refer to information, differentiate data generated by your own studies from other available information. Present work done by specific persons (including you) in past tense.

Describe generally acknowledged facts and main beliefs in present tense.

The Administration Rules

Administration Rules to Be Strictly Followed before Submitting Your Research Paper to Global Journals Inc.

Please read the following rules and regulations carefully before submitting your research paper to Global Journals Inc. to avoid rejection.

Segment draft and final research paper: You have to strictly follow the template of a research paper, failing which your paper may get rejected. You are expected to write each part of the paper wholly on your own. The peer reviewers need to identify your own perspective of the concepts in your own terms. Please do not extract straight from any other source, and do not rephrase someone else's analysis. Do not allow anyone else to proofread your manuscript.

Written material: You may discuss this with your guides and key sources. Do not copy anyone else's paper, even if this is only imitation, otherwise it will be rejected on the grounds of plagiarism, which is illegal. Various methods to avoid plagiarism are strictly applied by us to every paper, and, if found guilty, you may be blacklisted, which could affect your career adversely. To guard yourself and others from possible illegal use, please do not permit anyone to use or even read your paper and file.

Criterion for Grading a Research Paper (Compilation) by Global Journals

Please note that following table is only a Grading of "Paper Compilation" and not on "Performed/Stated Research" whose grading solely depends on Individual Assigned Peer Reviewer and Editorial Board Member. These can be available only on request and after decision of Paper. This report will be the property of Global Journals.

Topics	Grades		
	A-B	**C-D**	**E-F**
Abstract	Clear and concise with appropriate content, Correct format. 200 words or below	Unclear summary and no specific data, Incorrect form Above 200 words	No specific data with ambiguous information Above 250 words
Introduction	Containing all background details with clear goal and appropriate details, flow specification, no grammar and spelling mistake, well organized sentence and paragraph, reference cited	Unclear and confusing data, appropriate format, grammar and spelling errors with unorganized matter	Out of place depth and content, hazy format
Methods and Procedures	Clear and to the point with well arranged paragraph, precision and accuracy of facts and figures, well organized subheads	Difficult to comprehend with embarrassed text, too much explanation but completed	Incorrect and unorganized structure with hazy meaning
Result	Well organized, Clear and specific, Correct units with precision, correct data, well structuring of paragraph, no grammar and spelling mistake	Complete and embarrassed text, difficult to comprehend	Irregular format with wrong facts and figures
Discussion	Well organized, meaningful specification, sound conclusion, logical and concise explanation, highly structured paragraph reference cited	Wordy, unclear conclusion, spurious	Conclusion is not cited, unorganized, difficult to comprehend
References	Complete and correct format, well organized	Beside the point, Incomplete	Wrong format and structuring

INDEX

save our planet

Global Journal of Researches in Engineering

Visit us on the Web at www.GlobalJournals.org | www.EngineeringResearch.org
or email us at helpdesk@globaljournals.org

ISSN 9755861